DISSERTATIONES
TECHNOLOGIAE
UNIVERSITATIS
TARTUENSIS
84

MARIA MALOVERJAN

Optimizing cell-penetrating peptide-based nanoparticles for delivery of nucleic acid therapeutics

DISSERTATIONES TECHNOLOGIAE UNIVERSITATIS TARTUENSIS
84

DISSERTATIONES TECHNOLOGIAE UNIVERSITATIS TARTUENSIS
84

MARIA MALOVERJAN

Optimizing cell-penetrating peptide-based nanoparticles for delivery of nucleic acid therapeutics

UNIVERSITY OF TARTU
Press
1632

Institute of Technology, Faculty of Science and Technology, University of Tartu, Estonia

The dissertation was accepted for the commencement of the degree of Doctor of Philosophy in Biomedical Engineering on 17.06.2024, by the Joint Council of the Doctoral Program of Engineering and Technology of the University of Tartu.

Supervisors: Margus Pooga, PhD,
Professor of Chemical Biology,
Institute of Technology, University of Tartu, Estonia

Ana Rebane, PhD,
Professor of Molecular Medicine,
Institute of Biomedicine and Translational Medicine,
University of Tartu, Estonia

Reviewer: Helena Sork, PhD
Research Fellow in Nanobiotechnology
Institute of Technology, University of Tartu, Estonia

Opponent: Roland Brock, PhD,
Chair in Biochemistry,
Medical Center of the Radboud University, The Netherlands
Adjunct professor of Biochemistry,
Arabian Gulf University, Kingdom of Bahrain

Commencement: Auditorium 121, Nooruse 1, Tartu, Estonia, at 13.15 on August 26th, 2024

Publication of this thesis is granted by the Institute of Technology, Faculty of Science and Technology, University of Tartu.

ISSN 2228-0855 (print)
ISBN 978-9916-27-602-0 (print)
ISSN 2806-2620 (pdf)
ISBN 978-9916-27-603-7 (pdf)

Copyright: Maria Maloverjan, 2024

University of Tartu Press
www.tyk.ee

TABLE OF CONTENTS

LIST OF ORIGINAL PUBLICATIONS 7

LIST OF ABBREVIATIONS 8

INTRODUCTION 9

1. LITERATURE OVERVIEW 11
   1.1. Nucleic acid therapeutics 11
      1.1.1. Structure and function of therapeutic nucleic acids 12
      1.1.2. Nucleic acid-based therapies 15
   1.2. Delivery methods for therapeutic nucleic acids 17
      1.2.1. An overview of main nucleic acid delivery systems 18
      1.2.2. Cell-penetrating peptides as delivery vectors 20
   1.3. Uptake and trafficking of nanoparticles 25
      1.3.1. Endocytosis 25
      1.3.2. Intracellular trafficking of nanoparticles 26
      1.3.3. Internalization, trafficking, and endosomal escape of CPP/NA nanoparticles 28
   1.4. Non-structural factors affecting nanoparticle delivery 29
      1.4.1. Protein corona 29
      1.4.2. Role of calcium ions in transfection 33
      1.4.3. Other approaches to affect the potency of nanoparticles 34

2. AIMS OF THE STUDY 36

3. MATERIALS AND METHODS 37
   3.1. Cells 37
   3.2. Used CPPs and nucleic acids 38
   3.3. CPP/NA nanoparticle preparation 39
   3.4. Methods used to measure cellular association and biological effects of nanoparticles 39
   3.5. Methods used to study physical properties of nanoparticles 41
   3.6. Methods used to study cellular internalization of nanoparticles 41
   3.7. Methods used to analyze the protein corona of nanoparticles 42
   3.8. *In vivo* experiments 43

4. RESULTS AND DISCUSSION 44
   4.1. The role of protein corona in internalization and biological activity of the CPP/NA nanoparticles (Paper I) 44
      4.1.1. Protein corona can induce agglomeration of nanoparticles 44
      4.1.2. The composition of the protein corona depends on the serum used 45
      4.1.3. Adsorption of C3 depends on nanoparticle characteristics 47
      4.1.4. Protein corona affects cellular internalization and biological effects of nanoparticles 48

4.2. Calcium and magnesium ions enhance the CPP-mediated transfection of nucleic acids (Paper II) 48
4.2.1. Ca^{2+} and Mg^{2+} enhance the biological effect of PF14/SCO nanoparticles in a concentration-dependent manner 49
4.2.2. Ca^{2+}-supplemented nanoparticles are internalized via receptor-mediated endocytosis and efficiently escape from endosomes .. 50
4.2.3. Ca^{2+} supplementation works with different CPPs and cell lines 51
4.3. Optimizing PF14-mediated delivery of mRNA into cell lines, primary cells, and *in viv*o (Paper III) 52
4.3.1. Ca^{2+} ions enhance PF14-mediated delivery of mRNA into cell lines 53
4.3.2. PS80 enhances PF14-mediated delivery of mRNA into primary human keratinocytes 54
4.3.3. PF14/mRNA nanoparticles are internalized by cells via macropinocytosis and clathrin-mediated endocytosis 55
4.3.4. PF14 delivers mRNA in vivo in a mouse model of ICD upon local administration 56
5. CONCLUSIONS 58
SUMMARY IN ESTONIAN 60
REFERENCES 62
ACKNOWLEDGEMENTS 83
PUBLICATIONS 85
CURRICULUM VITAE 167
ELULOOKIRJELDUS 168

LIST OF ORIGINAL PUBLICATIONS

The thesis is based on the four original papers listed below:

I. Lorents A†, **Maloverjan M†**, Padari K, Pooga M. Internalisation and Biological Activity of Nucleic Acids Delivering Cell-Penetrating Peptide Nanoparticles Is Controlled by the Biomolecular Corona. Pharmaceuticals. 2021; 14(7):667.

II. **Maloverjan M**, Padari K, Abroi A, Rebane A, Pooga M. Divalent Metal Ions Boost Effect of Nucleic Acids Delivered by Cell-Penetrating Peptides. Cells. 2022; 11(4):756.

III. Periyasamy K†, **Maloverjan M†**, Biswas A, Remm A, Pook M, Rebane A, Pooga M. PepFect14 mediates the delivery of mRNA into human primary keratinocytes and in vivo. Front Pharmacol. 2023; 14:1219761.

The articles listed above are reprinted with the permission of the copyright owners.

Author's contribution:

I. I performed cell culture experiments and participated in manuscript writing and editing.

II. I performed all the experiments described in the publication, except electron microscopy, analyzed the data, and wrote the manuscript.

III. I performed experiments with cell lines and participated in manuscript writing and editing.

Other publications:

Biswas A†, **Maloverjan M†**, Padari K, Abroi A, Rätsep M, Wärmländer SKTS, Jarvet J, Gräslund A, Kisand V, Lõhmus R, Pooga M. Choosing an Optimal Solvent Is Crucial for Obtaining Cell-Penetrating Peptide Nanoparticles with Desired Properties and High Activity in Nucleic Acid Delivery. Pharmaceutics. 2023; 15(2):396.

LIST OF ABBREVIATIONS

Apo	apolipoprotein
ASO	antisense oligonucleotide
CPP	cell-penetrating peptide
DLS	dynamic light scattering
EDTA	ethylenediaminetetraacetic acid
EIPA	5-(N-ethyl-N-isopropyl) amiloride
FDA	U.S. Food and Drug Administration
ICD	irritant contact dermatitis
IL	interleukin
LF3000	Lipofectamine 3000
miRNA	microRNA
MMAX	Lipofectamine MessengerMAX
mRNA	messenger RNA
NA	nucleic acid
NF	NickFect
NP	nanoparticle
PC	protein corona
PCR	polymerase chain reaction
pDNA	plasmid DNA
PF	PepFect
PFA	paraformaldehyde
PMA	phorbol 12-myristate 13-acetate
Poly C	polycytidylic acid
Poly I	polyinosinic acid
PS80	polysorbate 80
PS-2'-OMe	phosphorothioate-2'-O-methyl
RISC	RNA-induced silencing complex
RNAi	RNA interference
RNAiMAX	Lipofectamine RNAiMAX
SCO	splice-correcting oligonucleotide
siRNA	small interfering RNA
SR	scavenger receptor
SR-A3	class A scavenger receptor 5
SR-A5	class A scavenger receptor 3
SSO	splice-switching oligonucleotide
TEM	transmission electron microscopy
UTR	untranslated region
5moU	5-methoxyuridine

INTRODUCTION

Gene therapy is a strategy aimed at treating or alleviating disease symptoms by manipulating gene expression, typically involving the introduction of exogenous nucleic acid molecules into the patient's cells. Multiple nucleic acid types can be successfully used for therapeutic purposes, enabling the treatment of hereditary, infectious, inflammatory, and other diseases. These therapeutic nucleic acids include plasmid DNA, gene-containing viral vectors, messenger RNA, and shorter nucleic acids such as microRNA, small interfering RNA, and antisense oligonucleotides.

However, the delivery of nucleic acids is challenging, limiting their efficiency *in vivo* and clinical use. The main issues when applying nucleic acids are their large size and highly negative charge. These properties lead to poor serum stability, with fast opsonization and elimination from the bloodstream. Furthermore, if nucleic acids reach their target cells, they cannot effectively penetrate the negatively charged hydrophobic plasma membrane. Finally, if cellular internalization occurs, most nucleic acid molecules get entrapped in acidic endosomes and are eventually degraded by lysosomal enzymes.

To tackle these issues, diverse delivery systems have been developed. They aim to protect nucleic acids from extra- and intracellular nucleases, diminish their opsonization and elimination from the bloodstream, effectively transfer nucleic acid cargoes through biological membranes, and facilitate their endosomal escape. Among these systems, cell-penetrating peptides (CPPs) have attracted significant attention as transfection agents due to the simplicity of their application, high efficacy, and low cytotoxicity.

CPPs, usually consisting of fewer than 30 amino acid residues, can transport a variety of cargoes into cells, including nucleic acids, proteins, antibodies, and small molecules. Typically being positively charged, CPPs readily form non-covalent nanoparticles with nucleic acids. CPPs have been shown to effectively deliver various types of nucleic acids *in vitro* and *in vivo*. However, CPPs are still not widely used in clinics, primarily because of their limited efficiency and poorly understood mechanism of action.

In this thesis, we address these concerns by examining the factors that limit the productive delivery of nucleic acids by CPPs and exploring ways to improve it. As a model peptide, we predominantly use PepFect14, an amphipathic stearylated CPP we have studied for years. First, we study the protein corona – a layer of proteins that forms around nanoparticles upon exposure to a serum-containing environment, such as the bloodstream, which can alter their properties and cause their rapid removal from the organism. We show that the protein corona composition varies depending on the origin of the serum used, thereby affecting nanoparticles' properties and efficiency. Secondly, we investigate the effects of divalent metal ions on the properties and efficiency of CPP/nucleic acid nanoparticles. Specifically, we analyze the effects of calcium and magnesium ions, demonstrating that they enhance the transfection efficiency of CPP/nucleic acid complexes, most

likely by facilitating their endosomal escape. Finally, we investigate the CPP-mediated delivery of messenger RNA into cell lines, primary cells, and *in vivo*, preparing nanoparticles with different compositions to achieve efficient cargo delivery. We demonstrate that while specific formulations exhibit high efficiency in cell culture, these results may not be readily applied to *in vivo* conditions.

In summary, our findings provide novel insights into the challenges associated with developing CPP/nucleic acid nanoparticles for clinical use and open potential avenues for enhancing their efficiency.

1. LITERATURE OVERVIEW

1.1. Nucleic acid therapeutics

Gene therapy aims to treat or alleviate the symptoms of diseases by altering gene expression, which typically involves the introduction of exogenous nucleic acids (NAs) into the organism. Various NA molecules with different structures and modes of action allow for the modulation of gene expression at both DNA and RNA levels.

A deficient or defective gene product can be supplemented or replaced by introducing a normal copy of the same gene, from which a functional protein is synthesized. To achieve this, genetic material can be introduced into cells within **plasmid DNA (pDNA)** [1, 2], which is then transcribed into RNA and translated into a functional protein. Alternatively, the transcription step can be omitted by using **messenger RNA (mRNA)** [3–5] instead, which is translated into the desired protein in the cell cytosol.

To eliminate an unwanted gene product, the expression of the respective gene has to be suppressed at the mRNA or DNA level. One way to achieve this is by using **antisense oligonucleotides (ASOs)** [6, 7]. ASOs are single-stranded DNA or RNA molecules that bind to their target mRNA, recruiting a nuclease RNase H that cleaves the mRNA. Additionally, ASOs can sterically block regulatory elements within their target mRNA, thus modulating its translation [8]. Some ASOs act at the DNA level. Thus, triplex-forming oligonucleotides (TFOs) are designed to form a triple helix with DNA, primarily with its oligopurine-rich tracts, and can modulate replication or transcription of genomic DNA [9, 10] or, if coupled with specific agents, induce its cleavage [11].

An initial product of transcription, pre-mRNA, contains both protein-coding exons and non-coding introns. Before translation, introns are removed in a complex process known as splicing [12]. Multiple elements within the pre-mRNA sequence are essential for splicing to occur correctly, such as 3' and 5' splice sites, splicing silencers, and enhancers. Mutations in these regions, as well as those creating aberrant splice sites, can cause splicing defects, resulting in the synthesis of non-functional or otherwise faulty proteins or causing degradation of mRNA due to the formation of premature stop codons [13, 14]. **Splice-switching oligonucleotides (SSOs)** bind splice-modulating regions in pre-mRNA, facilitating the synthesis of a functional protein form.

An alternative to using ASOs is harnessing **small interfering RNA (siRNA)** [15–17] and **microRNA (miRNA)** [18]. These double-stranded RNA molecules regulate gene expression through RNA interference (RNAi), which involves the controlled degradation or translational silencing of their complementary RNA molecules. Synthetic siRNA and miRNA molecules can be used to change gene expression in a desired way. In addition, oligonucleotides called **anti-miR** or **antagomiR** are designed to silence specific endogenous miRNA molecules, thus upregulating the expression of their target genes [19].

Several systems allow **genome editing** – modification of genomic DNA by introducing insertions, deletions, or replacements. These systems include zinc finger nucleases (ZFNs), transcription activator-like effector nucleases (TALENs),

and clustered regularly interspaced short palindromic repeat (CRISPR)-Cas nucleases. These engineered or bacterial nucleases usually induce double-stranded breaks in the target DNA, followed by DNA reparation by cellular systems, leading to gene addition, replacement, or inactivation [20, 21]. In addition, precise changes in the genome can be introduced with the help of base editors [22–24] or by co-delivering the nuclease and a donor DNA sequence, which will direct the change [25].

1.1.1. Structure and function of therapeutic nucleic acids

The current thesis primarily used SSOs, pDNA, mRNA, and siRNA. These four NA types, along with miRNA, are described below in more detail.

pDNA

pDNA is a double-stranded circular DNA molecule, usually several thousand base pairs in length. Plasmids are found mostly in prokaryotic organisms as extrachromosomal DNA molecules, often carrying bacterial virulence factors [26]. pDNA used in research and clinics for gene delivery is designed to contain genes of interest, as well as the elements necessary for their transcription in recipient cells, such as eukaryotic promoters and terminators. pDNA has to reach the cell nucleus to be transcribed by cellular RNA polymerase. Then, the mRNA transcript is exported into the cytosol and translated into the protein of interest. For research purposes, pDNA is usually propagated in bacteria, thus also containing prokaryotic origin of replication and a selection marker (usually an antibiotic resistance gene). In addition, such a pDNA can contain unmethylated CpG islands, which are characteristic of prokaryotes but can trigger immune responses in eukaryotes [27]. These prokaryotic elements can pose safety concerns when applying pDNA *in vivo* [28–30]. Minicircle plasmids are derivatives of conventional plasmids that overcome some of the challenges associated with using the latter. In contrast to conventional pDNA, minicircle plasmids lack bacterial genetic elements, thus having better safety profiles and providing higher levels of transgene expression [31].

mRNA

mRNA is an intermediary molecule between the DNA in the cell nucleus and the respective protein synthesized in the cytoplasm. mRNA is a single-stranded NA molecule with a nucleotide sequence corresponding to the coding sequence of a gene, including start and stop codons that determine the beginning and end of the resulting protein's amino acid sequence. mRNA also contains other elements necessary for translation, such as 5' and 3' untranslated regions (UTR), 5' cap structure, and 3' polyA tail.

mRNA can encode the entire spectrum of human proteins, which has led to the successful use of synthetic mRNA in research, medicine, and biotechnology. In contrast to DNA-based therapeutics, mRNA does not require delivery into the cell nucleus, as translation is the only step needed to get the desired product. This inherent characteristic makes mRNA an appealing tool for protein production.

Synthetic mRNA lacks modifications characteristic of mRNA transcripts naturally present in mammalian cells. Therefore, it is recognized by the organism as a foreign molecule, activating innate immune responses via toll-like receptors (TLR) [32]. In their Nobel prize-winning study, Katalin Kariko and Drew Weissmann showed that certain nucleoside modifications, such as m5C, m6A, m5U, s2U, and pseudouridine (ψ), significantly reduce the immunogenicity of synthetic mRNA [32]. The replacement of uridines within mRNA with ψ does not only reduce its immunogenicity but also improves its stability and translational efficiency [33]. In addition to ψ, uridines can be replaced with N1-methylpseudouridine (me(1)ψ) and 5-methoxyuridine (5moU) [34, 35]. Among these, 5moU provides the highest stability to the mRNA [36]. Another essential development is the mRNA cap, a structure found at the 5' end of eukaryotic mRNA [37]. It consists of a 7-methylguanosine (m7G) residue connected to the mRNA through a triphosphate bridge and plays a crucial role in translation initiation and mRNA stability. Eukaryotic mRNA can have three cap structures – cap 0, cap 1, or cap 2. These contain different numbers of 2'O-methyl groups, determining their immunogenicity through interactions with specific proteins [38, 39]. Synthetic cap analogs, such as Anti-Reverse Cap Analog (ARCA) [40] and CleanCap [41], mimic the natural cap structures. The ARCA closely mimics the cap 0 structure and possesses a sugar modification that prevents it from being incorporated into the mRNA in the incorrect orientation. The CleanCap method introduces the naturally occurring cap 1 structure into the mRNA [42].

SSOs

Splicing defects are associated with a variety of pathologies, such as neuromuscular disorders [43], hematological disorders [44], and cancers [45]. Impaired splicing leads to erroneous joining of exons and introns, resulting in the synthesis of malfunctioning protein products or the degradation of mRNA due to the formation of premature stop codons. To modify or correct aberrant splicing, SSOs have been developed. These are single-stranded RNA or DNA oligonucleotides that are typically 15 to 25 nucleotides in length. SSOs can induce splicing switching through several different mechanisms.

One example is **exon skipping**, where a faulty or mutated exon within a pre-mRNA (with mutations often causing the formation of premature stop codons and nonsense-mediated decay of mRNA) is deliberately excluded during the splicing process, leading to the production of a shorter mRNA encoding a partly functional protein [46, 47]. Another option is **splicing correction**, which involves blocking aberrant splice sites used in the splicing process instead of the normal ones [48, 49]. This approach results in the exclusion of introns or their portions erroneously included in mRNA, thus restoring normal splicing, and the SSOs acting in this way are known as **splice-correcting oligonucleotides (SCOs)**. Additionally, **exon recycling** can be used, i.e., the inclusion of an exon that is otherwise spliced out from pre-mRNA due to mutations [50, 51]. Finally, SSOs can act by **removing splicing factors** from tandem repeats. In this case, the pathology arises from the expansion of DNA tandem repeats, which causes the sequestration of splicing factors within these regions, impairing their normal function and leading to the

misregulation of alternative splicing. Applying an SSO complementary to these DNA regions, thus preventing the excessive binding of splicing factors, restores normal splicing [52].

SSOs do not require the recruitment of any cellular proteins, which opens possibilities for introducing various modifications into both the sugar and phosphate parts of the oligonucleotide backbone. Instead of a naturally occurring phosphodiester linkage, many SSOs contain a phosphorothioate (PS) backbone, which increases the stability of an oligonucleotide by increasing its resistance to nucleases and prolongs its half-life in the bloodstream [53]. PS modification can also affect plasma protein binding by an oligonucleotide (discussed in more detail in section 1.4.1), yielding better pharmacokinetic properties [54]. In addition, various modifications of ribose can be introduced. These are aimed at increasing stability, nuclease resistance, and target binding affinity of oligonucleotides, with examples including locked nucleic acid (LNA), unlocked nucleic acid (UNA), 2'-fluoro (2'-F), 2'-O-methyl (2'-OMe), and 2'-methoxyethyl (2'-MOE) substitutions [55–57]. Although widely used in the design of SSOs, modifications involving the 2'-O position of the ribose interfere with RNase H activity, thus having limited use for ASOs [56, 58]. Some modifications involve both the sugar and phosphate part of the NA backbone, such as peptide nucleic acid (PNA), morpholino, and tricyclo-DNA (tc-DNA) [59–61]. PS-2'-OMe modification, present in SCOs used in our research, has been shown to increase the translocation of oligonucleotides [62] into the cell nucleus, the site of action of SSOs.

siRNA and miRNA

SiRNA and miRNA are double-stranded small RNA molecules, usually 21 to 23 base pairs in length. These naturally occurring small RNA species mediate gene silencing through RNAi [63]. Endogenously, both siRNAs and miRNAs originate from long double-stranded RNA precursors. miRNAs are essential regulators of gene expression and originate from specific genes or introns of protein-coding genes. On the other hand, while also taking part in the control of gene expression, endogenous siRNAs are mostly believed to serve as an organism's defense mechanism against viruses and transposons [64, 65].

Long double-stranded precursors of small RNAs are processed by a nuclease Dicer into short double-stranded fragments with two-nucleotide overhangs at 3' ends. These fragments contain a guide (or antisense) strand complementary to the target sequence and a passenger (or sense) strand. They associate with the RNA-induced silencing complex (RISC), forming siRISC or miRISC, respectively, followed by the removal of the passenger strand. Then, the guide strand binds to the target mRNA. miRNA mainly interacts with 3'UTR of the target mRNA based on partial complementarity, inducing its translational repression or, more rarely, degradation [66]. Due to imperfect pairing, a single miRNA can have multiple targets, thereby regulating the expression of many genes. On the other hand, siRNA strongly pairs with its target RNA based on complete sequence complementarity, being specific to a single mRNA molecule and inducing its degradation. Interestingly, some siRNAs can also act in a miRNA-like mechanism, i.e., through imperfect complementarity [67, 68].

Although both exogenous siRNA and miRNA can be used to silence genes of interest, siRNA is more commonly applied. The high specificity and gene-silencing potency of siRNA have made it a powerful and widely used tool. In research and clinical settings, synthetic siRNA is introduced into cells to selectively silence genes of interest [69]. However, being highly susceptible to nuclease-mediated degradation, unmodified RNA has a very short half-life in the organism. Various nucleotide modifications can be introduced into siRNA sequences to enhance their stability, specificity, and delivery efficiency [70]. Similarly to the ones listed for SSOs, these include ribose modification, such as 2'-OMe, 2'-F, 2'-MOE, LNA, and UNA, as well as the phosphate backbone modifications, such as PS, phosphorodithioate, and triazole [71, 72]. However, to ensure the compatibility of synthetic siRNAs with the RISC complex, the modifications need to be introduced with caution, considering their types and positions. For example, modifications in the passenger strand are less likely to affect the function of siRNA than the ones introduced into the guide strand [70]. 3' overhangs of synthetic siRNAs, including the ones used in the research described in this thesis, are usually designed as deoxyribonucleotides to increase the stability of the molecule.

1.1.2. Nucleic acid-based therapies

Nucleic acid therapeutics approved for clinical use

There are currently over 20 NA-based therapeutics approved for clinical use by the FDA. Among them are six siRNAs, six ASOs, five SSOs, and two mRNAs [73].

Among the NA-based therapeutics currently approved by the FDA for clinical use, oligonucleotides are the most prevalent. Notably, the first NA drug, fomivirsen, is an RNase H-recruiting ASO approved for treating cytomegalovirus-induced retinitis in 1998 [74]. Currently, there are five SSOs approved for clinical use, out of which four, i.e., eteplirsen [75], golodirsen [76], viltolarsen [77, 78], and casimersen [79], are used to treat Duchenne muscular dystrophy (DMD) and one, nusinersen [80], for spinal muscular atrophy (SMA) [81]. There are more SSOs that, although not yet in clinics, are highly promising tools for treating diseases, such as X-linked agammaglobulinemia [48] and beta thalassemia [82]. All approved ASOs are chemically modified and delivered as naked oligonucleotides, i.e., without the aid of a delivery vehicle.

Recently, there has been a significant focus on mRNA therapy, driven by the success of two mRNA-based vaccines approved for clinical use that have played a crucial role in managing the coronavirus disease 2019 (COVID-19) pandemic, effectively limiting its spread and mitigating its severity [83, 84]. Among the NAs undergoing preclinical and clinical trials, mRNA-based candidate therapeutics are at the forefront [85, 86]. Synthetic mRNA can be a valuable tool for the treatment of a wide variety of conditions, with examples including infectious diseases, such as COVID-19 [87, 88], as well as cancer [89], inherited metabolic disorders [90], Alzheimer's disease [5], and heart injury [91].

The approved siRNA-based therapeutics include patisiran and vuttrisiran for hereditary transthyretin-mediated amyloidosis, givosiran for acute hepatic

porphyria, lumasiran and nedosiran for primary hyperoxaluria, and inclisiran for hypercholesterolemia [63, 73, 81, 92]. All of them, except patisiran, are conjugated to N-acetylgalactosamine (GalNAc), which binds to asialoglycoprotein receptors highly expressed in hepatocytes, facilitating the delivery of the siRNAs into the liver [93]. Patisiran, in contrast, is delivered by lipid nanoparticles [94].

Nucleic acid-based approaches for chronic inflammatory diseases

One of the possible applications of the nanoparticles we aim to develop is to treat chronic inflammatory diseases. Chronic inflammatory diseases are, for example, allergic diseases, such as atopic dermatitis and asthma, and are highly prevalent in both pediatric and adult populations [95, 96]. The two aforementioned diseases are often characterized by activation of type II immune responses involving T helper(h)2 cells, eosinophils, and increased blood immunoglobulin E (IgE) levels. In addition, during the chronic phase of tissue inflammation, pro-inflammatory cytokines, such as interleukin (IL)-1 [97], tumor necrosis factor α (TNF-α) [98], IL-6 [99], and interferon-γ (IFN-γ) [100], contribute to persistent activation of epithelial cells and cause tissue damage. Current strategies to manage chronic inflammatory diseases involve an array of treatments. These include topical or inhaled therapies, such as locally applied corticosteroids [101, 102] and topical calcineurin inhibitors for atopic dermatitis [103], as well as systemic corticosteroids [104] and immunomodulators (biologics) [105]. However, these treatments often require persistent application, may induce adverse effects, and their efficacy can be limited or diminished over time [95, 96]. Consequently, there is an ongoing demand for safer and more effective alternative approaches.

Immunomodulators target key molecules involved in immune responses, such as IgE, pro-inflammatory cytokines (IL-4, IL-13, thymic stromal lymphopoietin (TSLP), etc.), and their receptors, which play pivotal roles in the pathogenesis of chronic inflammatory diseases [106]. In contrast to suppressing pro-inflammatory proteins, an alternative approach would be to suppress their expression by targeting the precursor mRNA. Additionally, anti-inflammatory NAs or proteins could be supplemented by introducing them into cells or inducing their expression, respectively. This strategy would involve localized administration of anti-inflammatory NAs at the inflammation site. For instance, the anti-inflammatory miRNA miR-146a has been extensively studied and successfully delivered into cells, reducing inflammation markers [18, 107, 108]. This approach employs a synthetic miRNA with a sequence identical to the one of the endogenous miRNA already present in cells [18], which makes it potentially safer than introducing exogenous molecules foreign to an organism. Alternatively, the application of mRNA encoding anti-inflammatory cytokines or receptor antagonists, such as IL-1RA [109, 110], IL-10 [111, 112], IL-11 [113], IFN-λ [114], and transforming growth factor-β (TGF-β) [112], could also be beneficial. The recipient's cells would translate the mRNA into functional proteins, which could then function as therapeutic agents. Notably, a vector delivering such NA therapeutics should be non-cytotoxic and non-immunogenic to avoid eliciting any additional inflammation.

1.2. Delivery methods for therapeutic nucleic acids

Regardless of the type, the critical challenge while using NAs lies in their efficient delivery into the target cells and tissues. Being large and negatively charged molecules, NAs cannot penetrate hydrophobic cell membranes effectively. Furthermore, NAs are rapidly degraded by extra- and intracellular nucleases and are subjected to renal clearance. Additionally, NAs, especially RNA molecules, are chemically unstable, being prone to hydrolysis. Another concern associated with using NAs in live systems is their immunogenicity, which is especially prominent in the case of long RNA and DNA molecules [115–117].

Although chemically modified oligonucleotides have improved nuclease resistance, their delivery efficiency is still far from perfect. For not fully modified NAs, inefficient cellular delivery remains an even more serious issue. To address this, various delivery vehicles have been developed that aim to increase the stability and efficiency of NA, facilitate its translocation into cells, and avoid endosomal entrapment and subsequent degradation by lysosomal enzymes. The main types of NAs used in gene therapy and research, as well as the main systems used for their delivery, are highlighted in **Figure 1**.

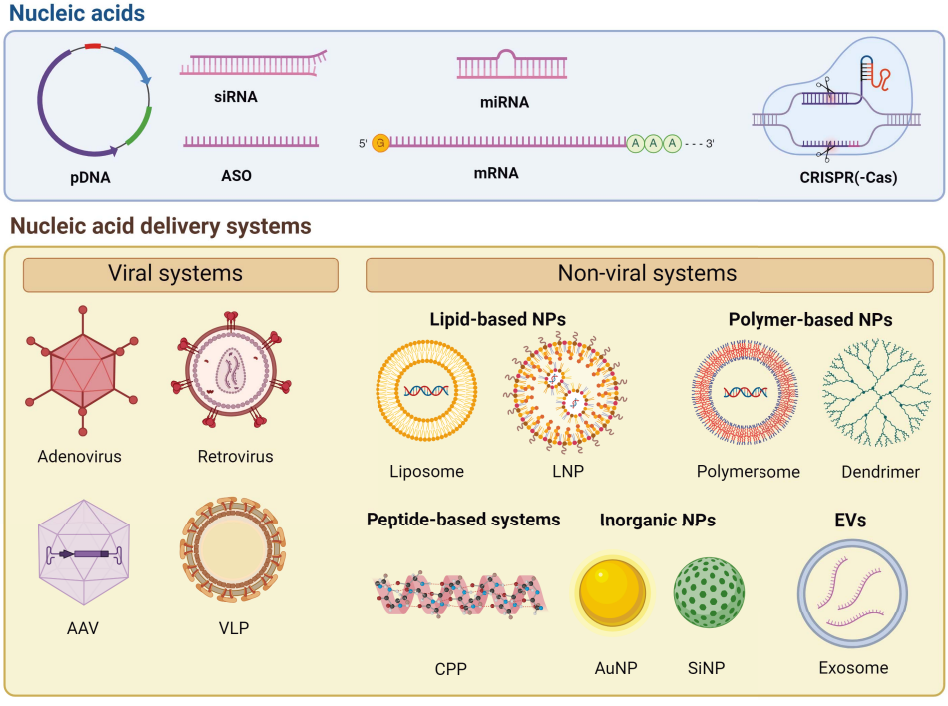

Figure 1. The main types of NAs used in gene therapy and research and the main types of the respective delivery systems are given with some examples. NP – nanoparticle, AAV – adeno-associated virus, LNP – lipid nanoparticle, VLP – virus-like particle, CPP – cell-penetrating peptide, AuNP – gold nanoparticle, SiNP – silica nanoparticle, EV – extracellular vesicle. CRISPR-Cas genome editors can be delivered to cells as DNA, RNA, or ribonucleoproteins [118].

1.2.1. An overview of main nucleic acid delivery systems

The systems utilized for NA delivery can be largely divided into viral and non-viral approaches. Viral approaches harness an inherent ability of **retroviruses** [119], **adenoviruses** [120], and **adeno-associated viruses** [121] to infect cells, delivering their genetic material with the included genes of interest, and can help to achieve short- or long-term expression, depending on the specific condition [122]. Although viral approaches offer highly efficient NA delivery and several such therapeutics have been approved for clinical use [123–126], these drugs are costly, can be eliminated from the organism due to the production of antibodies against the vector, and can exhibit severe side effects [127, 128].

Virus-like particles (VLPs) are virus-derived multiprotein structures that can self-assemble, mimicking the size and structure of native viruses, but lack viral genetic material. VLPs are highly immunogenic and can efficiently elicit immune responses during vaccination and cancer vaccination. Additionally, VLPs can transport various payloads into cells, including NAs [129, 130].

In addition to the abovementioned virus-based approaches, numerous non-viral methods have been developed to deliver therapeutic molecules, including NAs. Physical methods involve the application of physical forces to deliver materials into cells and are not further discussed in this thesis. Chemical methods are based on lipids, peptides, polymers, inorganic compounds, and extracellular vesicles and are described below in more detail.

Lipid-based nanoparticles

Liposomes are small spherical vesicles whose membrane is composed of a lipid bilayer. They can encapsulate hydrophilic compounds within their inner aqueous core, while hydrophobic molecules can reside in the membrane. Liposomes can have varying lipid compositions, including natural or synthetic lipids or phospholipids. Liposomes can be modified with peptides, dendrimers, polymers, etc., to improve their properties and transfection efficiency [131]. On the other hand, for NA delivery, cationic lipids are often used, forming lipid/NA complexes called **lipoplexes**. Unlike liposomes, lipoplexes do not exhibit a defined structure; instead, the lipids and NAs are intermixed due to electrostatic interactions. Although efficient NA carriers, lipoplexes are rapidly eliminated from the bloodstream and can activate the immune system due to their positive charge [132].

Lipid nanoparticles (LNPs) are more advanced vehicles that do not form a lipid bilayer, like classical liposomes, and do not form complexes with NAs based on electrostatic interactions, like lipoplexes. LNPs are composed of multiple components at specific proportions to ensure optimal encapsulation and delivery of a payload. These components usually include ionizable lipids, polyethylene glycol (PEG)ylated lipids, phospholipids, and cholesterol [132]. The use of ionizable lipids instead of cationic ones helps to overcome the drawbacks associated with the use of lipoplexes, as these lipids are uncharged at a neutral pH in the blood but become positively charged at lower pH values in endosomal compartments [133]. Notably, LNPs are used for cellular delivery of the two FDA-approved mRNA-

based vaccines, as well as for several mRNA-based cancer vaccines under development [134, 135] and siRNA-based therapeutics [136]. LNPs are usually slightly cytotoxic and immunogenic, therefore promoting immune system stimulation, which is advantageous for vaccination [137] and cancer immunotherapy [138].

Polymer-based nanoparticles

Polymer-based NA delivery systems usually consist of cationic polymers that interact with negatively charged NAs. Similarly to cationic lipids, they form with NAs stable complexes called **polyplexes** [139, 140]. For example, polyethyleneimine (PEI) contains multiple ionizable amine groups that promote complexation with NA, as well as subsequent endosomal escape of the complexes. Various compounds can be delivered with **polymeric nanoparticles (PNPs)**, including proteins, small molecules, and NAs. PNPs are highly versatile in composition and structure, including subtypes like polymersomes, polymer micelles, nanospheres, and dendrimers [141]. Among them, **dendrimers** are three-dimensional hyperbranched molecules, such as poly(propylene imine) (PPI), polyamidoamine (PAMAM), and poly-L-lysine (PLL) [142]. Dendrimers can encapsulate various cargoes, such as NAs and small molecules. Alternatively, cargo molecules can be conjugated or non-covalently attached to surface functional groups of dendrimers [142]. Despite their advantages, PNPs carry some risks, such as particle aggregation, toxicity, and hemolysis [141]. Encouragingly, some modifications of polymers, such as PEGylation, have been shown to mitigate their toxicity [142].

Peptide-based nanoparticles

Some natural peptides and proteins, such as those contained in venoms [143, 144], have an inherent ability to cross cell membranes. In addition to the natural prototypes, many more synthetic **cell-penetrating peptides** have been developed and harnessed to deliver various types of cargoes into cells. These are reviewed in more detail in subsection 1.2.2.

Inorganic nanoparticles

Inorganic materials commonly used for nanoparticle preparation are gold, iron oxide, and silica. **Gold nanoparticles (AuNPs)** are chemically inert and nontoxic and can be functionalized by attaching different moieties to their surface. Cargo molecules can be directly conjugated to gold nanoparticles via cleavable linkers, with the subsequent glutathione-mediated or photo-regulated release. Alternatively, AuNPs can be covered with ligands forming a monolayer, which then embeds non-covalently attached cargo [145]. Thus, AuNP functionalized with cationic ligands can non-covalently bind negatively charged NAs, delivering them into cells [146, 147]. **Silica nanoparticles (SiNPs)** are composed of silica oxide (SiO_2) and have controllable size, large surface area, and high biocompatibility. SiNPs can be either non-porous or mesoporous and can be used to deliver various therapeutic molecules, including NAs [19, 148, 149]. The surface of SiNPs can

be functionalized with various moieties, including lipids [150], polymers [151], gelatin [152], antibodies [153], and sugars [154], resulting in different functionalities and the ability to bind a wide variety of cargo molecules. Besides being highly biocompatible and non-toxic, like the abovementioned inorganic nanoparticles, **iron oxide nanoparticles (IONPs)** possess magnetic and semiconductor properties. These properties make them an attractive tool in various biomedical fields, such as developing antimicrobial agents, magnetic resonance imaging, cancer immunotherapy, and targeted drug delivery [155]. IONPs can be made of magnetite, hematite, maghemite, or mixed ferrites. Similarly to AuNPs and SiNPs, IONPs can be coated with various organic and inorganic molecules to possess different activities. IONPs have been harnessed to deliver various therapeutic NA molecules into tumors, including pDNA [156], miRNA [157], siRNA [158], and mRNA [159].

Extracellular vesicles

Extracellular vesicles (EVs) are membranous structures secreted into extracellular space by multiple cell types. It is mainly believed that they are used by cells as a means of communication – to exchange proteins, lipids, and NAs. The main types of EVs are **exosomes**, which originate from the endosomal system, and **microvesicles**, which originate from the plasma membrane [160, 161]. An NA cargo can be loaded into EVs either exogenously, after their purification and isolation, or endogenously, letting a donor cell sort the cargo into EVs before their isolation. EVs are naturally internalized by cells, which makes them an attractive tool for drug delivery. EVs have been used to deliver different types of NAs, such as siRNA [162], miRNA [163], mRNA [164], and ASO [165]. However, the difficulties in producing EVs are the main factor limiting their application. Normally, cells secrete EVs at low levels, resulting in low yields. In addition, the isolation process is laborious, expensive, and poorly standardized, leading to inconsistent doses of EVs and their contained molecules in the resulting formulations [166].

1.2.2. Cell-penetrating peptides as delivery vectors

Cell-penetrating peptides (CPPs) are short peptides that can traverse cell membranes, carrying a variety of payloads into cells. This has made them an attractive delivery system for therapeutic molecules, encouraging their extensive research and the design of numerous CPPs with different sequences, structures, and physicochemical properties. To date, although multiple CPPs designed for NA delivery have reached clinical trials [167], none have been clinically approved. Yet a CPP-based agent is in clinical use for protein delivery, illustrating the potential of these delivery vectors [168].

Properties and classification of cell-penetrating peptides

CPPs consist of 5 to 30 amino acid residues that can be easily modified to possess different activities [169, 170]. CPPs can be covalently [171, 172] or non-covalently attached to their cargoes and have been shown to mediate cellular delivery of different types of molecules, including NAs [173–175] peptides and proteins [176, 177], small-molecule drugs [178, 179], and antibodies [180]. There are different ways to classify CPPs. By their structure, CPPs are divided into cyclic and linear. Cyclic CPPs are a newer CPP class and can have several advantages, such as improved stability [181]. By their origin, CPPs can be classified into protein-derived, synthetic, and chimeric, with the latter being formed by combining two natural sequences. By their physicochemical properties, CPPs can be divided into three classes: cationic, hydrophobic, and amphipathic.

- **Cationic CPPs**: These peptides contain multiple positively charged residues essential for their cellular uptake. Positive charges are provided by arginine, lysine, and/or a non-natural amino acid ornithine. Most typical members of this class are arginine-rich peptides, such as the transactivator of HIV transcription (Tat) peptide [182, 183] and oligoarginines (R_n) [184]. Positively charged amino acid residues enable interaction with negatively charged plasma membrane glycoproteins and glycolipids, facilitating membrane translocation of such peptides. Most CPPs, regardless of the class, possess a positive charge.
- **Hydrophobic CPPs**: A limited number of CPPs are classified as hydrophobic. Comprising mostly apolar amino acid residues and having a low net charge, they include such members as C105Y [185], VPTLK [186], and KLPVM [187], as well as pepducins and stapled peptides. Pepducins are lipidated peptides derived from intracellular loops of transmembrane proteins, namely G-protein coupled receptors (GPCRs) [188]. Stapled peptides have side chains of two amino acids linked together with a hydrocarbon bridge, which forces the peptide to take an alpha-helical conformation and exposes the non-polar side chains to the surrounding environment, increasing hydrophobicity of the peptide [189].
- **Amphipathic CPPs**: These peptides feature a combination of hydrophobic and hydrophilic motifs and often form secondary structures [190], which are important for cell membrane permeation. Amphipathic CPPs can be classified into primary and secondary. In primary amphipathic CPPs, hydrophobic and hydrophilic domains are contained in their primary structure. In secondary amphipathic CPPs, the hydrophobic and hydrophilic regions form when a peptide acquires its secondary structure, such as alpha-helix, and as a result, positively charge residues gather on its one side and hydrophobic residues on the other. Examples of amphipathic CPPs include transportan (TP) [191] and its truncated version TP10 [192], penetratin [193], CADY [194], PepFect [195–197], and NickFect [107, 198] peptides. The cationic part of these peptides enables the formation of non-covalent complexes with NAs, while the non-polar residues promote penetration through the lipid bilayer.

Some of the most widely used CPPs are listed in **Table 1**.

Table 1. Some commonly used CPPs, their sequences, classes, and references.

Name	Sequence	Class	Ref.
TAT	GRKKRRQRRRPQ-a	Cationic	[183, 199]
Penetratin	RQIKIWFQNRRMKWKK-a	Amphipathic	[193]
Transportan	GWTLNSAGYLLGKINLKALAALAKKIL-a	Amphipathic	[191]
TP10	AGYLLGKINLKALAALAKKIL-a	Amphipathic	[192]
R9	RRRRRRRRR-a	Cationic	[200]
PepFect6	Stearyl-AGYLLGK^{f}INLKALAALAKKIL-a	Amphipathic	[201]
PepFect14	Stearyl-AGYLLGKLLOOLAAAALOOLL-a	Amphipathic	[196]
pVEC	LLIILRRRIRKQAHAHSK-a	Amphipathic	[202]
MAP	KLALKLALKALKAALKLA-a	Amphipathic	[203]
Melittin	GIGAVLKVLTTGLPALISWIKRKRQQ-a	Amphipathic	[144]
Pep-1	KETWWETWWTEWSQPKKKRKV-a	Amphipathic	[204]
CADY	GLWRALWRLLRSLWRLLWRA-cya	Amphipathic	[205]
MPG	GALFLGFLGAAGSTMGAWSQPKKKRKV-cya	Amphipathic	[206]

f – four molecules of a chloroquine analog (trifluoromethylquinoline) are coupled at this position via lysine tree; a – C-terminal amide: cya – C-terminal cysteamide; O – ornithine

PepFect14

In the studies included in the current thesis, we predominantly focused on PepFect14 (PF14), an amphipathic CPP from the PepFect series that was designed by Ezzat and colleagues in 2011 based on stearylated TP10 [196, 207]. When designing PF14, in the structure of stearyl-TP10, lysines and isoleucines were replaced with ornithines and leucines, with ornithine being a non-proteinogenic amino acid, due to which PF14 is less susceptible to serum proteases than its parent peptide [196]. The stearyl moiety coupled to the N-terminus of PF14 increases transfection efficiency, promoting membrane penetration [195, 208, 209]. With a high positive charge of +5, PF14 readily forms non-covalent complexes with NAs, enabling stable nanoparticle preparation upon simple mixing. In solution, PF14 takes an alpha-helical structure and, due to its stearyl moiety, self-assembles into uniform spherical nanoparticles, most likely micelles or liposomes [210]. PF14 is an efficient carrier with low cytotoxicity and has been shown to mediate cellular delivery of multiple NA types, including pDNA [174, 211], siRNA [212, 213], miRNA [107, 214], ASOs [196, 215, 216], and mRNA [217]. The helical wheel projection of PF14 and the general scheme of its complexation with NAs are shown in **Figure 2**.

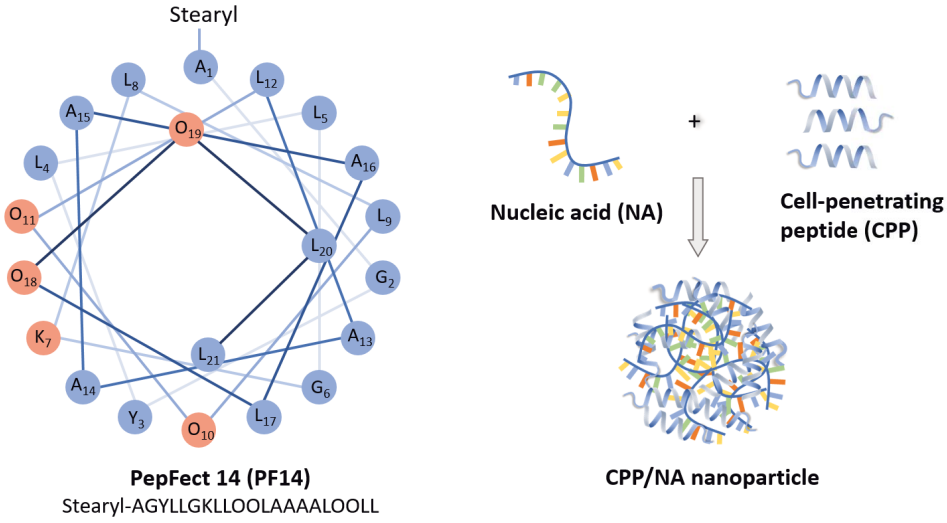

Figure 2. Structure of PF14 and nanoparticle formation between CPP and NA. A: Helical wheel projection and sequence of PF14. The stearyl moiety is coupled to the N-terminus of the peptide, and the C-terminus is amidated. Amino acids on a red background are positively charged, and on a blue background are apolar. B: General scheme of complexation of NA by a CPP.

CPP/NA complexes

CPPs have been extensively used to deliver different NAs, including siRNA, miRNA, SCO, and pDNA, both via covalent and non-covalent coupling. The covalent method denotes the chemical conjugation of a CPP with its cargo, most often via disulfide bonding. This approach can be favorable for delivering non-charged NAs, such as PNA [218, 219], but can also be used for charged NAs, such as siRNA [218, 219]. Additionally, it often allows for forming more defined and easier-to-characterize active agents than the non-covalent formulation approach. However, such an approach has a risk of altering the biological activity of cargo and requires more time and cost than association by simple mixing. Thus, for negatively charged NAs, non-covalent complexing is often preferred, especially in the case of larger NA molecules such as mRNA and pDNA. Based on electrostatic and hydrophobic interactions, CPPs readily form stable complexes with negatively charged NAs, making nanoparticle preparation simple and time-efficient. Furthermore, it enables more efficient cargo release in cells and maintains full biological activities of both complex components. Complexation of a negatively charged NA and a positively charged CPP can result in nanoparticles possessing a positive, neutral, or negative charge, primarily depending on the ratio of the components [220]. Interestingly, it has been shown that nanoparticles with strong positive or negative charges are eliminated from circulation faster than neutral ones [221]. On the other hand, such strongly charged particles have higher colloidal stability, i.e., a reduced risk of aggregation, due to stronger repulsion forces between the particles possessing the same charge [222].

The exact architecture of non-covalent nanoparticles depends on the specific NA and CPP. Firstly, the size of NA is important. It has been shown that the same CPP forms differently-sized particles with pDNA, siRNA, and SCO, with CPP/pDNA complexes being the largest and CPP/SCO complexes the smallest [223]. In addition to electrostatic interactions, hydrophobic interactions can also play a significant role in the formation of CPP/NA nanoparticles. Thus, the hydrophobicity of an NA (e.g., highly increased hydrophobicity of PS 2'OMe oligonucleotides) and a CPP (e.g., N-terminal lipidation) can affect nanoparticle formation between the two. Finally, different types of NAs have different spatial rigidity, with some of them, such as pDNA, possessing stable secondary and tertiary structures and others, such as SCO and siRNA, being more labile. Several CPP/NA nanoparticle formation models have been proposed (**Figure 3**).

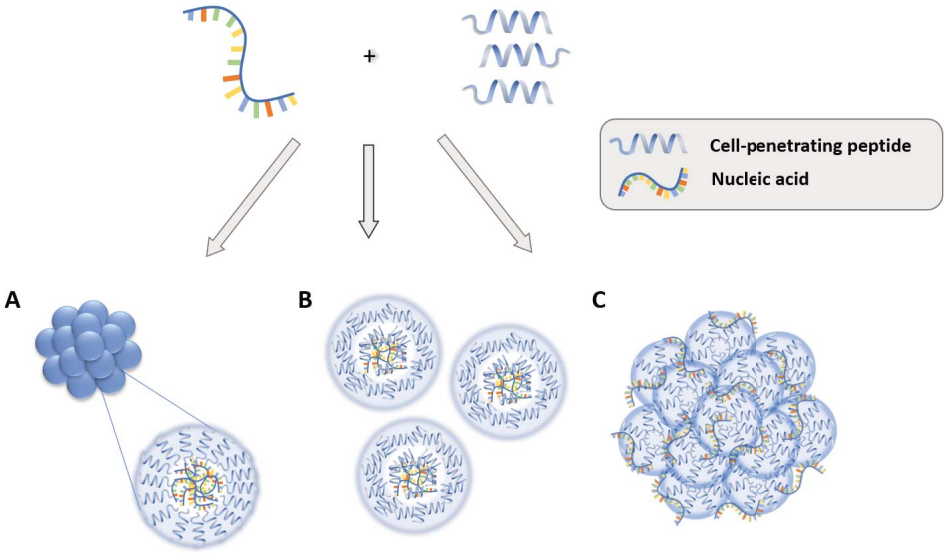

Figure 3. Proposed models of nanoparticle formation between CPP and NA. A: A model of nanoparticle formation where NA becomes encapsulated by a CPP, and then larger conglomerates form. B: A model of complexation of siRNA and a pH-sensitive CPP proposed by Pärnaste *et al.* In this model, siRNA complexed by an optimal number of CPP molecules forms a core, and excess CPP forms a shell around it. C: A model of PF14/SCO nanoparticle formation proposed by Lehto *et al.* In their model, a CPP forms small micelles, which then assemble into larger agglomerates, and NA binds to these agglomerates.

For example, Bosguerin *et al.* pictured self-assembling nanoparticles consisting of different NAs and simple, PEGylated or lipidated CPPs as multi-grained complexes where each grain consists of an NA core and a CPP shell surrounding it [224] (**Figure 3A**). Pärnaste *et al.* proposed a model for the formation of siRNA nanoparticles with pH-sensitive CPPs. In this model, the core of a nanoparticle consists of CPP molecules bound to siRNA at an optimal ratio, surrounded by a shell composed of self-assemblies formed by excess CPP molecules [225]

(**Figure 3B**). The authors stated that once in acidic endosomes, the shell of such nanoparticles would start collapsing due to the CPP acquiring an increasingly positive charge and growing repulsion between the molecules. Finally, Lehto *et al.* proposed a model of the formation of nanoparticles between oligonucleotides and acylated CPPs [226] (**Figure 3C**). In their model, CPP complexes/micelles form first and then assemble into larger conglomerates. NA molecules bind to these conglomerates, so both the CPP and the NA are exposed to the surrounding environment.

It is worth noting that the charge of PF14 is not significantly influenced by a decrease in pH [225]. Thus, it is unlikely that PF14 follows the second model. Since PF14 itself forms micelles in solution [210], it is also not likely that the micelles become entirely reorganized or disrupted to accommodate NA in the center, as the first model implies. Thus, we consider it most likely that PF14/NA nanoparticles form according to the third model (**Figure 3C**), with peptide micelles accommodating NA on their surface and between peptide molecules. Both electrostatic interactions between phosphates in NA backbone and CPP's ornithines and lysine, as well as hydrophobic interactions between nitrogen bases and hydrophobic amino acids mediate such complexation.

1.3. Uptake and trafficking of nanoparticles

Despite the internalization of CPPs being reported in a wide variety of cell types, the specific internalization mechanism is not well understood. It varies considerably depending on the CPP, cargo, and physicochemical features of nanocomplexes [227]. In addition, the same particle can be internalized via different mechanisms, depending on the cell type [228]. Although CPPs may utilize direct plasma membrane translocation [229–231], endocytosis is believed to be the primary route for CPPs to enter the cells [232–234].

1.3.1. Endocytosis

Endocytosis is a process that cells harness for the uptake of extracellular materials. It can be non-specific as well as receptor-mediated. Receptor-mediated internalization is used by some viruses to enter host cells and can also be triggered by metabolites such as cholesterol and iron, hormones, proteins, and nanoparticles [235]. Multiple types of receptors can induce endocytosis, such as transferrin receptors [236], low-density lipoprotein receptors (LDLR) [237], epidermal growth factor receptors (EGFR) [238], mannose receptors [239], and scavenger receptors [240].

Endocytosis can be divided into two main types: phagocytosis and pinocytosis. **Phagocytosis** is a specialized form of endocytosis used by phagocytes, such as neutrophils and macrophages, for the targeted engulfment of relatively large particles, such as pathogens [241]. In contrast, **pinocytosis** is a more general process utilized by various cell types, involving the non-specific uptake of fluid

and small particles from the surrounding environment. Pinocytosis can be divided into macropinocytosis, clathrin-dependent, caveolin-dependent, and clathrin- and caveolin-independent endocytosis, and the latter can be dynamin-dependent or -independent [242]. It should be mentioned that there are alternative ways to classify endocytic pathways [243]. Cells can use different types of endocytosis to internalize particles with different compositions.

Ways to study endocytosis

Several methods are available to determine the route or routes of endocytosis utilized by particles or compounds to enter cells. The most commonly employed approach involves the suppression of individual endocytic pathways. This can be achieved by using pharmacological inhibitors targeting key proteins involved in specific pathways [244], by siRNA-mediated knockdown of these proteins [247], or by overexpressing a non-functional analog of a protein regulating a specific endocytic pathway, which is then incorporated into the pathway instead of a functional copy [245].

However, this approach has certain limitations. Multiple factors can influence the efficiency and toxicity of pharmacological inhibitors, including the composition of the cell culture media, cell seeding density, passage number, etc. [246] It has been observed that, for some inhibitors, distinguishing between uptake-inhibiting and cytotoxic effects is challenging [246]. The efficiency of some inhibitors may also depend on incubation time, while others can affect multiple types of endocytosis, complicating the interpretation of the results [246]. Furthermore, when one pathway is suppressed, cells may adapt by switching to alternative pathways or overcompensating for the suppressed function [247]. Consequently, interpreting results obtained from such experiments can be challenging, and their reproducibility may be low [246].

An alternative approach, not based on suppression, involves cell imaging to detect the colocalization of a molecule of interest with specific endocytic structures. To label specific vesicles, cells can be transduced with fluorescently labeled proteins known to reside in these vesicles, such as EEA1 and Rab5 in early endosomes [248] or caveolin-1 in caveolae [249]. Alternatively, low molecular mass probes can be used to label specific vesicles, such as LysoSensor, which fluoresces in the acidic environment of lysosomes [250]. Finally, immunocytochemistry can be applied to fixed cells, wherein specific cellular structures are stained using specific antibodies, and colocalization with compounds of interest is subsequently analyzed [251].

1.3.2. Intracellular trafficking of nanoparticles

Once internalized, a nanoparticle is trafficked through intracellular vesicles called endosomes [252]. After that, it can be either trafficked back to the plasma membrane, sent to the trans-Golgi network (TGN), directed into lysosomes for degradation, or escape into the cytosol (**Figure 4**). Endosomes undergo maturation,

during which intraluminal pH decreases and endosome composition is altered, with the most remarkable changes being in phosphatidylinositol phospholipid composition of an endosomal membrane and recruitment of different Rab GTPases [253, 254]. With a pH of about 6.5 [255], early endosomes are the least acidic vesicles in an endo-lysosomal pathway. Early endosomes are the main sorting point: from there, a compound can be directed into recycling endosomes, into TGN, or into the lysosomal pathway to be eventually degraded by lysosomal hydrolases (**Figure 4**). Late endosomes have a pH of around 5.5 and, due to the higher number of intraluminal vesicles, are also known as multivesicular bodies. Upon transition from early to late endosome, Rab5 is swapped for Rab7 [256], which is essential for the transition and migration of an endosome towards the cell nucleus along a microtubule. Eventually, a late endosome fuses with a lysosome with a highly acidic pH (up to 4.5) to form an endolysosome, where organic compounds, including peptides and NAs, are degraded by lysosomal hydrolases [257]. A bioactive compound has to escape from endosomes to the cytosol before endosomal pH decreases and hydrolytic enzymes degrade the molecule [258]. Endosomal escape is a significant bottleneck for many transfection systems that determines how large a fraction of the molecules can reach their intracellular target. Vectors, such as CPPs, are aimed to provide efficient endosomal escape so that their cargo can avoid degradation and reach its intracellular target.

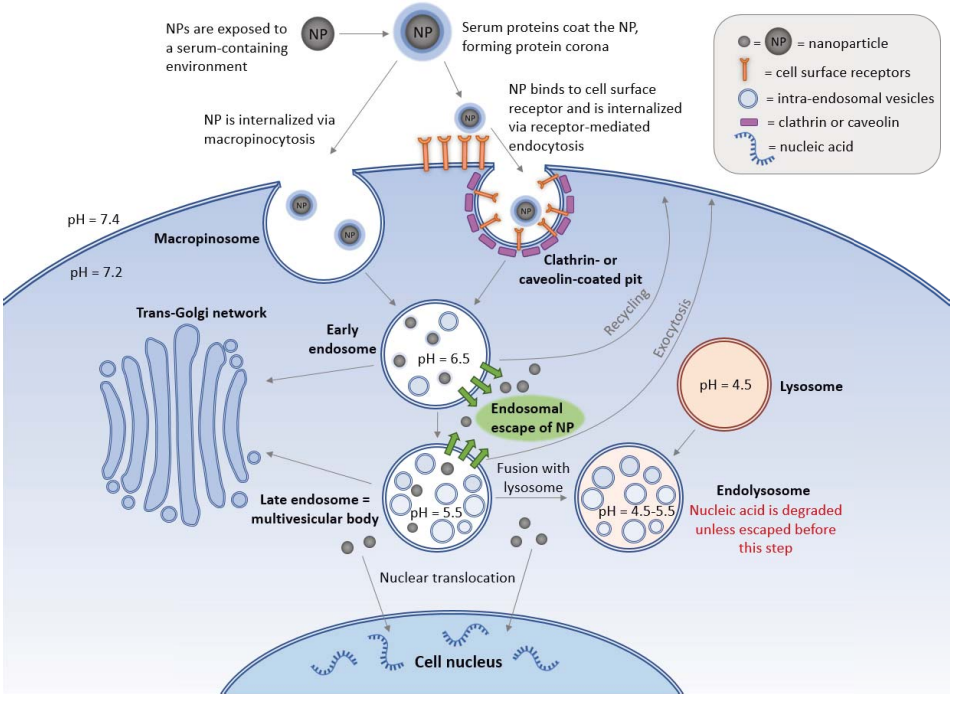

Figure 4. Schematic illustration of cellular internalization and trafficking, exemplified by an NA-delivering nanoparticle.

Dysregulation of endosomal pH can lead to impaired clearance of proteins directed for degradation and disrupted turnover of membrane receptors, causing pathological changes in cell metabolism. For example, cancer cells can have elevated endosomal pH that plays a critical role in their malignancy [259]. The presence of large, highly acidic vesicles has been associated with increased migration and metastasis of breast cancer [260]. Furthermore, disrupted endosomal acidification is likely to play a significant role in the pathogenesis of Alzheimer's disease and other neurological disorders [261, 262]. In healthy cells, cell type-dependent regulation of endosomal pH has been linked to varying susceptibility of different cell types to viral infection [263].

1.3.3. Internalization, trafficking, and endosomal escape of CPP/NA nanoparticles

CPP/NA nanoparticles are internalized by cells through endocytosis, meaning that they are trafficked through the endo-lysosomal network and need to escape to the cytosol for the NA cargo to execute its biological function. It has been shown that the cellular uptake of PF14/NA nanoparticles is primarily mediated by scavenger receptors, namely SR-A3 (SCARA3) and SR-A5 (SCARA5) [264–267], which are present in commonly used HeLa cells and many other cell types. A family of scavenger receptors is large and diverse, and recently, a consensus definitive classification of scavenger receptors has been proposed [268]. Interestingly, SR-A3 and SR-A5 are not constantly present on the plasma membrane but become recruited once the cells are exposed to suitable ligands [264].

It is known that PF14/SCO nanoparticles are internalized via macropinocytosis and caveolin-dependent endocytosis [264, 266], while for PF14/pDNA nanoparticles, caveolin-dependent endocytosis has been shown to be the main route of internalization [174]. It has been demonstrated that PF14/SCO nanoparticles are not trafficked into the endoplasmic reticulum or TGN, likely staying in endo-lysosomal compartments [264]. However, these particles predominantly accumulate in and escape from non-acidic vesicles without significant colocalization with the acidic lysosomes during the first hours of transfection [264]. This can be due to caveolin-mediated endocytosis playing an important role in their internalization, as caveosomes have a higher pH than other endocytic vesicles [269], or to the fact that PF14 may interfere with endosomal acidification [270].

Some NAs, such as SCO and pDNA, must reach the cell nucleus to execute their intended biological function. In addition to passively getting there during cell division, such NAs can reach the nucleus actively within hours after transfection [264]. It is known that pDNA associates in cells with multiple proteins that then mediate its transport across the microtubule network and through the nuclear pore complex [271]. For PS oligonucleotides, it has been shown that they are actively shuttled into the cell nucleus once they reach the cytosol [272]. Thus, endosomal escape remains the most critical step limiting the efficiency of NAs. This issue is mitigated by using delivery vehicles, such as CPPs. However, even

when complexed with a CPP, only a small portion of NA cargo escapes from endosomes [264, 273, 274], with endosomal escape remaining the major bottleneck limiting the efficiency of the CPP/NA complexes.

Many ways have been explored to enhance the endosomal escape of CPPs and their cargo molecules by introducing certain features into the structure of CPPs. For example, membrane fusion can be facilitated by coupling a peptide with a fatty acid, as in the case of PF14. Endosomal escape can be enhanced by incorporating multiple histidine residues into the CPP sequence, resulting in the "proton sponge" effect – an increasing protonation of a CPP at the acidic pH with the subsequent osmotic swelling and destabilization of endosomes [275]. In addition, endosomolytic residues can be incorporated into the CPP structure, such as chloroquine analogs in PF6 [201]. Similarly to chloroquine, a peptide derived from hemagglutinin-2 (HA2) of influenza virus has been shown to significantly enhance the efficiency of CPP-mediated transfection when fused with a CPP [276]. At low pH values, HA2 undergoes a conformational change, exposing its α-helix structure that fuses with the endosomal membrane, leading to the release of complexes.

1.4. Non-structural factors affecting nanoparticle delivery

Often, nanoparticles that are efficient *in vitro* can show much worse performance *in vivo*. One of the reasons for this discrepancy is that various proteins present in biological fluids coat the particles, changing their biomolecular interface, which can lead to their inactivation and elimination from the bloodstream before they reach their intended target [277, 278]. However, this coating can also have certain positive effects on nanoparticles, and, importantly, its composition can be manipulated to affect the fate of nanoparticles in a desired way. In addition to proteins passively binding to nanoparticle surface, certain compounds can be used as excipients during nanoparticle preparation and/or transfection. These excipients can affect the properties of nanoparticles, enhancing their productive uptake by cells.

1.4.1. Protein corona

Cell culture media usually contains serum that provides cultured cells with the necessary nutrients. However, serum proteins can significantly affect the properties and colloidal stability of nanoparticles introduced into the media [222], as, after contact with the serum-containing milieu, nanoparticles are rapidly coated by a layer of proteins called protein corona (PC) [279–282] (**Figure 5**). Still, CPP-mediated delivery of NAs *in vitro* often results in efficient and homogeneous uptake of the complexes by cells and a high functional effect of the cargo. However, application of the same delivery system in animal models *in vivo* is usually much less efficient [283, 284]. The same discrepancy can be observed in the case of lipid-based [285] and other types of nanoparticles [286, 287]. One of

the reasons for this is the different milieu in cell culture conditions and the organism. Cell culture conditions are static, lacking a constant flow of bloodstream and immune cells. Sometimes, transfection is carried out in serum-free cell culture media [288]. However, even if serum-containing media is used, such serum is usually derived from cattle and is heat-inactivated, not containing active components of the complement system and not fully resembling *in vivo* conditions [222]. Thus, the PC forming around nanoparticles *in vitro* and *in vivo* can have different compositions, affecting nanoparticles' properties and cellular internalization in various ways. Understanding the formation and effects of the PC is highly important for applying nanoparticles in serum-containing environments.

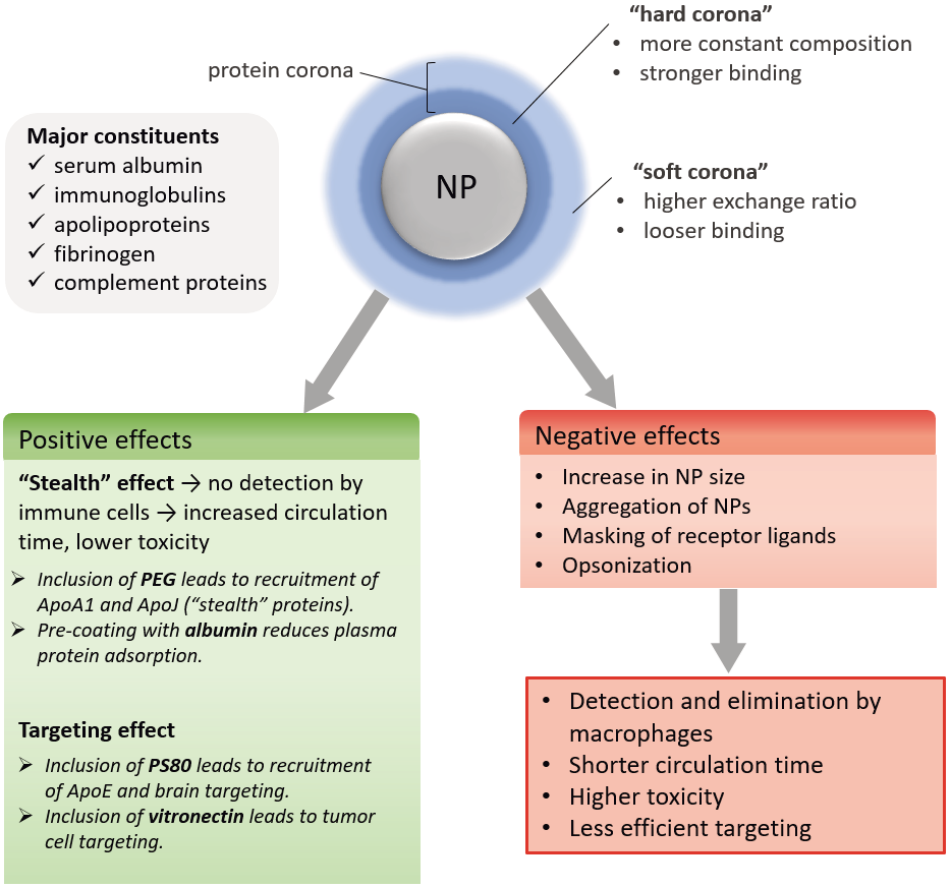

Figure 5. Architecture, composition, and possible effects of protein corona on nanoparticle properties and fate [289–295]. NP – nanoparticle, PEG – polyethylene glycol, Apo – apolipoprotein, PS80 – polysorbate 80.

Formation of protein corona around nanoparticles

After contact with biological fluids, e.g., blood, plasma proteins rapidly coat nanoparticles, forming a PC. As a result of this coating, not a synthetic nanoparticle itself, but rather its biomolecular PC interacts with target cells [296]. PC is classified into hard and soft, with hard PC corresponding to the inner layer of proteins that bind more stably at higher amounts and soft PC corresponding to the outer layer of proteins that bind more loosely and are more likely to be exchanged [297] (**Figure 5**). PC forms due to the competitive affinity-based adsorption of proteins, so the abundance of a protein in the milieu does not necessarily correlate with its abundance in PC [298]. Accordingly, when plasma concentration increases, proteins in PC with lower affinities can be replaced by those with lower plasma concentration but higher affinities [298]. For example, for oligonucleotides with PS backbone, it has been shown that while the proteins that are highly abundant in plasma, such as albumin, immunoglobulin G (IgG), transferrin, and complement component 3 (C3), bind such oligonucleotides with micromolar dissociation constants (K_d), less abundant ones can bind them with nanomolar K_d [54].

Composition of protein corona

Multiple factors affect the composition of the PC that nanoparticles acquire. Firstly, the composition of a PC is influenced by the physical properties of a nanoparticle, such as size [299, 300], shape [301], surface charge [302, 303], and hydrophobicity [303]. Secondly, it is affected by environmental factors such as temperature [304], pH [54, 305], and salt concentration [54]. Third, the composition of a PC largely depends on the type of biological fluid to which the nanoparticles are exposed. Thus, PC has different compositions in gastrointestinal tract fluids [306], lung surfactant [307], and different blood-derived liquids, such as whole blood, plasma, or serum [308–310]. Interestingly, even patients with different diseases, such as various types of cancers, provide nanoparticles with different PC [311, 312].

Most nanoparticles are designed for intravenous administration, and the composition of PC forming around nanoparticles in the bloodstream is best studied. Typically, the most abundant proteins present in PC forming in the presence of blood plasma are serum albumin, IgG, apolipoproteins, fibrinogen, and clusterin [297]. These proteins participate in coagulation, complement activation, and pathogen recognition. PC forming around some commonly used particle types is well-studied. For example, nearly 70 proteins coat AuNPs, the most abundant being fibrinogen [299]. The most abundant constituents of the PC forming around LNPs are serum albumin, C3, IgG, and apolipoprotein (Apo) E [313]. Besides nanoparticles, also naked NAs are coated with serum proteins. It has been shown that oligonucleotides with PS backbone predominantly bind serum albumin, IgG, apolipoproteins, C3, and transferrin [314]. Interestingly, the PS backbone has a major effect on PC composition, enhancing the association of an oligonucleotide with plasma proteins, reducing its renal clearance, and facilitating its translocation into peripheral tissues from the injection site [54].

Effects of protein corona on nanoparticles

As PC creates an entirely new biomolecular interface between nanoparticles and biological media, it can also significantly alter their properties and cellular internalization (**Figure 5**). The effects of PC become most significant when applying nanoparticles in live systems, and some positive and negative effects of PC *in vivo* are discussed below.

Adsorption of "stealth" proteins into PC, such as ApoA1 and ApoJ, can reduce nanoparticle-induced toxicity and increase their circulation time by masking them from immune cells [294]. However, more often, PC has the opposite effect. Firstly, PC can negatively affect nanoparticles by altering their physical properties. Specifically, PC increases the size of a particle [299], which can be undesirable for certain applications. Furthermore, it can lead to nanoparticle aggregation, making them more likely to be eliminated by macrophages or through the liver and kidneys [315]. Additionally, the adsorption of opsonizing proteins such as C3 can trigger an immune response, increasing nanoparticle toxicity and inducing their elimination from the bloodstream [296, 297]. Finally, PC can interfere with the targeted delivery of nanoparticles by masking the ligands that interact with receptors on the cell surface [316, 317].

By investigating the effects of PC with different compositions, it is possible to influence the nanoparticles' properties, pharmacokinetics, and cellular internalization by modulating the composition of PC forming around them [296, 297]. For example, the simplest way to mitigate PC-caused clearance is the incorporation of PEG, a near-neutral and hydrophilic polymer, into nanoparticles, which reduces the adsorption of opsonizing proteins and can induce the adsorption of stealth proteins into PC, thus reducing nanoparticle elimination by macrophages [294, 318]. Pre-coating with serum albumin has also been shown to reduce plasma protein adsorption and prolong nanoparticle circulation time [295, 319, 320], which has already found application in clinics [321].

Furthermore, nanoparticles can be designed to adsorb blood proteins that promote targeting to specific cells. For example, coating nanoparticles with polysorbate 80 (PS80) promotes the adsorption of ApoE, which, in turn, facilitates nanoparticle binding to LDLR and their transport across the blood-brain barrier [290–292]. A pre-formed PC comprising vitronectin has been harnessed to target tumor cells. Specifically, an arginine-glycine-aspartic acid (RGD) motif of vitronectin interacted with αVβ3 integrins overexpressed on the surface of the target tumor cells [293]. Nanoparticles conjugated with retinol were shown to preferentially adsorb retinol-binding protein, which in turn targeted the nanoparticles into hepatic stellate cells [322]. Similarly, the pre-adsorption of antibodies can mediate the targeting of the nanoparticles to specific cell types [323]. Interestingly, patisiran, the only FDA-approved siRNA-based drug not conjugated with GalNAc, is predominantly accumulating in the liver due to the presence of ApoE in its PC, which enables the targeting of hepatocytes [285].

Despite the significant impact that PC has on nanoparticles, the composition and effects of PC on CPP/NA nanoparticles have not been well-studied. However, some effects that serum can have on these particles are described. For example,

it has been shown that the CPP/NA nanoparticles' zeta potential and stability are reduced in the presence of serum while their size increases [265, 324]. Due to the presence of polyanions such as heparan sulfates, serum can trigger premature disintegration of CPP/NA complexes, reducing their biological effect. It has also been shown that the opsonization of CPP/NA nanoparticles can be reduced by lowering the nitrogen-to-phosphate (N/P) ratio of the nanoparticles [220]. Still, the exact composition and effects of PC forming around CPP/NA nanoparticles need further investigation.

1.4.2. Role of calcium ions in transfection

Calcium ions are known to play multiple roles in cell metabolism. Calcium signaling plays a crucial role in mitochondrial metabolism [325], cell division [326], as a second messenger in cell signaling pathways [327], apoptosis [328], autophagy [329], clathrin-mediated endocytosis [330, 331], and translocation of receptors to the plasma membrane [266], to name just a few.

It was shown that the entry of CPPs into cells is accompanied by a temporary increase in intracellular calcium concentration [332, 333]. According to this change, CPPs can be divided into two groups [332]. Specifically, amphipathic CPPs cause an influx of calcium ions, which triggers plasma membrane repair response and lysosomal blebbing, while non-amphipathic CPPs do not have such an effect. Furthermore, the depletion of extracellular calcium ions has been shown to reduce the internalization and biological activity of CPP/NA nanoparticles [332]. In line with this, Hori and colleagues showed in 2015 that the effect of oligonucleotides can be enhanced by increasing extracellular calcium concentration, i.e., simply by adding calcium chloride into transfection media [334]. The authors proposed that calcium ions trigger the formation of nanosized particles from serum components, which, in turn, facilitate the transfection of NA (**Figure 6B**). Goldshtein *et al.* showed in 2016 that calcium can condense naked siRNA to nanoparticles, promoting its cellular uptake and endosomal escape [335] (**Figure 6A**). Recently, Baoum and coauthors used calcium to facilitate CPP/NA nanoparticle transfection, showing that adding calcium provides highly efficient delivery of NAs with low toxicity [336–338]. The authors proposed that calcium acts by "softly crosslinking" functional groups of NA and CPP [336] (**Figure 6C**).

Despite being chemically similar, other metal ions did not show the same effects on NA transfection. Goldshtein *et al.* showed in 2016 that Mg^{2+} and Ba^{2+}, despite forming with siRNA nanoparticles physically similar to the ones that Ca^{2+} forms, do not increase gene silencing [335]. Similarly, Hori *et al.* showed in 2015 that while adding calcium to the cell culture media significantly enhances the efficiency of synthetic oligonucleotides, magnesium does not act in the same way [334].

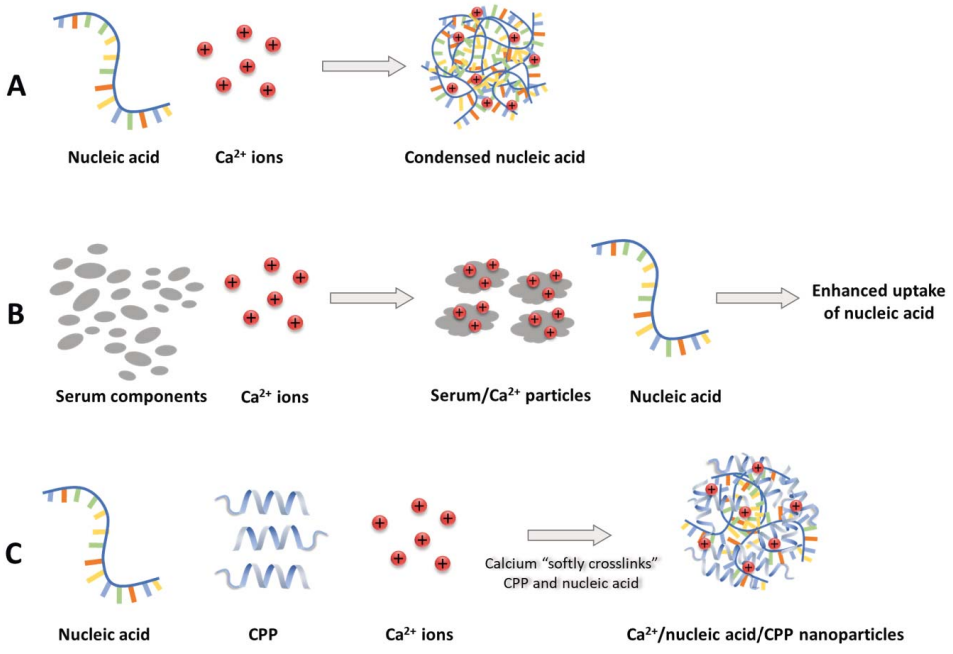

Figure 6. Proposed mechanisms of Ca^{2+}-induced increase in NA efficiency. A: Ca^{2+} ions condense NA to nanoparticles. B: Ca^{2+} ions interact with serum components, and the complexes assist NA transfection. C: Ca^{2+} ions are included in CPP/NA complexes. NA – nucleic acid, CPP – cell-penetrating peptide.

1.4.3. Other approaches to affect the potency of nanoparticles

In addition to structural changes in the vehicle (see paragraph 1.3.3), the delivery of nanoparticles can be improved by incorporating certain additives. In the research described in this thesis, we used Ca^{2+} ions (already described above), chloroquine, and PS80 as additives to CPP/NA complexes. These, as well as several more additives that have been shown to affect NA delivery, are discussed below.

Chloroquine is an endosomolytic compound that is used in malaria treatment and prevention. Its effect is due to its ability to increase the pH of the parasite's digestive vacuole, thus interfering with its hemoglobin digestion and detoxification [339]. Chloroquine has also been shown to have applications for the treatment and prevention of other diseases, such as viral infections [340–342], rheumatoid arthritis [343], and systemic lupus erythematosus [344]. Additionally, chloroquine is known to significantly enhance the delivery of nanoparticles by inhibiting endosomal acidification and, at higher doses, destabilizing endosomes and causing rupture of the endosomal membrane [345–350]. Its mechanism in transfection is as follows. Being a weak base, chloroquine diffuses into endosomes. In the acidic endosomal environment, it becomes protonated, leading to an increase in endosomal pH and endosome destabilization.

PS80, also known as Tween 80, is a non-ionic surfactant shown to promote the crossing of the blood-brain barrier by nanoparticles, thus mediating their translocation into the brain [351] (also see paragraph 1.4.1). It has been used for cerebral delivery of LNPs carrying siRNA [352] and plasmid DNA [353]. PS80 acts by recruiting apolipoproteins, specifically ApoE, into the PC of nanoparticles, which then associates with the respective receptors, LDLR, LDLR-related protein 1 (LRP1), and others [354], that are abundant on the surface of endothelial cells of the blood-brain barrier. However, besides the brain, these receptors can be found throughout the body, for example, in the liver [355]. Thus, if included in nanoparticles, PS80 can potentially enhance their delivery into various cell types. Notably, modifying PNPs with PS80 enhanced the internalization of the nanoparticles into cultured cells, supposedly by increasing the plasma membrane fluidity [356].

Multiple other compounds have been investigated as transfection enhancers. In 2022, Bost and coauthors found two small molecules, **CMP05** and **CMP05-7**, that greatly increased the SSO's transfection and the resulting biological effect at low micromolar concentrations by inducing its endosomal escape [357]. Interestingly, compounds as simple as **glucose**, **sucrose**, and **mannitol** were able to synergistically increase CPP internalization by a wide variety of cell lines and primary cells due to the hyperosmotic effect [358]. Bell *et al.* enhanced the efficiency of mRNA transfection with CPPs into adherent human gastric cancer cells by adding to them TLR antagonist **E6446** [359]. E6446 supposedly acts by suppressing the innate immune response, being a five times more efficient transfection enhancer than chloroquine. In another study, it was shown that the cellular delivery of SCO or enhanced green fluorescent protein (EGFP) by hydrophilic CPPs could be improved by adding **pyrenebutyrate** as a counteranion to increase the hydrophobicity of the complexes and promote plasma membrane penetration [360, 361]. Pre-treatment with another additive, **1,2-benzisothiazolin-3-one (BIT)**, was shown to facilitate the uptake of a CPP TAT and TAT-conjugated GFP or pro-apoptotic peptide KLA in different cell lines in a concentration-dependent manner [362]. It has been shown that adding **transferrin** to liposomes that were surface-modified with CPPs can improve cellular internalization and brain translocation of the complexes [363]. As mentioned above, adding **PEG** to nanoparticles can prolong their circulation time *in vivo* by improving their stability and reducing toxicity and immunogenicity with minimal loss of biological activity [294, 318]. Finally, it was found that coating CPP complexes with siRNA or pDNA with **chondroitin sulfate A** conjugated with a mucolytic agent **mannitol** can increase the mucus penetration by reducing nanoparticles' surface charge and viscosity of mucus [364].

In addition, different **preparation techniques** can yield nanoparticles with improved properties. For example, cryo-concentration of NF55/pDNA nanoparticles, which implies lyophilization of prepared complexes with subsequent reconstitution in water, was shown to produce nanoparticles that had higher stability against enzymatic degradation, better colloidal properties, longer shelf-life, and improved biological activity [365].

2. AIMS OF THE STUDY

The current thesis aims to investigate the factors determining the properties and efficiency of CPP/NA nanoparticles, as well as the ways to increase the efficiency of NA delivery by varying nanoparticle composition. The aims of individual papers summarized in this thesis were as follows:

Paper I To analyze the composition of the PC forming around CPP/NA nanoparticles in the presence of sera derived from different species and its effects on the nanoparticles.

Paper II To examine the effects of calcium and magnesium ions added to the CPP/NA nanoparticles during the preparation step.

Paper III To investigate ways to enhance the delivery efficiency of mRNA with PF14 into cell lines, primary cells, and *in vivo*.

3. MATERIALS AND METHODS

The methods used here are described in detail in the papers included in the current thesis, and the following section only provides a brief overview of the selected methods.

3.1. Cells

Throughout the current thesis, several cell lines were used, including HeLa [366], HaCaT [367], and reporter cell lines HeLa pLuc 705 [368], HeLa EGFP 654 [369], and U87 MG-Luc2 [370]. Additionally, human primary keratinocytes were used in Paper III.

HeLa is a widely used cell line derived from human cervical cancer. HeLa pLuc 705 and HeLa EGFP 654 are HeLa-derived cell lines mimicking human beta-thalassemia. These cells are used as a model for studying splicing correction. They contain the reporter genes (firefly luciferase or EGFP gene, respectively) interrupted by the human beta-globin second intron. This intron contains an aberrant splicing-inducing mutation at position 705 or 654, respectively. Mutations in either of these positions create a cryptic splice site, which is used during splicing, leading to the retention of a part of an intron in mRNA and the synthesis of a defective protein. When SCO with a complementary sequence blocks the aberrant splice site, splicing occurs normally, and luciferase or EGFP, respectively, can be detected, reflecting the efficiency of SCO transfection. U87 MG-Luc2 is a human glioblastoma-derived cell line that contains the luciferase gene stably incorporated in its genome and constitutively expresses firefly luciferase, thus being suitable for siRNA transfection experiments. Finally, HaCaT, human immortalized keratinocytes, were used as an intermediate step between the cancer-derived cell lines and primary keratinocytes.

All cells were maintained at 37 °C in a humid atmosphere that contained 5% CO_2. All cell lines were cultured in Dulbecco's Modified Eagle Media (DMEM) containing 4.5 g/L of glucose, 10% (v/v) fetal bovine serum (FBS), and 1% (v/v) penicillin-streptomycin solution. Keratinocytes were cultured in a keratinocyte serum-free media (KC-SFM) supplemented with recombinant epidermal growth factor (EGF), bovine pituitary extract, and antibiotic solution (5 U/mL penicillin and 5 μg/mL streptomycin). Cells were grown on 6 cm or 10 cm cell culture dishes and were split once reaching about 90% confluency by treating them with 0.05%–0.1% trypsin-EDTA solution and transferring about 20% of cells to a dish with the fresh cell culture media.

3.2. Used CPPs and nucleic acids

In all articles included in the current thesis, a PF14 was primarily used for NA transfection. In papers I and II, we also used the following peptides: PF6, NF70, NF71, NF72, NF55, and C22-PF14. The sequences and references for all CPPs used are provided in **Table 2**.

Table 2. CPPs used in the studies included in the current thesis, their sequences, N-terminal fatty acid moieties, and references.

CPP	Sequence	Fatty acid	Reference
PF14	AGYLLGKLLOOLAAAALOOLL-a	C18	[196]
PF6	AGYLLGK^{f}INLKALAALAKKIL-a	C18	[201]
NF70 = H52	HHHHYHHGOeILLKALKALAKAIL-a	C20	[275]
NF71 = H31	HHYHHGO^{e}ILLKALKALAKAIL-a	C18	[275]
NF72 = H82	HHHHHHYHHGO^{e}ILLKALKALAKAIL-a	C20	[275]
NF55	AGYLLGO^{e}INLKALAALAKAIL-a	C18	[198]
C22-PF14	AGYLLGKLLOOLAAAALOOLL-a	C22	[220]

f – four molecules of chloroquine analog (trifluoromethylquinoline) are coupled at this position via lysine tree; e – next amino acid is coupled to the ornithine's side chain, i.e. to δ NH_2 group, not α NH_2; a – C-terminal amide.

For splicing switching, the PS-2'-OMe SCOs were used. Depending on the assay, the 5' end of an oligonucleotide was labeled with either Cy5, biotin, or a nanogold tag (d = 1.4 nm) or was not modified. The following SCOs were used: SCO-705 [368] and SCO-654 [371]. SCO-705 targets position 705 in beta-globin intron inserted into the firefly luciferase gene of HeLa pLuc 705 cells. Similarly, SCO-654 targets position 654 in the same intron inserted into the EGFP gene of HeLa EGFP 654 cells.

The following protein-encoding NAs were used: mRNA and pDNA. We used four mRNAs: mRNA encoding firefly luciferase (mRNA-luc), mCherry (mRNA-mCherry), EGFP (mRNA-EGFP), and Cy5-labeled mRNA encoding EGFP (Cy5-mRNA-EGFP). All mRNAs contained 5moU residues and a modified cap structure – ARCA or CleanCap. We used a plasmid encoding firefly luciferase (pGL3).

Finally, siRNA targeting firefly luciferase (siRNA-luc) was applied for gene knockdown. As siRNA leads to a reduction in luciferase expression and in the resulting luminescence, which is not well distinguishable from toxicity, a non-targeting siRNA (siRNA-neg) was used as a negative control.

NAs used in the studies are summarized in **Table 3**.

Table 3. Nucleic acids with different sequences used in the studies included in the current thesis, their sequences or structural features, and manufacturers. For siRNA, only the sequence of the guide strand is shown.

Nucleic acid	Sequence/structure	Manufacturer
SCO-705	5'-CCUCUUACCUCAGUUACA-3'	Microsynth or Metabion
SCO-654	5'-GCUAUUACCUAAACCCAG-3'	Microsynth or Metabion
siRNA-luc	5'-GGACGAGGACGAGCACUUCTT-3'	Microsynth
siRNA-neg	5'-AGGUAGUGUAAUCGCCUUGTT-3'	Microsynth
pGL3	4.7 kbp, Mw = 3055 kDa	Promega
mRNA-luc	CleanCap, 5moU	TriLink Biotechnologies
mRNA-mCherry	CleanCap, 5moU	APExBIO Technology
mRNA-EGFP	ARCA, 5moU	APExBIO Technology

SCO-705 – SCO targeting position 705 in human beta-globin intron 2; SCO-654 – SCO targeting position 654 in human beta-globin intron 2; siRNA-luc – siRNA targeting firefly luciferase; siRNA-neg – non-targeting negative control siRNA; pGL3 – plasmid encoding firefly luciferase; mRNA-luc – mRNA encoding luciferase; mRNA-mCherry – mRNA encoding mCherry; mRNA-EGFP – mRNA encoding EGFP; ARCA – anti-reverse cap analog; 5moU – 5-methoxyuridine.

3.3. CPP/NA nanoparticle preparation

For nanoparticle preparation, we used a non-covalent association of CPP and NA. To form nanoparticles, we mixed NA and CPP in Milli-Q (MQ) water in $1/10^{th}$ of the final volume. After letting nanoparticles form for 15 min at room temperature (RT), we added ions or other excipients to the mixture, if indicated. After 15 min, fully formed particles were applied to the cells by adding them into cell media (1:9 v:v). The following final concentrations were used for functional studies if not indicated otherwise: 100 nM SCO with 500 nM CPP (molar ratio 5), 0.8 ng/µl mRNA with 1 µM CPP (charge ratio 2), 15 nM siRNA with 255 nM CPP (molar ratio 17), and 1.1 ng/µl pDNA with 1.3 µM CPP (charge ratio 2). For microscopy, 2× higher concentrations were usually applied to provide higher detected signals.

3.4. Methods used to measure cellular association and biological effects of nanoparticles

The functional effects of NAs that induce or suppress luciferase expression (SCO-705, siRNA-luc, mRNA-luc, and pGL3) were measured by luminometry. The effects of fluorescent or fluorescence-enhancing NAs (SCO-654, Cy5-SCO-654, mRNA-mCherry, mRNA-EGFP, and Cy5-mRNA-EGFP) were analyzed using flow cytometry, fluorescence microscopy, and confocal microscopy.

Luminometry is a rapid and straightforward approach to quantify the amount of luciferase expressed by cells. It is a highly sensitive method, exhibiting signal

differences that can span up to millions-fold. This technique allows for the fast and convenient assessment of numerous conditions in a single experiment from a 96-well plate. A key drawback of this approach is its dependence on the number of cells per well. Nonetheless, if cells are evenly seeded and minimal toxicity of the test solutions is confirmed through cell viability measurements, this approach provides a comprehensive overview of the effectiveness of the tested compounds while remaining time- and cost-effective. To measure luciferase expression, after incubation with test solutions, cells were washed with phosphate-buffered saline (PBS) and incubated with 20 µl of a lysis buffer (containing 1% v:v of Triton X-100) per well at –25 °C until the samples froze. Once thawed at RT, 70 µL of luciferase substrate solution (containing 1 mM luciferin) was added per 96-well plate well, and the solutions were transferred to a white 96-well plate for luminescence signal detection.

Flow cytometry enables the quantification of fluorescent signals at the single-cell level, providing various information, including cell size, viability, and signal distribution across the population. Unlike luminometry, it is independent of cell number, allowing for quick analysis of multiple samples from a 96-well plate. Its primary drawbacks include reduced time efficiency and a higher cost. For the flow cytometry, cells were incubated with the solutions of interest, washed with PBS, and incubated with the trypsin-EDTA solution until detached. After that, 4′,6-diamidino-2-phenylindole (DAPI) solution in PBS (final concentration of DAPI 0.5 µg/mL) was added to each well, and cells were resuspended thoroughly. After 5 min of incubation, the signals were measured with an Attune NxT flow cytometer, and at least 5000 live cells were analyzed per well of a 96-well plate.

Confocal laser scanning microscopy (CLSM) is a quick and informative approach to examine the effects and cellular localization of the molecules of interest. Unlike luminometry and flow cytometry, this approach is rather qualitative than quantitative, although quantifying signals from obtained images still enables some degree of quantification. We performed live-cell microscopy or prepared fixed-cell samples. For fixed specimen preparation, cells were seeded onto 12 mm ⌀ cover glasses. 24 h post-transfection, the cells were washed with PBS and fixed by incubation with 4% paraformaldehyde (PFA) for 15 min at RT, cell nuclei were stained with DAPI, and the cover glasses were mounted onto glass slides with 80% glycerol. The images were obtained using a confocal laser scanning microscope Olympus FluoView FV1000 or Olympus FV1200MPE at the wavelengths optimal for the detection of DAPI ($\lambda_{ex/em}$ = 405/461 nm), EGFP ($\lambda_{ex/em}$ = 473/510 nm), mCherry ($\lambda_{ex/em}$ = 587/610 nm), and Cy5 ($\lambda_{ex/em}$ = 633/664 nm).

3.5. Methods used to study physical properties of nanoparticles

Dynamic light scattering (DLS) is a technique employed to measure the size of colloidal particles and their distribution in a liquid media. It relies on detecting fluctuations in light scattering caused by particles moving within the solution. The movement of larger particles is slower, resulting in more gradual intensity fluctuations, while smaller particles cause rapid fluctuations due to their faster movement. Analyzing these fluctuations allows determining the size of the particles within the sample. Additionally, this method can be used to measure the zeta potential of the nanoparticles, which reflects their surface charge and colloidal stability. Zeta potential measurement is based on the electrophoretic mobility of nanoparticles – how they migrate in response to an applied electric field. A highly positive or negative zeta potential indicates strong repulsive forces between nanoparticles, resulting in greater colloidal stability. For DLS analysis, we prepared CPP/NA nanoparticles as described above, diluted 1:100 in MQ water, and measured the nanoparticles' hydrodynamic diameter and zeta potential using the ZetaSizer Nano ZSP instrument [372].

Transmission electron microscopy (TEM) is a method that enables the visualization of nanoscale objects at very high resolution and can reveal their morphology and precise cellular localization. The equipment for TEM is expensive, and the procedure is laborious, but this method is often irreplaceable in the nanoscience field. Here, we used TEM to reveal the size and morphology of nanoparticles, as well as their intracellular localization. Nanoparticles were formed as described above. For negative staining, the sample was spread and absorbed onto copper grids covered with Formvar film and a carbon layer. The grids were exposed to 2% aqueous uranyl acetate to visualize the particles. After removing the excess stain with filter paper, specimens were air-dried and examined at 120 kV accelerating voltage with FEI Tecnai G2 Spirit transmission electron microscope [107, 372].

3.6. Methods used to study cellular internalization of nanoparticles

Endocytosis of a compound or a particle can occur via one or several parallel routes (see section 1.3). One of the ways to pinpoint the particular endocytosis route is by inhibiting its different pathways (e.g., [288]). Among the most commonly used pharmacological inhibitors of endocytosis, chlorpromazine can inhibit clathrin-mediated endocytosis as it interferes with the formation of plasma membrane-bound clathrin-coated pits [373]. Cytochalasin D inhibits actin polymerization, affecting mainly macropinocytosis [374]. Nystatin is a polyene antibiotic that binds cholesterol, which is essential for the formation of caveolin-containing endosomes and lipid rafts [375–377]. EIPA, i.e., 5-(N-ethyl-N-isopropyl)

amiloride, is an inhibitor of Na^+–H^+ exchanger, mainly affecting macropinosomes by slowing down their acidification [378, 379].

To inhibit endocytosis, the cells were pre-incubated for 30 min with cell culture media containing the abovementioned inhibitors to ensure suppression of the pathways of interest. Then, nanoparticle-containing solutions were added, and the cells were incubated with inhibitors and nanoparticles for 4 h. After this, the media with inhibitors and nanoparticles was replaced with a fresh growth media, and the expression of a reporter protein was measured the next day.

To evaluate the efficiency of **endosomal escape** of differently prepared nanoparticles, we used an endosome-destabilizing compound, chloroquine. Analyzing the extent of the increase in reporter protein expression in the presence of chloroquine enables determining, which nanoparticles benefit the most from it and which are less susceptible to its action. If adding chloroquine does not increase the biological effect of the cargo, it can be concluded that these particles successfully escape from endosomes already, as they do not benefit from additional endosome destabilization. The cells were incubated with nanoparticles and 100 μM chloroquine for 4 h. Next, the solutions were replaced with fresh cell culture media, and the effects were measured after an additional 20 h of incubation.

To evaluate the role of **class A scavenger receptors (SR-A3 and SR-A5)** in transfection and biological efficiency of differently prepared nanoparticles [264, 265], SR-A inhibitors polyinosinic acid (Poly I) [380–382] and fucoidan [383–385] were used. Structurally similar compounds without inhibiting properties, polycytidylic acid (Poly C) and galactose, respectively, were used as negative controls. Cells were first incubated for 1 h in inhibitor-containing media ($9/10^{th}$ of final volume). Then, 10× nanoparticle solutions ($1/10^{th}$ of the final volume) were added, and the effects were measured after 24 h of incubation.

3.7. Methods used to analyze the protein corona of nanoparticles

The PC, a layer of proteins adsorbed onto the surface of nanoparticles in a serum-containing environment, can be analyzed for its composition and major constituents using various methods such as silver staining, Western blotting, and mass spectrometry. To analyze PC forming on CPP/NA nanoparticles, these were prepared using either biotinylated SCO or biotinylated pDNA. First, the nanoparticles were incubated with the serum of interest, leading to the formation of PC. Then, streptavidin beads were used to capture the nanoparticles through the streptavidin-biotin interaction. Finally, PC-coated nanoparticles were isolated from the solution by using magnetic separation.

Protein separation with **silver staining** was used to analyze the composition of the protein-containing samples. This method involves protein denaturation with subsequent separation according to molecular mass on polyacrylamide gel. The separated proteins are visualized by binding silver ions, which are then reduced, leading to the formation of dark bands. This method provides information

about the approximate size and abundance of proteins. We used **Western blotting** to identify specific proteins in a sample. In this method, proteins are denatured, separated, bound to a membrane, and then the membrane is incubated with the primary and secondary antibodies. Finally, we used **mass-spectrometry** for more precise identification and characterization of proteins. For that, a mixture of proteins was subjected to trypsin digestion, and the resulting peptides were identified based on their mass-to-charge ratios.

3.8. *In vivo* experiments

In paper III, we analyzed the delivery of mRNA by PF14 *in vivo* in a mouse model of irritant contact dermatitis (ICD). This model mimics keratinocyte responses characteristic of chronic skin inflammation, such as AD [386], and was used in this study due to its simplicity [107]. We used six-to-ten-week-old C57BL/6J mice. CPP/mRNA nanoparticles were prepared as described above, and before injection, the complexes were mixed with a 5% glucose solution. Then, the solutions were injected subcutaneously into mouse ears (20 µl/ear), and inflammation resembling ICD was induced by topically applying 0.2% phorbol 12-myristate 13-acetate (PMA) in acetone to mouse ears. **Ear thickness** was measured directly after injection and 24 h later to identify possible ear swelling due to inflammation. Mouse ears were analyzed by **immunofluorescence**. For this, they were fixed in 4% PFA, cryosectioned, and stained with antibodies specific to the proteins expressed from the transfected mRNA. Following that, confocal microscopy of the samples was performed. Additionally, for the identification of possible changes in gene expression, total RNA was isolated from mouse blood, and **reverse transcription-quantitative PCR (RT-qPCR)** of genes encoding several cytokines was performed.

4. RESULTS AND DISCUSSION

4.1. The role of protein corona in internalization and biological activity of the CPP/NA nanoparticles (Paper I)

After contact with biological fluids, e.g., after intravenous injection, various proteins rapidly coat nanoparticles, forming a layer known as protein corona. The formation of the PC establishes a new "bio-nano interface" between the nanoparticles and the biological media. This interface, rather than the nanoparticles themselves, interacts with blood cells, endothelial lining, and the target cells. The PC can have many different effects on the properties and fate of nanoparticles in the organism. Although in some cases, PC can mask nanoparticles from immune cells or promote their targeting, more often, its effects are negative, ranging from the increased size of nanoparticles to their elimination by immune cells. The formation of the PC often explains why nanoparticles that are highly effective *in vitro* fail to produce the expected effects *in vivo* [277, 278, 387]. Although the PC plays a vital role in the biodistribution and efficiency of nanoparticles, the PC of CPP/NA complexes has not been thoroughly studied.

In Paper I, we aimed to analyze the composition and effects of the PC formed around CPP/NA nanoparticles in the presence of sera derived from three different organisms: calf, mouse, and human. Bovine serum was utilized as a representative of most cell culture systems, while murine serum represents the most typical animal model. Human serum represents the actual target organism in which a drug will be used.

4.1.1. Protein corona can induce agglomeration of nanoparticles

In this study, we prepared nanoparticles using three different CPPs – PF14, C22-PF14, or NF55 and two different NAs – SCO or pDNA. First, we measured the particles' hydrodynamic diameter and zeta potential by DLS. All nanoparticles had a hydrodynamic diameter ranging from 90 to 210 nm. Those formed with pGL3 had a positive zeta potential, while those with SCO were negatively charged. The difference between the zeta potential of CPP/SCO and CPP/pDNA nanoparticles can be attributed to the different N/P ratios used to prepare nanoparticles. Specifically, an N/P ratio of 2 was used for CPP/pDNA nanoparticles, and an N/P ratio of 1.5 for CPP/SCO nanoparticles, meaning that in the former, the positively charged CPP was in a higher excess, contributing to the higher surface charge.

It has previously been shown that PC formation enhances nanoparticle size [299] and can reduce their stability [265, 324]. To analyze the colloidal properties of the CPP/NA nanoparticles, we associated PF14 with biotin-labeled SCO and tagged the formed complexes with 10 nm gold via neutravidin for detection by TEM. To reveal the effect of PC, nanoparticles were incubated with 50% bovine, murine, or human serum, which resembles *in vivo* conditions. In the absence of serum, mostly single nanoparticles or small clusters were detected by TEM.

However, the nanoparticles possessing PC tended to form larger agglomerates with a size of several hundred nanometers. This was similar for all three sera used. Furthermore, PC was dense enough to make nanoparticles *per se* visible, unlike the nanoparticles formed in water that could only be detected based on their nanogold tags.

These results indicate that CPP/NA nanoparticles, similar to other nanoparticle types, may aggregate in *in vivo* conditions due to the formation of PC. A similar effect of PC on nanoparticle aggregation has been shown for polystyrene nanoparticles [388]. Interestingly, the opposite has been observed for gold nanoparticles, where the formation of hard PC led to higher colloidal stability of the formulations [389]. Overall, PC can affect nanoparticle colloidal stability differently, ranging from stabilization to aggregation [390]. Our results indicate that the latter scenario is likely to take place in the case of CPP/NA nanoparticles. When nanoparticles are applied *in vivo*, their aggregation can lead to harmful consequences, such as clogging small lung capillaries [391]. However, it is worth noting that, although representing well *in vivo* conditions in terms of serum concentrations, the experimental settings *in vitro* are highly static, lacking the flow properties of the bloodstream. Thus, the aggregation *in vivo* is likely milder than detected here.

4.1.2. The composition of the protein corona depends on the serum used

Next, we aimed to analyze the composition of the PC formed in different sera around CPP/NA nanoparticles. For the majority of nanoparticles, the main constituents of the PC are proteins that are abundant in serum and involved in transport, coagulation, and complement activation. These typically include serum albumin, immunoglobulins, apolipoproteins, fibrinogen, clusterin, and complement components [297]. Here, we wanted to determine whether this applies to CPP/NA nanoparticles.

First, we aimed to obtain general information about the composition of the PC. For this purpose, we used protein separation with silver staining. Nanoparticles formed with biotinylated pDNA were captured on neutravidin beads and incubated with 50% bovine or murine serum. Then, the adsorbed proteins were separated using gel electrophoresis and visualized with silver staining. Analysis of different time points showed that the PC formed as early as 5 minutes after incubation with serum, and its composition changed over time, consistent with previous results [298, 389]. The major constituent of the PC formed in both sera was a protein approximately 70 kDa in size, most likely serum albumin. However, the composition of the PC differed between the two sera, as indicated by different band patterns. Interestingly, it appeared that the composition of the PC was very similar in the case of nanoparticles prepared with PF14 and NF55, suggesting that it was not highly dependent on the CPP used.

Next, to determine the exact composition of the PC, we performed mass spectrometry of proteins adsorbed to the nanoparticles. We analyzed the composition of the PC formed around naked pDNA and CPP/pDNA nanoparticles in bovine, murine, and human serum (**Table 4**). As expected, serum albumin was highly represented in all coronae, being prevalent in the PC of naked pDNA and PF14/pDNA nanoparticles incubated in bovine serum, as well as in the PC of naked pDNA incubated with human serum. However, in the PC of PF14/pDNA nanoparticles incubated in human serum, C3 was the most abundant protein, followed by serum albumin and α-2-macroglobulin. In murine serum, apolipoprotein B-100 (ApoB-100) was the most abundant among all the identified proteins, followed by fibronectin and C3.

Table 4. The main constituents of PC formed around naked pDNA and PF14/pDNA nanoparticles in the presence of different sera, from more (top) to less (bottom) abundant.

Bovine serum		Murine serum		Human serum	
pDNA	**PF14/pDNA**	**pDNA**	**PF14/pDNA**	**pDNA**	**PF14/pDNA**
Albumin	Albumin	ApoB-100	ApoB-100	Albumin	C3
α-2-macrogl.	α-2-macrogl.	C3	Fibronectin	α-1-antitrypsin	Albumin
Serotransferrin	C3	Fibronectin	C3	α-2-macrogl.	α-2-macrogl.
C3	Serotransferrin	Murinogl.-1	Murinogl.-1	Haptoglobin	C4-B
ApoA-I	ApoA-I	α-2-macrogl.	α-2-macrogl.	C3	Serotransferrin
α-1-antitrypsin	Inter-α-tr. inh.	Albumin	Albumin	Serotransferrin	α-1-antitrypsin
Inter-α-tr. inh.	Prothrombin	Serotransferrin	Fibrinogen β	Apo A-I	Apo A-I

α-2-macrogl. – α-2-macroglobulin; albumin – serum albumin; ApoB-100 – apolipoprotein B-100; C3 – complement component 3; C4-B – complement component 4-B; Murinogl.-1 – murinoglobulin-1; ApoA-I – apolipoprotein A-I; inter-α-tr. inh. – inter-α-trypsin inhibitor heavy chain H2; fibrinogen β – fibrinogen β chain. Red – likely increases the elimination of nanoparticles; green – likely reduces the elimination of nanoparticles; blue – is involved in the binding and transporting of biomolecules; yellow – is involved in blood coagulation and hemostasis; not colored – other functions.

Thus, the composition of the PC varied greatly depending on the serum used but remained relatively consistent for different nanoparticles incubated with the same serum. Nevertheless, all the major constituents of the coronae were proteins involved in transport, blood coagulation, and pathogen recognition. As expected, the PC of pDNA and PF14/pDNA nanoparticles comprised proteins that could positively and negatively affect nanoparticle biodistribution and efficiency. For example, serum albumin, present at high levels in the PC of all formulations, has been shown to prolong the circulation time of nanoparticles, prevent the adsorption of opsonizing serum proteins, and facilitate the successful delivery of nanoparticles to peripheral tissues [295, 319, 320]. Other proteins identified in the PC of the analyzed nanoparticles, such as apolipoproteins, α-2-HS-glycoprotein (also known as fetuin-A), serotransferrin, etc., are involved in the binding and transport of various biomolecules in the bloodstream. Among them, fetuin has been shown to mark nanoparticles for recognition by cells via scavenger receptors [392], thus

increasing their cellular uptake and likely promoting the activity of the cargo, as scavenger receptors are essential for PF14/NA nanoparticle internalization [265]. Finally, proteins involved in blood coagulation and hemostasis, such as α-2-macroglobulin, prothrombin, fibrinogen, and α-1-antitrypsin, are also adsorbed into the PC of CPP/NA nanoparticles. Among them, α-2-macroglobulin has been shown to increase the elimination of the nanoparticles, thus reducing their efficiency [393]. Similarly, opsonization by C3 has a highly negative effect, promoting the phagocytosis of nanoparticles [394, 395].

4.1.3. Adsorption of C3 depends on nanoparticle characteristics

C3 is a protein that can significantly affect the fate of nanoparticles. Being the most abundant complement protein in serum, C3 is required for the activation of the complement system via all three pathways [396], mediating opsonization and subsequent elimination of compounds from the bloodstream. As C3 was identified in the PC of all CPP/NA nanoparticles, we analyzed amounts of C3 adsorbed on different nanoparticles more closely with Western blot. For this, we incubated CPP/NA nanoparticles either with serum or with plasma, bearing in mind that in serum, complement is inactivated by heat, so that incubation with plasma better represents real *in vivo* conditions.

As expected, significantly more C3 adsorbed to the nanoparticles in plasma than in serum. In the case of CPP/pDNA nanoparticles incubated in murine serum or plasma, adsorption of C3 was not significantly dependent on the CPP used, although nanoparticles with NF55 showed a tendency to adsorb more C3 than those with PF14 and C22-PF14. As expected, the adsorption of C3 to pDNA was time-dependent, increasing with longer incubation periods. When comparing naked pDNA and CPP/pDNA nanoparticles, it could be noted that C3 is associated with naked pDNA at a higher level, suggesting that CPPs may reduce complement-triggered inactivation and elimination of the cargo.

When naked SCO, SCO/PF14, and SCO/NF55 nanoparticles were incubated with murine serum, the adsorption of C3 was similar in the case of naked SCO and SCO/PF14 nanoparticles. However, the adsorption was significantly elevated in the case of NF55/SCO nanoparticles. Interestingly, in plasma, all nanoparticles adsorbed a rather equal amount of C3. The tendency of NF55/NA nanoparticles to adsorb more C3 than PF14/NA and C22-PF14/NA nanoparticles from serum can be attributed to the higher hydrophobicity of NF55 [198] and its complexes with NAs, compared to the other CPPs. Hydrophobic nanoparticles are known to adsorb more C3 than hydrophilic ones [303, 397].

Overall, the complexation of pDNA with CPPs reduced the adsorption of C3 into PC compared with naked pDNA, which would most likely translate to reducing elimination and prolonging the circulation time of the nanoparticles *in vivo*. In the case of SCO, no such effect was observed, with CPP/SCO nanoparticles absorbing the amount of C3 equal to or higher than the naked SCO. This discrepancy between the two NA types is likely due to the SCO having a PS backbone. It is known that oligonucleotides lacking a PS backbone are subjected

to rapid renal clearance, and PS largely determines protein interactions of oligonucleotides, significantly prolonging their half-life [314].

4.1.4. Protein corona affects cellular internalization and biological effects of nanoparticles

Next, we aimed to determine whether the efficiency of SCO in cell culture depends on the serum with which PF14/SCO nanoparticles were incubated during the preparation step. For that, we prepared non-covalent complexes of SCO and PF14, incubated them with different sera, and added them to cells for 1 hour. Our results showed that the uptake of fluorescently labeled SCO by HeLa cells varied significantly depending on the serum used, being the highest in the case of bovine serum and the lowest in the case of human serum. This indicates that PCs with different compositions interact differently with cell surface receptors, affecting cellular binding and uptake of the nanoparticles. Confocal microscopy also showed that the nanoparticles were not targeted into acidic endosomes during the first hour of incubation, consistent with earlier results [264].

Next, we measured the splice-correcting effect of SCO in HeLa pLuc 705 cells when SCO was transfected within PF14 nanoparticles incubated with different sera. Consistent with the uptake experiments, the biological effect of SCO was the highest when the PF14/SCO nanoparticles were incubated with bovine serum and the lowest with human serum. The efficiency of the nanoparticles being the highest in bovine serum can be attributed to the fact that HeLa cells are typically cultured in the presence of this serum, and CPPs are selected based on the uptake efficiency in this milieu. Thus, the PC that forms on PF14 nanoparticles in bovine serum likely triggers endocytosis by HeLa cells more efficiently than the PC assembling in murine or human serum. In addition, unlike in human and murine serum, the most abundant protein in PC forming in bovine serum is serum albumin (**Table 4**), which can favor cellular binding and uptake of the nanoparticles.

4.2. Calcium and magnesium ions enhance the CPP-mediated transfection of nucleic acids (Paper II)

In Paper II, we focused on enhancing the productive transfection of CPP/NA nanoparticles. Our previous research indicated that the cellular entry of CPP nanoparticles is accompanied by an influx of calcium ions [332, 333]. Additionally, it has been shown that the depletion of Ca^{2+} in the intra- and extracellular environment leads to a reduction in the CPP uptake [332]. Several other groups before us investigated adding Ca^{2+} to NAs and NA-containing nanoparticles, showing that calcium supplementation can positively affect NA delivery [334–338]. Magnesium, although chemically similar to calcium, was shown not to enhance transfection of oligonucleotides when added to cell culture media [334] and gene knockdown when added to siRNA [335]. However, its effects were never tested

with CPP/NA complexes. Thus, we aimed to investigate whether adding calcium and magnesium ions to the CPP/NA nanoparticles at the preparation step would be advantageous for their cellular internalization and the resulting biological effect of the cargo.

4.2.1. Ca^{2+} and Mg^{2+} enhance the biological effect of PF14/SCO nanoparticles in a concentration-dependent manner

First, we tested the supplementation of PF14/SCO nanoparticles with Ca^{2+} and Mg^{2+} in HeLa pLuc 705 reporter cells, a model cell line for studying splicing correction. We prepared nanoparticles by mixing SCO and PF14 in MQ water and then, after a 15-minute incubation, adding varying concentrations of $CaCl_2$ and $MgCl_2$. After forming nanoparticles, we added them to the cells and measured the efficiency of splicing correction after a 24-hour incubation. The supplementation of PF14/SCO nanoparticles with Ca^{2+} and Mg^{2+} resulted in a multiple-fold increase in reporter protein expression compared to non-supplemented nanoparticles. The effects of the ions were concentration-dependent, being significant at 30 μM ion concentration (final concentration in cell culture media), reaching the maximum at 1 to 5 mM, and decreasing at higher concentrations. Calcium was generally more efficient than magnesium, providing up to a 9-fold increase in reporter protein expression compared to non-supplemented PF14/SCO nanoparticles, as opposed to an up to 6.4-fold increase provided by magnesium. Additionally, we tested whether the effects were already present at the mRNA level. As expected, both Ca^{2+} and Mg^{2+} increased the amount of correctly spliced luciferase mRNA in the HeLa pLuc 705 cell, as confirmed by PCR. DLS showed that adding the ions to the PF14/SCO nanoparticles slightly increased their size, with non-supplemented PF14/SCO nanoparticles having a hydrodynamic diameter of 230 nm and those supplemented with Ca^{2+} or Mg^{2+} ranging from 300 to 400 nm. The zeta potential of the particles slightly increased upon adding the ions, from 9.3 mV to 10–15 mV, respectively.

We then analyzed cellular association and intracellular distribution of (Ca^{2+}/)PF14/SCO complexes by confocal microscopy and flow cytometry, using fluorescently labeled SCO (SCO-Cy5). Adding Ca^{2+} and Mg^{2+} into nanoparticles enhanced the cellular association of the complexes to some extent, but only by up to 1.8 fold. However, the intracellular distribution of the SCO changed significantly, as confirmed by confocal microscopy. Strong Cy5 fluorescence was detected in cell nuclei of cells transfected with calcium-supplemented PF14/SCO-Cy5 nanoparticles, as opposed to predominantly cytoplasmic localization in the case of complexes prepared without added Ca^{2+}. This is in good concordance with the increased biological activity of SCO, as a larger proportion of the oligonucleotide reached the cell nucleus, its site of action. TEM analysis confirmed the cellular internalization, which mainly occurred through macropinocytosis, and endosomal escape of the calcium-supplemented PF14/SCO nanoparticles. Furthermore, nanogold-labeled SCO was detected at a higher level in the nuclei of cells

incubated with Ca^{2+}/PF14/SCO nanoparticles than of those incubated with non-supplemented complexes. These findings indicate that Ca^{2+} and Mg^{2+} most likely act not only by increasing cellular internalization of PF14/SCO nanoparticles but predominantly by facilitating the endosomal escape of SCO, thus increasing its productive delivery, which otherwise remains very low [264, 273]. The cytoplasmic delivery, in turn, leads to nuclear translocation, as has been previously shown for PS oligonucleotides [272].

To investigate the effect of Ca^{2+} on nanoparticles with different proportions of the components, we prepared PF14/SCO complexes at different molar ratios. Among molar ratios of 1:1, 3:1, 5:1, 10:1, and 20:1 (PF14:SCO), Ca^{2+} exhibited the most significant impact on the nanoparticles prepared at molar ratios 3:1 and 5:1, with the latter demonstrating the most consistent effects and the highest biological response to the delivered SCO. As we increased the molar ratio beyond 5:1, the advantage provided by Ca^{2+} diminished, although the efficiency of non-supplemented complexes rose. Despite calcium ions strongly binding to NAs [398], the high positive charge of nanoparticles containing PF14 in excess might hinder the incorporation of positively charged calcium ions. It is worth noting that an excess of CPP can lead to increased cytotoxicity of the complexes, making nanoparticles with lower peptide concentrations preferable unless delivery efficiency is compromised. Adding Ca^{2+} to nanoparticles presents an excellent solution, enabling the preparation of highly efficient nanoparticles by combining relatively low concentrations of the transfection agent and the ions.

4.2.2. Ca^{2+}-supplemented nanoparticles are internalized via receptor-mediated endocytosis and efficiently escape from endosomes

It has been demonstrated that class A scavenger receptors, specifically SR-A3 and SR-A5, play a crucial role in the internalization of PF14/SCO nanoparticles by cultured human cells [264–267]. To explore the internalization pathways of calcium-supplemented nanoparticles, we used scavenger receptor inhibitors, Poly I and fucoidan. We employed the HeLa pLuc 705 reporter system, transfecting the cells with PF14/SCO nanoparticles supplemented with either 0.3 mM or 3 mM $CaCl_2$. We found that luminescence was significantly reduced when SR-A3/5 receptors were inhibited, indicating their involvement in the internalization. However, higher concentrations of the inhibitors were necessary to suppress the internalization of calcium-supplemented nanoparticles compared to non-supplemented ones. This suggests that while PF14/SCO nanoparticles primarily enter cells via receptor-mediated endocytosis, calcium-supplemented nanoparticles may employ alternative routes not dependent on the scavenger receptors. Additionally, it could indicate that the calcium-supplemented nanoparticles have a higher affinity for the receptors, enabling them to compete with the inhibitors for binding more effectively.

Next, we applied an endosome-destabilizing compound, chloroquine, to assess whether endosomal escape is a limiting step for calcium-supplemented PF14/SCO nanoparticles, similar to non-supplemented ones [196]. For this, we added nanoparticles to the cells in media containing 100 μM chloroquine for 4 hours, then replaced the solutions with fresh media and measured luminescence the next day. While the biological effect of non-supplemented SCO/PF14 nanoparticles was significantly enhanced by chloroquine, calcium-supplemented nanoparticles did not rely on it as much, with the impact of chloroquine decreasing with increasing calcium concentration. This again supports the hypothesis that calcium acts by destabilizing endosomes and facilitating the endosomal escape of nanoparticles.

Previously, it has been shown that simply adding calcium chloride into the transfection media can significantly enhance the biological effect of an oligonucleotide [334]. However, the concentration of Ca^{2+} used in that study was 9 mM, much higher than the efficient concentrations in our experiments. In line with this, we showed that adding Ca^{2+} to PF14/SCO complexes during the preparation of nanoparticles resulted in about 3-fold higher splicing correction than supplementing the media with the same amount of Ca^{2+} and adding already formed complexes after that. This suggests that Ca^{2+} is integrated into the complexes/nanoparticles, as proposed by Baoum and colleagues [336], rather than assisting transfection in some other way. This hypothesis was later corroborated in our subsequent study [210], where we performed an energy dispersive X-ray (EDX) analysis of PF14/SCO nanoparticles supplemented with Ca^{2+} and Mg^{2+} and showed that calcium and magnesium, respectively, are present in the complexes.

In addition to these experiments, we analyzed the applicability of different preparation schemes for calcium-supplemented nanoparticles. Pre-mixing $CaCl_2$ with PF14 before adding SCO resulted in a somewhat lower biological effect of the oligonucleotide than all the other mixing schemes, which included adding Ca^{2+} to pre-formed PF14/SCO complexes, mixing all three components simultaneously, and pre-mixing Ca^{2+} and SCO before adding peptide. Calcium can lead to the aggregation of proteins [399–401], so it is possible that its pre-mixing with PF14 results in interactions that do not favor subsequent complexation with NA.

4.2.3. Ca^{2+} supplementation works with different CPPs and cell lines

Next, we aimed to determine whether the effect of calcium ions applies in different conditions. For that, we used a wider selection of CPPs, including PF6, which contains four chloroquine-like moieties that enhance its ability to escape from endosomes; NickFect-type peptides NF70, NF71, NF72, and NF55; and a PF14 analog with a longer fatty acid moiety C22-PF14. Adding Ca^{2+} had varying effects on the nanoparticles of SCO with these peptides. Ca^{2+} strongly increased the biological effect of SCO delivered within the complexes with C22-PF14, NF55, and NF71 but had little to no effect on nanoparticles prepared with NF70, NF72, and PF6. The possible reason is that all three latter CPPs were designed

for the delivery of siRNA and act in a pH-dependent manner. All three contain modifications that facilitate endosomal escape by inducing a proton sponge effect, i.e., the chloroquine-like moieties in PF6 and multiple histidines in NF70 and NF72. It again indicates that calcium ions primarily act by facilitating endosomal escape of the nanoparticles and fail to increase the efficiency of CPPs that are already fairly good at escaping from endosomes.

Next, we also tested the effects of Ca^{2+} and Mg^{2+} in different cell lines and with different NAs. First, we used another reporter cell line with aberrant splicing, HeLa EGFP 654. Upon hybridization of SCO-654 to an aberrant splice site, functional EGFP is produced, and fluorescence can be detected. Confocal microscopy and flow cytometry showed that both Ca^{2+} and Mg^{2+} increased the expression of EGFP in a concentration-dependent manner, and the difference between the two was negligible. Next, we tested supplementation with Ca^{2+} and Mg^{2+} of PF14/siRNA nanoparticles and of siRNA alone. Interestingly, calcium, but not magnesium ions, enhanced the siRNA-mediated gene knockdown in U87 MG-Luc2 cells without a CPP. The ability of calcium ions to mediate siRNA delivery was already shown earlier [335]. This is an interesting specificity of siRNA, as none of the ions could increase the efficiency of naked SCO in HeLa pLuc 705 cells or, as we tested later, the delivery of pDNA or mRNA. In the case of CPP/siRNA complexes, both calcium and magnesium ions increased the knockdown, but calcium was much more efficient than magnesium at all siRNA concentrations tested. This suggests that the effects of Ca^{2+} and Mg^{2+} are quantitatively and/or qualitatively different, which may only become apparent in the case of some types of cargoes. Remarkably, calcium and magnesium were non-toxic to HeLa pLuc 705 and U87 MG-Luc2 cells at efficient concentrations alone or in combination with PF14.

In addition to Ca^{2+} and Mg^{2+}, we also tested the effects of several other biologically relevant metal ions on PF14/SCO nanoparticles, and surprisingly, a few of them were efficient in HeLa pLuc 705 cells. Namely, Na^{+} and Al^{3+} increased splicing correction by SCO similar to that of Ca^{2+}, while Fe^{3+}, Zn^{2+}, and Mn^{2+} were cytotoxic. However, the effects of these and other ions in different experimental settings are yet to be determined.

4.3. Optimizing PF14-mediated delivery of mRNA into cell lines, primary cells, and *in vivo* (Paper III)

Inspired by the success of mRNA-based vaccines against COVID-19 [87, 88], we aimed to investigate the efficiency of CPP-mediated delivery of mRNA into cell lines, primary cells, and *in vivo*. Being able to encode every protein in the human body, mRNA can potentially be used for the treatment of a wide variety of conditions, with examples, besides infectious diseases, including Alzheimer's disease [5], inherited metabolic disorders [90], cancer [89], and heart injury [91]. Our main objective, however, was the potential treatment of chronic inflammatory disorders, where NA-based therapeutics, including the ones based on mRNA, are

a promising approach for conditions such as asthma, psoriasis, and ICD. Our research group has been studying the ways to combat these diseases with NA-based therapeutics, predominantly miRNA, for years [18, 107, 108, 402]. Here, we employed a mouse model of ICD, a widespread inflammatory skin disorder where tissue damage is caused by innate immune system activation [403]. Potentially, chronic inflammatory skin diseases could be treated by administering mRNA encoding anti-inflammatory cytokines or receptor inhibitors, which then can act as therapeutics [169]. Ideally, the vehicle used for delivering such therapeutic mRNA should support the function of the cargo and be non-cytotoxic and non-immunogenic, making CPPs suitable candidates.

A substantial amount of research has already been conducted regarding CPP-mediated mRNA delivery. There are multiple ways to prepare nanoparticles of a CPP and mRNA, such as covalent conjugation [404], incorporation of lipids [405] and polymers [406], as well as non-covalent complexation of CPP and mRNA. In a recent study, Kim *et al.* showed that upon non-covalent complexation, amphipathic peptides significantly outperform cationic ones in mRNA delivery to cancer cells [407]. In an exciting research by Brand *et al.* [217], PF14 was used to deliver mRNA into tumor cells in a mouse model of ovarian cancer. Remarkably, the authors showed that applying PF14-based nanocomplexes led to a high expression of the mRNA-encoded protein in tumor-associated tissue, outperforming a commercial lipid-based mRNA transfection agent [217, 408].

4.3.1. Ca^{2+} ions enhance PF14-mediated delivery of mRNA into cell lines

In this study, we used four different reporter mRNAs: one encoding firefly luciferase (mRNA-luc), two encoding fluorescent proteins (mRNA-EGFP and mRNA-mCherry), and a fluorescently labeled one (Cy5-mRNA-EGFP). All the used mRNAs were around 1000 nucleotides long and contained modified uridines (see **Table 3**). We prepared PF14/mRNA complexes by mixing the components in MQ water at a charge ratio of 2 and letting nanoparticles form for 30 minutes at room temperature. In addition, we supplemented the nanoparticles with four additives that could potentially increase cellular internalization and endosomal escape of the complexes: Ca^{2+}, Mg^{2+}, chloroquine, and PS80. Among these, Ca^{2+} and Mg^{2+} were tested in our previous study and showed great promise for enhancing the productive delivery of various NAs. Chloroquine is a well-known compound that enhances the endosomal escape of the particles [345]. Finally, PS80 promotes brain translocation of NA-bearing nanoparticles by inducing the adsorption of specific serum proteins into PC [351]. In addition, PS80 has also been shown to promote pDNA uptake by cultured cells and enhance its biological effect, presumably by increasing plasma membrane fluidity and activating endocytosis [356]. Thus, we decided to supplement PF14/mRNA nanoparticles with these four compounds and their combinations to detect their individual as well as possible synergistic effects.

First, we evaluated the physical characteristics of the nanoparticles. While naked mRNAs formed clusters/aggregates with a diameter of over 500 nm, all PF14/mRNA nanoparticles prepared at a charge ratio of 2 were around 120 nm in diameter, except for the ones with mRNA-mCherry, which had a larger diameter of around 300 nm. All PF14/mRNA nanoparticles had a positive zeta potential of around +30 mV, while mRNA alone was negatively charged and PF14 was positively charged, as expected. None of the additives markedly changed the size or zeta potential of the nanoparticles. Overall, these results showed that all the tested nanoparticles had suitable parameters for further experiments.

Next, we assessed the biological effects of the nanoparticles in cell lines. We used two cell lines: HeLa cells, a cancerous cell line typically used in *in vitro* experiments, and HaCaT cells, a human keratinocyte-derived immortalized cell line, which we considered a model representing an intermediate step between cell lines of cancerous origin and primary keratinocytes. The biological effects of the mRNA/PF14 nanoparticles were rather similar in the two cell lines and with two mRNAs tested, mRNA-luc and mRNA-mCherry. All the nanoparticles, non-supplemented and supplemented with additives, induced the expression of reporter proteins. However, among the additives, only Ca^{2+} enhanced the expression of mRNA-encoded mCherry and luciferase reporters. The increase in expression provided by calcium was multiple-fold and concentration-dependent, similar to that observed for other NA types (Paper II). The addition of Mg^{2+} to the PF14/mRNA nanoparticles showed some tendency for a concentration-dependent increase in protein expression from mRNA, which was not statistically significant. Interestingly, the supplementation with PS80 and its combinations with other additives slightly reduced the expression of reporter proteins. Together with our previous research, these data indicate that the effects of different additives largely depend on the NA used. The cell viability assessment showed that most complexes were not toxic to HeLa and HaCaT cells. However, nanoparticles supplemented with PS80 and its combinations with other additives significantly reduced the viability of HaCaT cells, also inducing a slight decrease in the viability of HeLa cells, which was not statistically significant.

4.3.2. PS80 enhances PF14-mediated delivery of mRNA into primary human keratinocytes

Next, we transfected mRNA with PF14 into primary human keratinocytes, also supplementing the PF14/mRNA nanoparticles with additives and their combinations. Calcium was excluded from these experiments, as it is known to induce differentiation of keratinocytes [409, 410]. To test the internalization and intracellular distribution of the complexes, we harnessed Cy5-mRNA-EGFP. All the PF14/mRNA complexes with and without additives were internalized into cells, as confirmed by confocal microscopy. A slightly lower amount of mRNA was associated with cells when PS80 and Mg^{2+} were added to the nanoparticles, as evidenced by the reduced Cy5 signal. The EGFP signal was relatively low in all

conditions, indicating inefficient translation of Cy5-labeled mRNA-EGFP in keratinocytes. Thus, we next analyzed the expression by using mRNA-EGFP and mRNA-luc.

The transfection of mRNA-EGFP within all tested nanoparticles, both non-supplemented and supplemented with the three additives, led to EGFP expression in keratinocytes. Among the additives, PS80 tended to increase EGFP expression from mRNA-EGFP, as detected in confocal microscopy, which appeared to be significant when the same samples were analyzed by flow cytometry. Additionally, the supplementation of PF14/mRNA-luc nanoparticles with PS80 provided a significant, around 34-fold increase in luminescence compared to non-supplemented complexes. At the same time, chloroquine and Mg^{2+} did not produce any increase in luciferase expression. It has previously been shown that PS80 enhances cellular internalization and expression from pDNA in cell lines, probably by increasing cell membrane fluidity and activating endocytosis [356]. Most likely, it acts similarly in the case of keratinocytes. However, the cytotoxicity assessment showed that keratinocytes were more sensitive than cell lines, with PF14/mRNA nanoparticles supplemented with most additives, especially PS80, interfering with cell viability. Thus, although primary human keratinocytes can be successfully transfected with PF14/mRNA nanoparticles, and the efficiency of such transfection can be enhanced by supplementing nanoparticles with certain compounds, such as PS80, it is essential to keep in mind the higher sensitivity of primary cells compared to cell lines.

4.3.3. PF14/mRNA nanoparticles are internalized by cells via macropinocytosis and clathrin-mediated endocytosis

Although it is known that CPPs enter cells predominantly via endocytosis, the exact mechanism is not fully understood and can vary depending on many factors, such as cell type, properties of CPP and its cargo, etc. Thus, we further analyzed the internalization routes of CPP/mRNA nanoparticles by inhibiting different routes of endocytosis. We used the following inhibitors: EIPA to inhibit macropinocytosis, chlorpromazine to inhibit clathrin-mediated endocytosis, and nystatin to inhibit caveolin-mediated endocytosis. In addition to PF14/mRNA nanoparticles, we tested the particles supplemented with the most efficient additives, i.e., Ca^{2+} and PS80 in cell lines and keratinocytes, respectively.

Among the inhibitors, EIPA significantly reduced the reporter protein expression in HeLa cells, indicating that macropinocytosis is the main route of internalizing PF14/mRNA particles by these cells. This result was expected, as macropinocytosis is known to be highly and constitutively active in cancer cells [411]. In the case of HaCaT cells, both EIPA and chlorpromazine caused a significant decrease in the expression of the reporter protein, suggesting that, in addition to macropinocytosis, clathrin-mediated endocytosis was involved in the uptake of the calcium-supplemented PF14/mRNA nanoparticles by cells. Although EIPA and chlorpromazine significantly reduced EGFP expression in keratinocytes, the

effects were not statistically significant. In all three cell types, the effects of the inhibitors were more prominent in the case of PF14/mRNA nanoparticles supplemented with Ca^{2+} and PS80, respectively, compared to the non-supplemented ones. This can be attributed to the higher expression of the reporter protein in the case of supplemented nanoparticles, which provides a higher amplitude of fluorescence signal and enables better detection of an inhibitor-induced reduction of the signal. It should be noted that some of the inhibitors negatively affected cell viability. Specifically, EIPA decreased the viability of the cell lines to some extent, while chlorpromazine compromised the viability of keratinocytes.

It is worth noting that while inhibition of endocytic routes is widely used and provides valuable information about the mechanisms of internalization of various compounds, this strategy has significant limitations. Multiple factors may affect the efficiency and toxicity of the inhibitors, including the composition of the cell culture media, pre-incubation and overall exposure duration, cell seeding density, passage number, etc. [246, 379, 412]. Still, based on our data, we concluded that PF14/mRNA nanoparticles are mainly internalized by HeLa cells via macropinocytosis and by HaCaT cells and primary keratinocytes – most likely by a combination of macropinocytosis and clathrin-mediated endocytosis.

4.3.4. PF14 delivers mRNA *in vivo* in a mouse model of ICD upon local administration

To assess the effectiveness of PF14-mediated mRNA delivery *in vivo* into the skin under inflammatory conditions, we utilized a mouse model of ICD [403]. This model mimics keratinocyte responses characteristic of chronic skin inflammation, such as AD, and was used in this study due to its simplicity [107, 386]. We injected PF14/mRNA, PF14/mRNA/Mg^{2+}, and PF14/mRNA/PS80 complexes subcutaneously into mouse ears, with a subgroup of mice undergoing induction of ICD-like inflammation via topical application of PMA to their ears. PMA-induced skin inflammation involves swelling, increased vascular permeability, and substantial infiltration of inflammatory cells [413]. This model had been previously used to evaluate the anti-inflammatory effects of miRNA nanoparticles formed with PF6 and NF71 [107, 108]. To determine whether a compound or a particle exhibits inflammatory or anti-inflammatory properties, ear thickness is measured before and 24 h after treatment. As our particles did not contain anti-inflammatory mRNA, our first focus was assessing whether mRNA-containing nanoparticles can be delivered and produce protein and whether they induce an unwanted inflammatory response in mice. The administration of nanoparticles did not result in a significant change in ear thickness, whether in PMA-treated or untreated ears, suggesting an absence of inflammation and immune response induced by the nanoparticles. Additionally, levels of inflammatory cytokines in mouse blood were measured via RT-qPCR. The results indicated that levels of inflammatory cytokines in treated mice were not elevated compared to control mice, further confirming the absence of nanoparticle-induced toxicity.

To analyze mRNA transfection and expression of the mRNA-encoded reporter protein, mouse ears were cryosectioned and examined using confocal microscopy. PF14 successfully delivered Cy5-mRNA-EGFP into mouse ears, as evidenced by the Cy5 signal observed upon subcutaneous injection of the nanoparticles. Interestingly, while the Cy5 signal was detected in both untreated and PMA-treated ears, a higher amount was observed in the PMA-treated ears. Similarly, the expression of mRNA-encoded EGFP was also higher in inflamed ears than non-inflamed ones. This phenomenon could be attributed to the loosening of tight junctions between cells during inflammation [414, 415], facilitating the spread of complexes.

Unexpectedly, neither $CaCl_2$ nor PS80 enhanced the internalization of PF14/mRNA complexes or the biological effect of the delivered mRNA. Since we detected reporter protein expression in a relatively low number of cells, further optimization of subcutaneous CPP-mediated mRNA delivery is necessary. The fact that some additives enhanced the expression of an mRNA-encoded protein in cell culture but failed to exhibit similar effects *in vivo* highlights that results obtained in the former system cannot always be directly translated to the latter. One reason, as mentioned in Paper I, could be the formation of a PC around nanoparticles, which can have significantly different compositions in cell culture media and mouse tissue, thereby substantially altering the properties of nanoparticles and their cellular internalization. Another reason is the mechanically different environment: while in cell culture experiments, the nanoparticles can freely move in the solution and spread across the cell population, *in vivo*, the migration of the particles is physically constrained. PC-bearing particles tend to be larger and more prone to aggregation than those formed in aqueous solution, which can hinder the spreading and cellular internalization of PF14/mRNA complexes in our *in vivo* experiments. This limitation is partially resolved by inducing inflammation and ear swelling, resulting in wider mRNA distribution and higher expression of the encoded protein. In addition, although no inflammation was detected in transfected ears, immune cells, such as tissue macrophages, can mediate the clearance of the particles. Finally, *in vivo*, nanoparticles can be carried away from their site of action by blood flow.

Nevertheless, PF14 delivered mRNA into mouse ears *in vivo*, mediating the expression of the reporter protein, with PF14/mRNA nanoparticles being non-immunogenic. Still, further optimization of such delivery and developing new carrier peptides for mRNA delivery *in vivo* are required.

5. CONCLUSIONS

CPPs show great potential as vehicles for NA delivery in biotechnology and biomedicine. However, their application is limited by an incomplete understanding of their mechanisms of action and by their insufficient potency at delivering cargo molecules.

The main goal of the current thesis was to examine the limiting factors affecting the activity of CPP/NA nanoparticles by analyzing the effects and composition of the protein corona formed around them in the presence of blood serum and to study ways to increase the efficiency of such nanoparticles by supplementing them with different additives. The key findings of the current thesis are listed below.

Paper I:

- In the presence of serum, PC quickly forms around CPP/NA nanoparticles.
- PC can increase the size of nanoparticles and trigger their aggregation.
- PC with different compositions is formed in the presence of bovine, murine, and human serum.
- The main constituents of all analyzed protein coronae were proteins involved in transport, blood coagulation, and complement system.
- C3, the protein inducing the activation of the complement system and elimination of nanoparticles, was present at a high level in all analyzed coronae.
- Complexation with CPP can protect NAs with phosphodiester backbone from opsonization by C3.
- Cellular uptake of CPP/NA nanoparticles and the resulting biological efficiency in eukaryotic cells depend on the PC forming around them.

Paper II:

- Calcium and magnesium ions increase the efficiency of SCO delivered into cultured cells by PF14 in a concentration-dependent manner, with the effect of calcium being higher than that of magnesium.
- Calcium and magnesium ions slightly increase the hydrodynamic diameter and zeta potential of PF14/SCO nanoparticles.
- Calcium supplementation increases the nuclear localization of SCO delivered by PF14.
- Calcium ions most likely act by facilitating the endosomal escape of the nanoparticles.
- Calcium supplementation is efficient in the case of different CPPs, NAs, and cell lines, although the effects vary depending on the composition of complexes.
- Calcium, but not magnesium, can mediate transfection of naked siRNA.
- Other biologically relevant ions may have effects similar to calcium and magnesium, but this topic requires further investigation.

Paper III

- PF14 forms with mRNA nanoparticles ranging from 100 to 300 nm and having a positive surface charge of approximately +30 mV.
- The tested additives – Ca^{2+}, Mg^{2+}, chloroquine, and PS80 – do not significantly alter physical properties of the nanoparticles.
- PF14 can deliver mRNA into cell lines, primary cells, and *in vivo* into mouse ears.
- Ca^{2+} supplementation enhances PF14-mediated transfection of mRNA into cell lines and PS80 supplementation – into primary human keratinocytes.
- HeLa cells predominantly internalize PF14/mRNA nanoparticles via macropinocytosis, while HaCaT cells and primary human keratinocytes also utilize clathrin-mediated endocytosis.
- PF14/mRNA nanoparticles are non-immunogenic *in vivo* upon subcutaneous injection.
- Neither Mg^{2+} nor PS80 significantly increases PF14-mediated delivery of mRNA *in vivo* in a mouse model of ICD despite showing promising results *in vitro*.

SUMMARY IN ESTONIAN

Rakkudesse penetreeruvatel peptiididel põhinevate nanopartiklite omaduste optimeerimine nukleiinhapete transpordiks

Nukleiinhapetel põhinev geeniekspressiooni muutmine on leidnud üha enam rakendamist biotehnoloogias ja biomeditsiinis, nii kaasasündinud kui omandatud haiguste raviks. Paraku ei ole sellised molekulid organismis alati piisavalt stabiilsed ning suure molekulmassi ja negatiivse laengu tõttu ei suuda need läbida bioloogiliste membraanide barjääre. Sellest tulenevalt on välja töötatud mitmeid kandursüsteeme nukleiinhapete transpordiks, mis suurendavad nende stabiilsust organismis ning võimaldavad nende efektiivset toimetamist märklaudrakkude ja -molekulideni. Üheks selliseks transportsüsteemiks on rakkudesse penetreeruvad peptiidid (RPP). Need on kuni 30 aminohappe pikkused peptiidid, mis on reeglina positiivselt laetud ning koonduvad nukleiinhapetega mittekovalentseteks nanoosakesteks. RPP-dega vahendatud transport on efektiivne rakukultuuris, aga elusorganismides kasutamiseks vajab see siiski veel optimeerimist. Üheks suurimaks takistuseks, mis piirab RPP-dega transpordi efektiivsust, on toimeaine ehk nukleiinhappe lagundamine endosoomides ja lüsosoomides. Teiseks oluliseks faktoriks, mille tõttu isegi need RPP-d, mis näitavad kõrget efektiivsust rakukultuuris, on tihtipeale väheefektiivsed elusorganismis, on nn valgukrooni moodustumine nanoosakeste pinnale. Valgukroon on verevalkude kiht, mis tekib verre sattuvate osakeste pinnale ja võib põhjustada osakeste agregatsiooni, suurendada toksilisust ja suunata organismist eemaldamist.

Käesolevas töös uurisime tegureid, mis piiravad RPP/nukleiinhape komplekside efektiivsust, ning viise, kuidas seda efektiivsust suurendada. Mudelpeptiidina kasutasime PepFect14 (PF14), amfipaatset stearüülitud peptiidi, mille laeng on +5. Esimeses artiklis analüüsisime valgukrooni teket PF14/oligonukleotiidi ja PF14/plasmiidi osakeste pinnale erinevate loomade vereseerumites. Näitasime, et osakestele moodustuv valgukroon võib suurendada nende diameetrit ja põhjustada agregatsiooni, mida tuleb arvesse võtta osakeste *in vivo* rakendamisel. Teiseks kirjeldasime hiire-, veise- ja inimseerumis tekkiva valgukrooni koostist, näidates, et selle suurima osa moodustavad transpordi, verehüübe ja immuunreaktsiooni tekkes osalevad valgud. Lisaks sellele näitasime, et valgukroon mõjutab oluliselt osakeste transfektsiooni ja efektiivsust rakukultuuris, osutades taas selle olulisusele osakeste disainis. Valgukrooni koostise modifitseerimist ja selle abil osakeste omaduste muutmist on rakendatud teiste osakeste tüüpide puhul. Tulevikus võib see osutuda perspektiivikaks ka RPP-del põhinevate osakeste puhul.

Teises artiklis uurisime Ca^{2+} ja Mg^{2+} ioonide mõju RPP/nukleiinhape osakeste omadustele ja efektiivsusele. Näitasime, et PF14 ja oligonukleotiidist koosnevate osakeste suurus ja pinnalaeng suurenevad mõnevõrra, kui osakestesse on lisatud divalentsete metalliioonid. Nii kaltsium kui ka magneesium suurendasid PF14/nukleiinhape osakeste efektiivsust rakukultuuris mitmekordselt, toimides erinevate nukleiinhapete ja rakuliinide puhul, samas ioonide efektid varieerusid sõltuvalt

kasutatud RPP-st. Meie tulemused näitavad, et lisatud ioonide efekt põhineb tõenäoliselt endosoomidest vabanemise suurendamisel, mille tõttu suurem osakaal rakkudesse jõudnud nukleiinhappest satub tsütoplasmasse ja annab bioloogilist efekti. Lisaks sellele näitasime, et selliste osakeste sisenemiseks rakkudesse on olulised püüdurretseptorid, nimelt SR-A3 ja SR-A5, mis teadaolevalt osalevad ka ilma ioonide lisamiseta valmistatud PF14/nukleiinhape osakeste rakkudesse sisenemises. Avastasime, et mõned teised positiivselt laetud ioonid võivad omada kaltsiumile ja magneesiumile sarnast mõju PF14/oligo osakeste transfektsioonile, kuid see on eraldi uuringut vajav teema.

Kolmandas artiklis uurisime mRNA transfektsiooni PF14 abil. mRNA on suure potentsiaaliga ravimolekul, ning mRNA-l põhinevaid ravimeid töötatakse välja paljude haiguste raviks, alustades infektsioonhaigustest ja lõpetades vähiga. Meie moodustasime osakesed mRNA-st ja PF14 ning lisasime neile Ca^{2+}, Mg^{2+}, klorokviini ja polüsorbaat 80 (PS80) suurendamaks osakeste efektiivsust. Näitasime, et PF14 moodustab mRNA-ga 100–300 nm hüdrodünaamilise diameetriga ja positiivse pinnalaenguga osakesi. PF14 oli võimeline viima mRNA-d rakuliinidesse, primaarsetesse keratinotsüütidesse ja *in vivo* hiirte kõrvarakkudesse. Ca^{2+} ioonid suurendasid mitmekordselt PF14/mRNA komplekside transfektsiooni rakuliinidesse ning PS80 omas tugevat positiivset efekti keratinotsüütide puhul. Vaatamata ülalmainitud lisandite kõrgele efektiivsusele *in vitro*, ei suurendanud need PF14/mRNA osakeste sisenemist ja reportervalgu ekspressiooni *in vivo*. Tähelepanuväärselt, oli PF14 võimeline sisestama mRNA hiirte kõrvarakkudesse ning transfektsioon ei kutsunud esile immuunsüsteemi aktivatsiooni. Meie tulemustest võib järeldada, et PF14 on sobiv kandja mRNA jaoks, aga see transportsüsteem vajab optimeerimist.

Kokkuvõtteks, käesolevas töös käsitlesime RPP-vahendatud nukleiinhapete transfektsiooni erinevate nurkade alt: uurisime selle efektiivsust piiravaid tegureid, nagu valgukrooni teke ja endosoomidesse jäämine; osakeste efektiivsuse suurendamist divalentsete metalliioonide lisamise abil; ning suhteliselt vähe uuritud mRNA transfektsiooni RPP-dega. Antud töö laiendab teadmisi RPP-dest ja nendega vahendatud transpordist rakkudesse, püstitades uusi küsimusi ja tuues esile edasist uurimist vajavaid suundi.

REFERENCES

1. Tran, T.H., et al. Modulation of macrophage functional polarity towards anti-inflammatory phenotype with plasmid DNA delivery in cd44 targeting hyaluronic acid nanoparticles. *Scientific Reports* **5** (2015).
2. Wang, W., et al. An injectable conductive hydrogel encapsulating plasmid DNA-enos and adscs for treating myocardial infarction. *Biomaterials* **160**, 69–81 (2018).
3. Pardi, N., et al. MRNA vaccines – a new era in vaccinology. *Nature Reviews Drug Discovery* **17**, 261–279 (2018).
4. Thess, A., et al. Sequence-engineered mRNA without chemical nucleoside modifications enables an effective protein therapy in large animals. *Molecular Therapy* **23**, 1456–1464 (2015).
5. Lin, C.Y., et al. Messenger RNA-based therapeutics for brain diseases: An animal study for augmenting clearance of beta-amyloid by intracerebral administration of neprilysin mRNA loaded in polyplex nanomicelles. *Journal of Controlled Release* **235**, 268–275 (2016).
6. Hill, S.F., Meisler, M.H. Antisense oligonucleotide therapy for neurodevelopmental disorders. *Developmental Neuroscience* **43**, 247–252 (2021).
7. Di Fusco, D., et al. Antisense oligonucleotide: Basic concepts and therapeutic application in inflammatory bowel disease. *Frontiers in Pharmacology* **10** (2019).
8. Sasaki, S., et al. Steric inhibition of 5′ UTR regulatory elements results in upregulation of human CFTR. *Molecular Therapy* **27**, 1749–1757 (2019).
9. Duvalvalentin, G., et al. Specific inhibition of transcription by triple helix-forming oligonucleotides. *Proceedings of the National Academy of Sciences of the United States of America* **89**, 504–508 (1992).
10. Li, C., et al. Triplex-forming oligonucleotides as an anti-gene technique for cancer therapy. *Frontiers in Pharmacology* **13** (2022).
11. Strobel, S.A., Dervan, P.B. Site-specific cleavage of a yeast chromosome by oligonucleotide-directed triple-helix formation. *Science* **249**, 73–75 (1990).
12. Chen, M., Manley, J.L. Mechanisms of alternative splicing regulation: Insights from molecular and genomics approaches. *Nature Reviews Molecular Cell Biology* **10**, 741–754 (2009).
13. Khajavi, M., et al. Nonsense-mediated mRNA decay modulates clinical outcome of genetic disease. *European Journal of Human Genetics* **14**, 1074–1081 (2006).
14. Nickless, A., et al. Control of gene expression through the nonsense-mediated RNA decay pathway. *Cell and Bioscience* **7** (2017).
15. Zahir-Jouzdani, F., et al. Sirna delivery for treatment of degenerative diseases, new hopes and challenges. *Journal of Drug Delivery Science and Technology* **45**, 428–441 (2018).
16. Chalbatani, G.M., et al. Small interfering RNAs (siRNAs) in cancer therapy: A nano-based approach. *International Journal of Nanomedicine* **14**, 3111–3128 (2019).
17. Song, E.W., et al. Rna interference targeting fas protects mice from fulminant hepatitis. *Nature Medicine* **9**, 347–351 (2003).
18. Rebane, A., et al. Microrna-146a alleviates chronic skin inflammation in atopic dermatitis through suppression of innate immune responses in keratinocytes. *J Allergy Clin Immunol* **134**, 836–847 e11 (2014).
19. Tao, Y.Y., et al. Delivery of microRNA-33 antagomirs by mesoporous silica nanoparticles to ameliorate lipid metabolic disorders. *Frontiers in Pharmacology* **11** (2020).

20. Zheng, Q.P., et al. Precise gene deletion and replacement using the CRISPR/Cas9 system in human cells. *Biotechniques* **62** (2017).
21. Li, H.Y., et al. Applications of genome editing technology in the targeted therapy of human diseases: Mechanisms, advances and prospects. *Signal Transduction and Targeted Therapy* **5** (2020).
22. Komor, A.C., et al. Programmable editing of a target base in genomic DNA without double-stranded DNA cleavage. *Nature* **533**, 420–+ (2016).
23. Nishida, K., et al. Targeted nucleotide editing using hybrid prokaryotic and vertebrate adaptive immune systems. *Science* **353** (2016).
24. Gaudelli, N.M., et al. Programmable base editing of a.T to g.C in genomic DNA without DNA cleavage. *Nature* **551**, 464–+ (2017).
25. Kim, H., Kim, J.S. A guide to genome engineering with programmable nucleases. *Nature Reviews Genetics* **15**, 321–334 (2014).
26. Carattoli, A. Plasmids and the spread of resistance. *International Journal of Medical Microbiology* **303**, 298–304 (2013).
27. Klinman, D.M., et al. Contribution of CPG motifs to the immunogenicity of DNA vaccines. *Journal of Immunology* **158**, 3635–3639 (1997).
28. Chen, Z.Y., et al. Silencing of episomal transgene expression by plasmid bacterial DNA elements in vivo. *Gene Therapy* **11**, 856–864 (2004).
29. Pang, A.S.D. Production of antibodies against bacillus-thuringiensis delta-endotoxin by injecting its plasmids. *Biochemical and Biophysical Research Communications* **202**, 1227–1234 (1994).
30. Valera, A., et al. Expression of the neomycin-resistance (neo) gene induces alterations in gene expression and metabolism. *Human Gene Therapy* **5**, 449–456 (1994).
31. Gaspar, V., et al. Minicircle DNA vectors for gene therapy: Advances and applications. *Expert Opinion on Biological Therapy* **15**, 353–379 (2015).
32. Karikó, K., et al. Suppression of RNA recognition by toll-like receptors:: The impact of nucleoside modification and the evolutionary origin of RNA. *Immunity* **23**, 165–175 (2005).
33. Karikó, K., et al. Incorporation of pseudouridine into mRNA yields superior nonimmunogenic vector with increased translational capacity and biological stability. *Molecular Therapy* **16**, 1833–1840 (2008).
34. Morais, P., et al. The critical contribution of pseudouridine to mRNA COVID-19 vaccines. *Frontiers in Cell and Developmental Biology* **9** (2021).
35. Moradian, H., et al. Chemical modification of uridine modulates mRNA-mediated proinflammatory and antiviral response in primary human macrophages. *Molecular Therapy-Nucleic Acids* **27**, 854–869 (2022).
36. Li, B., et al. Effects of chemically modified messenger RNA on protein expression. *Bioconjugate Chemistry* **27**, 849–853 (2016).
37. Ramanathan, A., et al. MRNA capping: Biological functions and applications. *Nucleic Acids Research* **44**, 7511–7526 (2016).
38. Inagaki, M., et al. Cap analogs with a hydrophobic photocleavable tag enable facile purification of fully capped mRNA with various cap structures. *Nature Communications* **14** (2023).
39. Devarkar, S.C., et al. Structural basis for m7g recognition and 2′-o-methyl discrimination in capped RNAs by the innate immune receptor rig-i. *Proceedings of the National Academy of Sciences of the United States of America* **113**, 596–601 (2016).
40. Jemielity, J., et al. Novel "anti-reverse" cap analogs with superior translational properties. *Rna* **9**, 1108–1122 (2003).

41. Vaidyanathan, S., et al. Uridine depletion and chemical modification increase Cas9 mRNA activity and reduce immunogenicity without HPLC purification. *Molecular Therapy-Nucleic Acids* **12**, 530–542 (2018).
42. Shanmugasundaram, M., et al. Recent advances in modified cap analogs: Synthesis, biochemical properties, and mRNA-based vaccines. *Chemical Record* **22** (2022).
43. Fairclough, R.J., et al. Therapy for Duchenne muscular dystrophy: Renewed optimism from genetic approaches. *Nat Rev Genet* **14**, 373–8 (2013).
44. Thein, S.L. The molecular basis of β-thalassemia. *Cold Spring Harbor Perspectives in Medicine* **3** (2013).
45. Fackenthal, J.D., Godley, L.A. Aberrant rna splicing and its functional consequences in cancer cells. *Disease Models & Mechanisms* **1**, 37–42 (2008).
46. Scoto, M., et al. Genetic therapies for inherited neuromuscular disorders. *Lancet Child & Adolescent Health* **2**, 600–609 (2018).
47. Aartsma-Rus, A., van Ommen, G.J. Antisense-mediated exon skipping: A versatile tool with therapeutic and research applications. *RNA* **13**, 1609–24 (2007).
48. Bestas, B., et al. Splice-correcting oligonucleotides restore BTK function in X-linked agammaglobulinemia model. *J Clin Invest* **124**, 4067–81 (2014).
49. Busslinger, M., et al. Beta+ thalassemia – aberrant splicing results from a single point mutation in an intron. *Cell* **27**, 289–298 (1981).
50. Hua, Y.M., et al. Antisense correction of smn2 splicing in the CNS rescues necrosis in a type iii sma mouse model. *Genes & Development* **24**, 1634–1644 (2010).
51. Hua, Y.M., et al. Antisense masking of an hnrnp a1/a2 intronic splicing silencer corrects smn2 splicing in transgenic mice. *American Journal of Human Genetics* **82**, 834–848 (2008).
52. Tanner, M.K., et al. Targeted splice sequencing reveals RNA toxicity and therapeutic response in myotonic dystrophy. *Nucleic Acids Research* **49**, 2240–2254 (2021).
53. Eckstein, F. Phosphorothioates, essential components of therapeutic oligonucleotides. *Nucleic Acid Therapeutics* **24**, 374–387 (2014).
54. Gaus, H.J., et al. Characterization of the interactions of chemically modified therapeutic nucleic acids with plasma proteins using a fluorescence polarization assay. *Nucleic Acids Res* **47**, 1110–1122 (2018).
55. Monia, B.P., et al. Evaluation of 2'-modified oligonucleotides containing 2'-deoxy gaps as antisense inhibitors of gene expression. *Journal of Biological Chemistry* **268**, 14514–14522 (1993).
56. Roberts, T.C., et al. Advances in oligonucleotide drug delivery. *Nat Rev Drug Discov* **19**, 673–694 (2020).
57. Nielsen, P., et al. Synthesis and evaluation of oligodeoxynucleotides containing acyclic nucleosides – introduction of 3 novel analogs and a summary. *Bioorganic & Medicinal Chemistry* **3**, 19–28 (1995).
58. Kim, Y. Drug discovery perspectives of antisense oligonucleotides. *Biomolecules & Therapeutics* **31**, 241–252 (2023).
59. Steffens, R., Leumann, C.J. Synthesis and thermodynamic and biophysical properties of tricyclo-DNA. *Journal of the American Chemical Society* **121**, 3249–3255 (1999).
60. Nan, Y.C., Zhang, Y.J. Antisense phosphorodiamidate morpholino oligomers as novel antiviral compounds. *Frontiers in Microbiology* **9** (2018).

61. Pellestor, F., Paulasova, P. The peptide nucleic acids (PNAs), powerful tools for molecular genetics and cytogenetics. *European Journal of Human Genetics* **12**, 694–700 (2004).
62. Aoki, Y., et al. Fine-tuning of phosphorothioate inclusion in 2′-o-methyl oligonucleotides contributes to specific cell targeting for splice-switching modulation. *Frontiers in Physiology* **12** (2021).
63. Jadhav, V., et al. Rna interference in the era of nucleic acid therapeutics. *Nature Biotechnology* (2024).
64. Hammond, S.M., et al. Post-transcriptional gene silencing by double-stranded RNA. *Nature Reviews Genetics* **2**, 110–119 (2001).
65. Agrawal, N., et al. Rna interference: Biology, mechanism, and applications. *Microbiology and Molecular Biology Reviews* **67**, 657–+ (2003).
66. O'Brien, J., et al. Overview of microRNA biogenesis, mechanisms of actions, and circulation. *Frontiers in Endocrinology* **9** (2018).
67. Carthew, R.W., Sontheimer, E.J. Origins and mechanisms of miRNAs and siRNAs. *Cell* **136**, 642–655 (2009).
68. Shang, R.F., et al. MicroRNAs in action: Biogenesis, function and regulation. *Nature Reviews Genetics* **24**, 816–833 (2023).
69. Ding, S.W. Rna-based antiviral immunity. *Nature Reviews Immunology* **10**, 632–644 (2010).
70. Lam, J.K.W., et al. Sirna versus miRNA as therapeutics for gene silencing. *Molecular Therapy-Nucleic Acids* **4** (2015).
71. Selvam, C., et al. Therapeutic potential of chemically modified siRNA: Recent trends. *Chemical Biology & Drug Design* **90**, 665–678 (2017).
72. Tang, Q.a.K., A. Rnai-based drug design: Considerations and future directions. *Nature Reviews Drug Discovery* (2024).
73. Belgrad, J., et al. Nucleic acid therapeutics: Successes, milestones, and upcoming innovation. *Nucleic Acid Therapeutics* **34**, 52–72 (2024).
74. Roehr, B. Fomivirsen approved for CMV retinitis. *J Int Assoc Physicians AIDS Care* **4**, 14–6 (1998).
75. Aartsma-Rus, A., Krieg, A.M. Fda approves eteplirsen for Duchenne muscular dystrophy: The next chapter in the eteplirsen saga. *Nucleic Acid Ther* **27**, 1–3 (2017).
76. Heo, Y.A. Golodirsen: First approval. *Drugs* **80**, 329–333 (2020).
77. Dhillon, S. Viltolarsen: First approval. *Drugs* **80**, 1027–1031 (2020).
78. Roshmi, R.R.a.Y., T. Viltolarsen: From preclinical studies to FDA approval. *Methods Mol Biol* **2587**, 31–41 (2023).
79. Shirley, M. Casimersen: First approval. *Drugs* **81**, 875–879 (2021).
80. Hoy, S.M. Nusinersen: First global approval. *Drugs* **77**, 473–479 (2017).
81. Egli, M., Manoharan, M. Chemistry, structure and function of approved oligonucleotide therapeutics. *Nucleic Acids Research* **51**, 2529–2573 (2023).
82. Hair, P., et al. Mipomersen sodium: First global approval. *Drugs* **73**, 487–493 (2013).
83. Hussain, A., et al. MRNA vaccines for COVID-19 and diverse diseases. *Journal of Controlled Release* **345** (2022).
84. Fang, E.Y., et al. Advances in COVID-19 mRNA vaccine development. *Signal Transduction and Targeted Therapy* **7** (2022).
85. Sasso, J.M., et al. The progress and promise of RNA medicine?An arsenal of targeted treatments. *Journal of Medicinal Chemistry* **65**, 6975–7015 (2022).
86. Kulkarni, J.A., et al. The current landscape of nucleic acid therapeutics (vol 16, pg 630, 2021). *Nature Nanotechnology* **16**, 841–841 (2021).

87. Polack, F.P., et al. Safety and efficacy of the bnt162b2 mRNA COVID-19 vaccine. *New England Journal of Medicine* **383**, 2603–2615 (2020).
88. Baden, L.R., et al. Efficacy and safety of the mRNA-1273 sars-cov-2 vaccine. *New England Journal of Medicine* **384**, 403–416 (2021).
89. Kubler, H., et al. Self-adjuvanted mRNA vaccination in advanced prostate cancer patients: A first-in-man phase i/iia study. *Journal for Immunotherapy of Cancer* **3** (2015).
90. Truong, B., et al. Lipid nanoparticle-targeted mRNA therapy as a treatment for the inherited metabolic liver disorder arginase deficiency. *Proceedings of the National Academy of Sciences of the United States of America* **116**, 21150–21159 (2019).
91. Sultana, N., et al. Optimizing cardiac delivery of modified mRNA. *Molecular Therapy* **25**, 1306–1315 (2017).
92. Curreri, A., et al. Rna therapeutics in the clinic. *Bioengineering & Translational Medicine* **8** (2023).
93. Akinc, A., et al. Targeted delivery of RNAi therapeutics with endogenous and exogenous ligand-based mechanisms. *Mol Ther* **18**, 1357–64 (2010).
94. Adams, D., et al. Patisiran, an RNAi therapeutic, for hereditary transthyretin amyloidosis. *New England Journal of Medicine* **379**, 11–21 (2018).
95. Ständer, S. Atopic dermatitis. *New England Journal of Medicine* **384**, 1136–1143 (2021).
96. Porsbjerg, C., et al. Asthma. *Lancet* **401**, 858–873 (2023).
97. Dinarello, C.A. Interleukin-1 in the pathogenesis and treatment of inflammatory diseases. *Blood* **117**, 3720–3732 (2011).
98. Popa, C., et al. The role of TNF-alpha in chronic inflammatory conditions, intermediary metabolism, and cardiovascular risk. *Journal of Lipid Research* **48**, 751–762 (2007).
99. Gabay, C. Interleukin-6 and chronic inflammation. *Arthritis Research & Therapy* **8** (2006).
100. Rebane, A., et al. Mechanisms of IFN-gamma-induced apoptosis of human skin keratinocytes in patients with atopic dermatitis. *J Allergy Clin Immunol* **129**, 1297–306 (2012).
101. Barnes, P.J. Inhaled corticosteroids in COPD: A controversy. *Respiration* **80**, 89–95 (2010).
102. Chiricozzi, A., et al. Topical corticosteroids for pediatric atopic dermatitis: Thoughtful tips for practice. *Pharmacological Research* **158** (2020).
103. Wollina, U. The role of topical calcineurin inhibitors for skin diseases other than atopic dermatitis. *American Journal of Clinical Dermatology* **8**, 157–173 (2007).
104. Rice, J.B., et al. Long-term systemic corticosteroid exposure: A systematic literature review. *Clinical Therapeutics* **39**, 2216–2229 (2017).
105. Plichta, J., et al. Biologic drugs in the treatment of chronic inflammatory pulmonary diseases: Recent developments and future perspectives. *Frontiers in Immunology* **14** (2023).
106. Dragonieri, S., Portacci, A., Quaranta, V. N. and Carpagnano, G. E. Advancing care in severe asthma: The art of switching biologics. *Advances in Respiratory Medicine* **92**, 110–122 (2024).
107. Carreras-Badosa, G., et al. Nickfect type of cell-penetrating peptides present enhanced efficiency for microRNA-146a delivery into dendritic cells and during skin inflammation. *Biomaterials* **262**, 120316 (2020).

108. Urgard, E., et al. Pre-administration of PepFect6-microRNA-146a nanocomplexes inhibits inflammatory responses in keratinocytes and in a mouse model of irritant contact dermatitis. *J Control Release* **235**, 195–204 (2016).
109. Deng, J., et al. Anti-inflammatory therapy for temporomandibular joint osteoarthritis using mRNA medicine encoding interleukin-1 receptor antagonist. *Pharmaceutics* **14** (2022).
110. Deng, R.H., et al. Chitosan/hyaluronic acid/plasmid-DNA nanoparticles encoding interleukin-1 receptor antagonist attenuate inflammation in synoviocytes induced by interleukin-1 beta. *Journal of Materials Science-Materials in Medicine* **29** (2018).
111. Gao, M.Z., et al. Modulating plaque inflammation via targeted mRNA nanoparticles for the treatment of atherosclerosis. *Acs Nano* **17**, 17721–17739 (2023).
112. Wang, W., et al. Adipose-derived stem cells enriched with therapeutic mRNA TGF-β3 and IL-10 synergistically promote scar-less wound healing in preclinical models. *Bioengineering & Translational Medicine* **9** (2024).
113. Trepicchio, W.L., et al. Interleukin-11 therapy selectively downregulates type I cytokine proinflammatory pathways in psoriasis lesions (vol 104, pg 1527, 1999). *Journal of Clinical Investigation* **105**, 396–396 (2000).
114. Won, J., et al. Inhaled delivery of interferon-lambda restricts epithelial-derived th2 inflammation in allergic asthma. *Cytokine* **119**, 32–36 (2019).
115. Mendes, B.B., et al. Nanodelivery of nucleic acids. *Nature Reviews Methods Primers* **2** (2022).
116. Shtykalova, S., et al. Non-viral carriers for nucleic acids delivery: Fundamentals and current applications. *Life-Basel* **13** (2023).
117. Lu, M., et al. Overcoming pharmaceutical bottlenecks for nucleic acid drug development. *Accounts of Chemical Research* **56**, 224–236 (2023).
118. Fajrial, A.K., et al. A review of emerging physical transfection methods for CRISPR/Cas9-mediated gene editing. *Theranostics* **10**, 5532–5549 (2020).
119. Hurford, R.K., et al. Gene-therapy of metastatic cancer by in-vivo retroviral gene targeting. *Nature Genetics* **10**, 430–435 (1995).
120. Boulis, N.M., et al. Adenoviral nerve growth factor and β-galactosidase transfer to spinal cord: A behavioral and histological analysis. *Journal of Neurosurgery* **90**, 99–108 (1999).
121. Azzouz, M., et al. Increased motoneuron survival and improved neuromuscular function in transgenic als mice after intraspinal injection of an adeno-associated virus encoding bcl-2. *Human Molecular Genetics* **9**, 803–811 (2000).
122. Bulcha, J.T., et al. Viral vector platforms within the gene therapy landscape. *Signal Transduction and Targeted Therapy* **6** (2021).
123. Zhang, W.W., et al. The first approved gene therapy product for cancer ad-p53 (gendicine): 12 years in the clinic. *Human Gene Therapy* **29**, 160–179 (2018).
124. Ylä-Herttuala, S. Endgame: Glybera finally recommended for approval as the first gene therapy drug in the european union. *Molecular Therapy* **20**, 1831–1832 (2012).
125. Schimmer, J., Breazzano, S. Investor outlook: Rising from the ashes; gsk's european approval of strimvelis for ADA-SCID. *Human Gene Therapy Clinical Development* **27**, 57–61 (2016).
126. Darrow, J.J. Luxturna: FDA documents reveal the value of a costly gene therapy. *Drug Discovery Today* **24**, 949–954 (2019).
127. Hacein-Bey-Abina, S., et al. Insertional oncogenesis in 4 patients after retrovirus-mediated gene therapy of scid-x1. *Journal of Clinical Investigation* **118**, 3132–3142 (2008).

128. Raper, S.E., et al. Fatal systemic inflammatory response syndrome in a ornithine transcarbamylase deficient patient following adenoviral gene transfer. *Molecular Genetics and Metabolism* **80**, 148–158 (2003).
129. Roldao, A., et al. Viruses and virus-like particles in biotechnology: Fundamentals and applications. *Comprehensive Biotechnology, Vol 1: Scientific Fundamentals of Biotechnology, 2nd Edition*, 625–649 (2011).
130. Nooraei, S., et al. Virus-like particles: Preparation, immunogenicity and their roles as nanovaccines and drug nanocarriers. *Journal of Nanobiotechnology* **19** (2021).
131. Gao, Y.G., et al. Recent advance of liposome nanoparticles for nucleic acid therapy. *Pharmaceutics* **15** (2023).
132. Samaridou, E., et al. Lipid nanoparticles for nucleic acid delivery: Current perspectives. *Advanced Drug Delivery Reviews* **154**, 37–63 (2020).
133. Semple, S.C., et al. Efficient encapsulation of antisense oligonucleotides in lipid vesicles using ionizable aminolipids: Formation of novel small multilamellar vesicle structures. *Biochimica Et Biophysica Acta-Biomembranes* **1510**, 152–166 (2001).
134. Chen, J.J., et al. Lipid nanoparticle-mediated lymph node-targeting delivery of mRNA cancer vaccine elicits robust cd8+ t cell response. *Proceedings of the National Academy of Sciences of the United States of America* **119** (2022).
135. Bevers, S., et al. MRNA-LNP vaccines tuned for systemic immunization induce strong antitumor immunity by engaging splenic immune cells. *Molecular Therapy* **30**, 3078–3094 (2022).
136. Akinc, A., et al. The onpattro story and the clinical translation of nanomedicines containing nucleic acid-based drugs. *Nat Nanotechnol* **14**, 1084–1087 (2019).
137. Alameh, M.G., et al. Lipid nanoparticles enhance the efficacy of mRNA and protein subunit vaccines by inducing robust t follicular helper cell and humoral responses (vol 54, pg 2877, 2021). *Immunity* **55**, 1136–1138 (2022).
138. Zhang, H.X., et al. Delivery of mRNA vaccine with a lipid-like material potentiates antitumor efficacy through toll-like receptor 4 signaling. *Proceedings of the National Academy of Sciences of the United States of America* **118** (2021).
139. Piotrowski-Daspit, A.S., et al. Polymeric vehicles for nucleic acid delivery. *Advanced Drug Delivery Reviews* **156**, 119–132 (2020).
140. Rai, R., et al. Polymeric nanoparticles in gene therapy: New avenues of design and optimization for delivery applications. *Polymers* **11** (2019).
141. Mitchell, M.J., et al. Engineering precision nanoparticles for drug delivery. *Nature Reviews Drug Discovery* **20**, 101–124 (2021).
142. Mendes, L.P., et al. Dendrimers as nanocarriers for nucleic acid and drug delivery in cancer therapy. *Molecules* **22** (2017).
143. Yandek, L.E., et al. Wasp mastoparans follow the same mechanism as the cell-penetrating peptide transportan 10. *Biochemistry* **48**, 7342–51 (2009).
144. Raghuraman, H., Chattopadhyay, A. Melittin: A membrane-active peptide with diverse functions. *Bioscience Reports* **27**, 189–223 (2007).
145. Duncan, B., et al. Gold nanoparticle platforms as drug and biomacromolecule delivery systems. *J Control Release* **148**, 122–7 (2010).
146. Kim, S.T., et al. Dendronized gold nanoparticles for siRNA delivery. *Small* **8**, 3253–6 (2012).
147. Sandhu, K.K., et al. Gold nanoparticle-mediated transfection of mammalian cells. *Bioconjug Chem* **13**, 3–6 (2002).

148. Fischer, T., et al. Cylindrical microparticles composed of mesoporous silica nanoparticles for the targeted delivery of a small molecule and a macromolecular drug to the lungs: Exemplified with curcumin and sirna. *Pharmaceutics* **13** (2021).
149. Song, Y.X., et al. Folic acid (fa)-conjugated mesoporous silica nanoparticles combined with mrp-1 sirna improves the suppressive effects of myricetin on non-small cell lung cancer (NSCLC). *Biomedicine & Pharmacotherapy* **125** (2020).
150. Zhu, J.J., et al. Angiopep-2 modi fi ed lipid-coated mesoporous silica nanoparticles for glioma targeting therapy overcoming BBB. *Biochemical and Biophysical Research Communications* **534**, 902–907 (2021).
151. Prabhakar, N., et al. Circumventing drug treatment? Intrinsic lethal effects of polyethyleneimine (PEI)-functionalized nanoparticles on glioblastoma cells cultured in stem cell conditions. *Cancers* **13** (2021).
152. Liao, Y.T., et al. Gelatin-functionalized mesoporous silica nanoparticles with sustained release properties for intracameral pharmacotherapy of glaucoma. *Journal of Materials Chemistry B* **5**, 7008–7013 (2017).
153. Qu, W., et al. Epcam antibody-conjugated mesoporous silica nanoparticles to enhance the anticancer efficacy of carboplatin in retinoblastoma. *Materials Science and Engineering C-Materials for Biological Applications* **76**, 646–651 (2017).
154. Taleghani, A.S., et al. Sugar-conjugated dendritic mesoporous silica nanoparticles as ph-responsive nanocarriers for tumor targeting and controlled release of deferasirox. *Materials Science and Engineering C-Materials for Biological Applications* **98**, 358–368 (2019).
155. Meng, Y.Q., et al. Recent trends in preparation and biomedical applications of iron oxide nanoparticles. *Journal of Nanobiotechnology* **22** (2024).
156. Hu, S.H., et al. Surfactant-free, lipo-polymersomes stabilized by iron oxide nanoparticles/polymer interlayer for synergistically targeted and magnetically guided gene delivery. *Advanced Healthcare Materials* **3**, 273–282 (2014).
157. Sun, Z.C., et al. Multimodality imaging of miRNA-16 iron nanoparticle reversing drug resistance to chemotherapy in a mouse gastric cancer model. *Nanoscale* **6**, 14343–14353 (2014).
158. Wang, K., et al. Iron-oxide-based nanovector for tumor targeted siRNA delivery in an orthotopic hepatocellular carcinoma xenograft mouse model. *Small* **12**, 477–487 (2016).
159. Luo, X., et al. Co-delivery of mRNA and spions through amino-este nanomaterials. *Nano Research* **11**, 5596–5603 (2018).
160. van Niel, G., et al. Shedding light on the cell biology of extracellular vesicles. *Nature Reviews Molecular Cell Biology* **19**, 213–228 (2018).
161. Doyle, L.M., Wang, M.Z. Overview of extracellular vesicles, their origin, composition, purpose, and methods for exosome isolation and analysis. *Cells* **8** (2019).
162. Didiot, M.C., et al. Exosome-mediated delivery of hydrophobically modified siRNA for huntingtin mRNA silencing. *Molecular Therapy* **24**, 1836–1847 (2016).
163. Rezaei, R., et al. Exosome-mediated delivery of functionally active miRNA-375-3p mimic regulates epithelial-mesenchymal transition (EMT) of colon cancer cells. *Life Sciences* **269** (2021).
164. Forterre, A.V., et al. Extracellular vesicle-mediated in vitro transcribed mRNA delivery for treatment of her2+ breast cancer xenografts in mice by prodrug cb1954 without general toxicity. *Molecular Cancer Therapeutics* **19**, 858–867 (2020).
165. Xu, H.Y., et al. A novel peptide-equipped exosomes platform for delivery of antisense oligonucleotides. *Acs Applied Materials & Interfaces* **13**, 10760–10767 (2021).

166. Oshchepkova, A., et al. Extracellular vesicles for therapeutic nucleic acid delivery: Loading strategies and challenges. *International Journal of Molecular Sciences* **24** (2023).
167. Bottens, R.A., Yamada, T. Cell-penetrating peptides (cpps) as therapeutic and diagnostic agents for cancer. *Cancers* **14** (2022).
168. Ravari, N.S., et al. Fabrication, characterization and evaluation of a new designed botulinum toxin-cell penetrating peptide nanoparticulate complex. *Daru-Journal of Pharmaceutical Sciences* **31**, 1–12 (2023).
169. Derakhshankhah, H., Jafari, S. Cell-penetrating peptides: A concise review with emphasis on biomedical applications. *Biomedicine & Pharmacotherapy* **108**, 1090–1096 (2018).
170. Reissmann, S. Cell penetration: Scope and limitations by the application of cell-penetrating peptides. *J Pept Sci* **20**, 760–84 (2014).
171. Yang, W.C., et al. Cell-free production of transducible transcription factors for nuclear reprogramming. *Biotechnology and Bioengineering* **104**, 1047–1058 (2009).
172. Chang, M., et al. Cellular internalization of fluorescent proteins via arginine-rich intracellular delivery peptide in plant cells. *Plant and Cell Physiology* **46**, 482–488 (2005).
173. Singh, T., et al. Versatility of cell-penetrating peptides for intracellular delivery of siRNA. *Drug Delivery* **25**, 1996–2006 (2018).
174. Veiman, K.L., et al. Pepfect14 peptide vector for efficient gene delivery in cell cultures. *Mol Pharm* **10**, 199–210 (2013).
175. Kurrikoff, K., et al. Status update in the use of cell-penetrating peptides for the delivery of macromolecular therapeutics. *Expert Opin Biol Ther* **21**, 361–370 (2021).
176. Gitton, Y., et al. Efficient cpp-mediated cre protein delivery to developing and adult CNS tissues. *Bmc Biotechnology* **9** (2009).
177. Wang, Z., et al. Cpp-mediated protein delivery in a noncovalent form: Proof-of-concept for percutaneous and intranasal delivery. *Protein and Peptide Letters* **21**, 1129–1136 (2014).
178. Uhl, P., et al. Coating of PLA-nanoparticles with cyclic, arginine-rich cell-penetrating peptides enables oral delivery of liraglutide. *Nanomedicine-Nanotechnology Biology and Medicine* **24** (2020).
179. Maity, S.K., et al. Cancer-cell-specific drug delivery by a tumor-homing cpp-gossypol conjugate employing a tracelessly cleavable linker. *Chemistry-a European Journal* **26**, 3010–3015 (2020).
180. de Cogan, F., et al. Topical delivery of anti-VEGF drugs to the ocular posterior segment using cell-penetrating peptides. *Investigative Ophthalmology & Visual Science* **58**, 2578–2590 (2017).
181. Park, S.E., et al. Cyclic cell-penetrating peptides as efficient intracellular drug delivery tools. *Molecular Pharmaceutics* **16**, 3727–3743 (2019).
182. Frankel, A.D., Pabo, C.O. Cellular uptake of the tat protein from human immunodeficiency virus. *Cell* **55**, 1189–1193 (1988).
183. Green, M., Loewenstein, P.M. Autonomous functional domains of chemically synthesized human immunodeficiency virus tat trans-activator protein. *Cell* **55**, 1179–88. (1988).
184. Futaki, S., et al. Arginine-rich peptides – an abundant source of membrane-permeable peptides having potential as carriers for intracellular protein delivery. *Journal of Biological Chemistry* **276**, 5836–5840 (2001).

185. Rhee, M., Davis, P. Mechanism of uptake of c105y, a novel cell-penetrating peptide. *J Biol Chem* **281**, 1233–40 (2006).
186. Kohli, H., et al. Designing of putative peptides for targeting pathological protein htt in Huntington's disease. *Heliyon* **7** (2021).
187. Zhang, Y., et al. Virus-mimicking mesoporous silica nanoparticles with an electrically neutral and hydrophilic surface to improve the oral absorption of insulin by breaking through dual barriers of the mucus layer and the intestinal epithelium. *Acs Applied Materials & Interfaces* **13**, 18077–18088 (2021).
188. Zhang, P., et al. Pepducins and other lipidated peptides as mechanistic probes and therapeutics. *Cell-Penetrating Peptides: Methods and Protocols, 2nd Edition* **1324**, 191–203 (2015).
189. Moiola, M., et al. Stapled peptides-a useful improvement for peptide-based drugs. *Molecules* **24** (2019).
190. Eiriksdottir, E., et al. Secondary structure of cell-penetrating peptides controls membrane interaction and insertion. *Biochim Biophys Acta* **1798**, 1119–28 (2010).
191. Pooga, M., et al. Cell penetration by transportan. *FASEB J.* **12**, 67–77 (1998).
192. Soomets, U., et al. Deletion analogues of transportan. *Biochim. Biophys. Acta* **1467**, 165–176 (2000).
193. Derossi, D., et al. The third helix of the antennapedia homeodomain translocates through biological membranes. *J. Biol. Chem.* **269**, 10444–10450 (1994).
194. Crombez, L., et al. A new potent secondary amphipathic cell-penetrating peptide for siRNA delivery into mammalian cells. *Molecular Therapy* **17**, 95–103 (2009).
195. Mae, M., et al. A stearylated cpp for delivery of splice correcting oligonucleotides using a non-covalent co-incubation strategy. *J Control Release* **134**, 221–7 (2009).
196. Ezzat, K., et al. Pepfect 14, a novel cell-penetrating peptide for oligonucleotide delivery in solution and as solid formulation. *Nucleic Acids Res* **39**, 5284–98 (2011).
197. Andaloussi, S.E., et al. Design of a peptide-based vector, pepfect6, for efficient delivery of siRNA in cell culture and systemically in vivo. *Nucleic Acids Res* **39**, 3972–87 (2011).
198. Freimann, K., et al. Optimization of in vivo DNA delivery with NickFect peptide vectors. *J Control Release* **241**, 135–143 (2016).
199. Vivés, E., et al. A truncated HIV-1 tat protein basic domain rapidly translocates through the plasma membrane and accumulates in the cell nucleus. *J. Biol. Chem.* **272**, 16010–16017 (1997).
200. Futaki, S., et al. Arginine-rich peptides. An abundant source of membrane-permeable peptides having potential as carriers for intracellular protein delivery. *J. Biol. Chem.* **276**, 5836–5840. (2001).
201. Andaloussi, S.E.L., et al. Design of a peptide-based vector, pepfect6, for efficient delivery of siRNA in cell culture and systemically. *Nucleic Acids Research* **39**, 3972–3987 (2011).
202. Elmquist, A., et al. Ve-cadherin-derived cell-penetrating peptide, pvec, with carrier functions. *Exp. Cell. Res.* **269**, 237–244. (2001).
203. Oehlke, J., et al. Cellular uptake of an α-helical amphipathic model peptide with the potential to deliver polar compounds into the cell interior non-endocytically. *Biochimica Et Biophysica Acta-Biomembranes* **1414**, 127–139 (1998).
204. Morris, M.C., et al. A peptide carrier for the delivery of biologically active proteins into mammalian cells. *Nat Biotechnol* **19**, 1173–6. (2001).
205. Crombez, L., et al. A new potent secondary amphipathic cell-penetrating peptide for siRNA delivery into mammalian cells. *Mol Ther* **17**, 95–103 (2009).

206. Simeoni, F., et al. Insight into the mechanism of the peptide-based gene delivery system mpg: Implications for delivery of siRNA into mammalian cells. *Nucleic Acids Res* **31**, 2717–24 (2003).
207. Anko, M., et al. Influence of stearyl and trifluoromethylquinoline modifications of the cell penetrating peptide tp10 on its interaction with a lipid membrane. *Biochim Biophys Acta* **1818**, 915–24 (2012).
208. Futaki, S., et al. Stearylated arginine-rich peptides: A new class of transfection systems. *Bioconjugate Chemistry* **12**, 1005–1011 (2001).
209. Tönges, L., et al. Stearylated octaarginine and artificial virus-like particles for transfection of siRNA into primary rat neurons. *Rna* **12**, 1431–1438 (2006).
210. Biswas, A., et al. Choosing an optimal solvent is crucial for obtaining cell-penetrating peptide nanoparticles with desired properties and high activity in nucleic acid delivery. *Pharmaceutics* **15** (2023).
211. Veiman, K.L., et al. Peg shielded MMP sensitive CPPs for efficient and tumor-specific gene delivery in vivo. *J Control Release* **209**, 238–47 (2015).
212. Ervin, E.H., et al. Targeted gene silencing in human embryonic stem cells using cell-penetrating peptide PepFect 14. *Stem Cell Res Ther* **10**, 43 (2019).
213. Srimanee, A., et al. Cell-penetrating peptides for siRNA delivery to glioblastomas. *Peptides* **104**, 62–69 (2018).
214. Urgard, E., et al. Comparison of peptide- and lipid-based delivery of mir-34a-5p mimic into ppc-1 cells. *Nucleic Acid Ther* **27**, 295–302 (2017).
215. Velez, M.V.L., et al. Delivery of antisense oligonucleotides for splice-correction of androgen receptor pre-mrna in castration-resistant prostate cancer models using cell-penetrating peptides. *Prostate* **82**, 657–665 (2022).
216. Cerrato, C.P., et al. Intracellular delivery of therapeutic antisense oligonucleotides targeting mRNA coding mitochondrial proteins by cell-penetrating peptides. *Journal of Materials Chemistry B* **8**, 10825–10836 (2020).
217. van den Brand, D., et al. Peptide-mediated delivery of therapeutic mRNA in ovarian cancer. *Eur J Pharm Biopharm* **141**, 180–190 (2019).
218. Ye, J.X., et al. Cellular uptake mechanism and comparative in vitro cytotoxicity studies of monomeric LMWP-siRNA conjugate. *Journal of Industrial and Engineering Chemistry* **63**, 103–111 (2018).
219. Moschos, S.A., et al. Lung delivery studies using siRNA conjugated to tat(48–60) and penetratin reveal peptide-induced reduction in gene expression and induction of innate immunity. *Bioconjugate Chemistry* **18**, 1450–1459 (2007).
220. Kurrikoff, K., et al. Effective in vivo gene delivery with reduced toxicity, achieved by charge and fatty acid-modified cell penetrating peptide. *Sci Rep* **7**, 17056 (2017).
221. Arvizo, R.R., et al. Modulating pharmacokinetics, tumor uptake and biodistribution by engineered nanoparticles. *PLoS One* **6**, e24374 (2011).
222. Moore, T.L., et al. Nanoparticle colloidal stability in cell culture media and impact on cellular interactions. *Chemical Society Reviews* **44**, 6287–6305 (2015).
223. Margus, H., et al. Characteristics of cell-penetrating peptide/nucleic acid nanoparticles. *Mol Pharm* **13**, 172–9 (2016).
224. Boisguérin, P., et al. Peptide-based nanoparticles for therapeutic nucleic acid delivery. *Biomedicines* **9** (2021).
225. Pärnaste, L., et al. The formation of nanoparticles between small interfering RNA and amphipathic cell-penetrating peptides. *Mol Ther Nucleic Acids* **7**, 1–10 (2017).

226. Lehto, T., et al. Saturated fatty acid analogues of cell-penetrating peptide pepfect14: Role of fatty acid modification in complexation and delivery of splice-correcting oligonucleotides. *Bioconjug Chem* **28**, 782–792 (2017).
227. Ruseska, I., Zimmer, A. Internalization mechanisms of cell-penetrating peptides. *Beilstein Journal of Nanotechnology* **11**, 101–123 (2020).
228. Sahay, G., et al. Endocytosis of nanomedicines. *Journal of Controlled Release* **145**, 182–195 (2010).
229. Pan, R., et al. Uptake mechanism and direct translocation of a new cpp for sirna delivery. *Molecular Pharmaceutics* **13**, 1366–1374 (2016).
230. Walrant, A., et al. Direct translocation of cell-penetrating peptides in liposomes: A combined mass spectrometry quantification and fluorescence detection study. *Anal Biochem* **438**, 1–10 (2013).
231. Jiao, C.Y., et al. Translocation and endocytosis for cell-penetrating peptide internalization. *J Biol Chem* **284**, 33957–65 (2009).
232. Trofimenko, E., et al. The endocytic pathway taken by cationic substances requires rab14 but not rab5 and rab7. *Cell Reports* **37** (2021).
233. Kondow-McConaghy, H.M., et al. Impact of the endosomal escape activity of cell-penetrating peptides on the endocytic pathway. *Acs Chemical Biology* **15**, 2355–2363 (2020).
234. Liu, B.R., et al. Endocytic trafficking of nanoparticles delivered by cell-penetrating peptides comprised of nona-arginine and a penetration accelerating sequence. *Plos One* **8** (2013).
235. Schwartz, A.L. Receptor cell biology – receptor-mediated endocytosis. *Pediatric Research* **38**, 835–843 (1995).
236. Ponka, P., Lok, C.N. The transferrin receptor: Role in health and disease. *International Journal of Biochemistry & Cell Biology* **31**, 1111–1137 (1999).
237. Yang, H.X., et al. Cholesterol in LDL receptor recycling and degradation. *Clinica Chimica Acta* **500**, 81–86 (2020).
238. Wang, Q., et al. Control of epidermal growth factor receptor endocytosis by receptor dimerization, rather than receptor kinase activation. *Embo Reports* **6**, 942–948 (2005).
239. Martinez-Pomares, L. The mannose receptor. *Journal of Leukocyte Biology* **92**, 1177–1186 (2012).
240. PrabhuDas, M., et al. Standardizing scavenger receptor nomenclature. *Journal of Immunology* **192**, 1997–2006 (2014).
241. Rosales, C., Uribe-Querol, E. Phagocytosis: A fundamental process in immunity. *Biomed Research International* **2017** (2017).
242. Chou, L.Y.T., et al. Strategies for the intracellular delivery of nanoparticles. *Chemical Society Reviews* **40**, 233–245 (2011).
243. Rennick, J.J., et al. Key principles and methods for studying the endocytosis of biological and nanoparticle therapeutics. *Nature Nanotechnology* **16**, 266–276 (2021).
244. Vercauteren, D., et al. The use of inhibitors to study endocytic pathways of gene carriers: Optimization and pitfalls. *Mol Ther* **18**, 561–9 (2010).
245. Vanderbliek, A.M., et al. Mutations in human dynamin block an intermediate stage in coated vesicle formation. *Journal of Cell Biology* **122**, 553–563 (1993).
246. Francia, V., et al. Limits and challenges in using transport inhibitors to characterize how nano-sized drug carriers enter cells. *Nanomedicine* **14**, 1533–1549 (2019).

247. Damke, H., et al. Clathrin-independent pinocytosis is induced in cells over-expressing a temperature-sensitive mutant of dynamin. *Journal of Cell Biology* **131**, 69–80 (1995).
248. Majzoub, R.N., et al. Fluorescence microscopy colocalization of lipid-nucleic acid nanoparticles with wildtype and mutant rab5-GFP: A platform for investigating early endosomal events. *Biochimica Et Biophysica Acta-Biomembranes* **1848**, 1308–1318 (2015).
249. Singh, R.D., et al. Selective caveolin-1-dependent endocytosis of glycosphingolipids. *Mol Biol Cell* **14**, 3254–65 (2003).
250. Ma, L., et al. Live-cell microscopy and fluorescence-based measurement of luminal pH in intracellular organelles. *Frontiers in Cell and Developmental Biology* **5** (2017).
251. Rabinowitz, S., et al. Immunocytochemical characterization of the endocytic and phagolysosomal compartments in peritoneal-macrophages. *Journal of Cell Biology* **116**, 95–112 (1992).
252. Scott, C.C., et al. Endosome maturation, transport and functions. *Seminars in Cell & Developmental Biology* **31**, 2–10 (2014).
253. Fuchs, R., et al. Acidification and ion permeabilities of highly purified rat-liver endosomes. *Journal of Biological Chemistry* **264**, 2212–2220 (1989).
254. Zhang, J., et al. Rab GTPases: The principal players in crafting the regulatory landscape of endosomal trafficking. *Computational and Structural Biotechnology Journal* **20**, 4464–4472 (2022).
255. Hu, Y.B., et al. The endosomal-lysosomal system: From acidification and cargo sorting to neurodegeneration. *Translational Neurodegeneration* **4** (2015).
256. Poteryaev, D., et al. Identification of the switch in early-to-late endosome transition. Cell **141**, 497–508 (2010).
257. Pillay, C.S., et al. Endolysosomal proteolysis and its regulation. *Biochemical Journal* **363**, 417–429 (2002).
258. Wan, Y., et al. Endosome escape strategies for improving the efficacy of oligonucleotide delivery systems. *Current Medicinal Chemistry* **22**, 3326–3346 (2015).
259. Kondapalli, K.C., et al. A leak pathway for luminal protons in endosomes drives oncogenic signalling in glioblastoma. *Nature Communications* **6** (2015).
260. Montcourrier, P., et al. Characterization of very acidic phagosomes in breast cancer cells and their association with invasion. *Journal of Cell Science* **107**, 2381–2391 (1994).
261. Prasad, H., Rao, R. Endosomal acid-base homeostasis in neurodegenerative diseases. *Organelles in Disease* **185**, 195–231 (2023).
262. Kondapalli, K.C., et al. An inside job: How endosomal na(+)/h(+) exchangers link to autism and neurological disease. *Frontiers in Cellular Neuroscience* **8** (2014).
263. Desai, T.M., et al. Ph regulation in early endosomes and interferon-inducible transmembrane proteins control avian retrovirus fusion. *Journal of Biological Chemistry* **292**, 7817–7827 (2017).
264. Juks, C., et al. The role of endocytosis in the uptake and intracellular trafficking of pepfect14-nucleic acid nanocomplexes via class a scavenger receptors. *Biochim Biophys Acta* **1848**, 3205–16 (2015).
265. Ezzat, K., et al. Scavenger receptor-mediated uptake of cell-penetrating peptide nanocomplexes with oligonucleotides. *FASEB J* **26**, 1172–80 (2012).
266. Juks, C., et al. Cell-penetrating peptides recruit type A scavenger receptors to the plasma membrane for cellular delivery of nucleic acids. *FASEB J* **31**, 975–988 (2017).

267. Lindberg, S., et al. A convergent uptake route for peptide- and polymer-based nucleotide delivery systems. *J Control Release* **206**, 58–66 (2015).
268. PrabhuDas, M.R., et al. A consensus definitive classification of scavenger receptors and their roles in health and disease. *Journal of Immunology* **198**, 3775–3789 (2017).
269. Pelkmans, L., et al. Caveolar endocytosis of simian virus 40 reveals a new two-step vesicular-transport pathway to the ER. *Nat Cell Biol* **3**, 473–83. (2001).
270. Räägel, H., et al. Cpp-protein constructs induce a population of non-acidic vesicles during trafficking through endo-lysosomal pathway. *J. Control. Release* **139**, 108–17 (2009).
271. Bai, H.Q., et al. Cytoplasmic transport and nuclear import of plasmid DNA. *Bioscience Reports* **37** (2017).
272. Lorenz, P., et al. Nucleocytoplasmic shuttling: a novel in vivo property of antisense phosphorothioate oligodeoxynucleotides. *Nucleic Acids Research* **28**, 582–592 (2000).
273. Finicle, B.T., et al. Simultaneous inhibition of endocytic recycling and lysosomal fusion sensitizes cells and tissues to oligonucleotide therapeutics. *Nucleic Acids Research* **51**, 1583–1599 (2023).
274. Gilleron, J., et al. Image-based analysis of lipid nanoparticle-mediated siRNA delivery, intracellular trafficking and endosomal escape. *Nat Biotechnol* **31**, 638–46 (2013).
275. Porosk, L., et al. Enhancement of siRNA transfection by the optimization of fatty acid length and histidine content in the cpp. *Biomater Sci* **7**, 4363–4374 (2019).
276. Liou, J.S., et al. Protein transduction in human cells is enhanced by cell-penetrating peptides fused with an endosomolytic ha2 sequence. *Peptides* **37**, 273–284 (2012).
277. Jain, P., et al. In-vitro in-vivo correlation (ivivc) in nanomedicine: Is protein corona the missing link? *Biotechnology Advances* **35**, 889–904 (2017).
278. Agnihotri, T.G., et al. In vitro-in vivo correlation in nanocarriers: From protein corona to therapeutic implications. *Journal of Controlled Release* **354**, 794–809 (2023).
279. Zhang, H.Z., et al. Quantitative proteomics analysis of adsorbed plasma proteins classifies nanoparticles with different surface properties and size. *Proteomics* **11**, 4569–4577 (2011).
280. Tenzer, S., et al. Rapid formation of plasma protein corona critically affects nanoparticle pathophysiology. *Nat Nanotechnol* **8**, 772–81 (2013).
281. Aggarwal, P., et al. Nanoparticle interaction with plasma proteins as it relates to particle biodistribution, biocompatibility and therapeutic efficacy. *Adv Drug Deliv Rev* **61**, 428–37 (2009).
282. Cedervall, T., et al. Understanding the nanoparticle-protein corona using methods to quantify exchange rates and affinities of proteins for nanoparticles. *Proc Natl Acad Sci U S A* **104**, 2050–5 (2007).
283. Blanco, E., et al. Principles of nanoparticle design for overcoming biological barriers to drug delivery. *Nat Biotechnol* **33**, 941–51 (2015).
284. Zhao, Z., et al. Effect of physicochemical and surface properties on in vivo fate of drug nanocarriers. *Adv Drug Deliv Rev* **143**, 3–21 (2019).
285. Francia, V., et al. The biomolecular corona of lipid nanoparticles for gene therapy. *Bioconjug Chem* **31**, 2046–2059 (2020).
286. Paunovska, K., et al. A direct comparison of in vitro and in vivo nucleic acid delivery mediated by hundreds of nanoparticles reveals a weak correlation. *Nano Lett* **18**, 2148–2157 (2018).

287. Malcolm, D.W., et al. The effects of biological fluids on colloidal stability and sirna delivery of a ph-responsive micellar nanoparticle delivery system. *ACS Nano* **12**, 187–197 (2018).
288. Bazaz, S., et al. Novel orthogonally hydrocarbon-modified cell-penetrating peptide nanoparticles mediate efficient delivery of splice-switching antisense oligonucleotides in vitro and in vivo. *Biomedicines* **9** (2021).
289. Li, H.M., et al. The protein corona and its effects on nanoparticle-based drug delivery systems. *Acta Biomaterialia* **129**, 57–72 (2021).
290. Kim, H.R., et al. Low-density lipoprotein receptor-mediated endocytosis of pegylated nanoparticles in rat brain endothelial cells. *Cellular and Molecular Life Sciences* **64**, 356–364 (2007).
291. Göppert, T.M., Müller, R.H. Polysorbate-stabilized solid lipid nanoparticles as colloidal carriers for intravenous targeting of drugs to the brain:: Comparison of plasma protein adsorption patterns. *Journal of Drug Targeting* **13**, 179–187 (2005).
292. Göppert, T.M., Müller, R.H. Plasma protein adsorption of tween 80-and poloxamer 188-stabilized solid lipid nanoparticles. *Journal of Drug Targeting* **11**, 225–231 (2003).
293. Caracciolo, G., et al. Selective targeting capability acquired with a protein corona adsorbed on the surface of 1,2-dioleoyl-3-trimethylammonium propane/DNA nanoparticles. *ACS Appl Mater Interfaces* **5**, 13171–9 (2013).
294. Schöttler, S., et al. Protein adsorption is required for stealth effect of poly(ethylene glycol)- and poly(phosphoester)-coated nanocarriers. *Nature Nanotechnology* **11**, 372–377 (2016).
295. Ogawara, K., et al. Pre-coating with serum albumin reduces receptor-mediated hepatic disposition of polystyrene nanosphere: Implications for rational design of nanoparticles. *J Control Release* **100**, 451–5 (2004).
296. Nguyen, V.H., Lee, B.J. Protein corona: A new approach for nanomedicine design. *Int J Nanomedicine* **12**, 3137–3151 (2017).
297. Corbo, C., et al. The impact of nanoparticle protein corona on cytotoxicity, immunotoxicity and target drug delivery. *Nanomedicine (Lond)* **11**, 81–100 (2016).
298. Monopoli, M.P., et al. Physical-chemical aspects of protein corona: Relevance to in vitro and in vivo biological impacts of nanoparticles. *J Am Chem Soc* **133**, 2525–34 (2011).
299. Dobrovolskaia, M.A., et al. Interaction of colloidal gold nanoparticles with human blood: Effects on particle size and analysis of plasma protein binding profiles. *Nanomedicine* **5**, 106–17 (2009).
300. Tenzer, S., et al. Nanoparticle size is a critical physicochemical determinant of the human blood plasma corona: A comprehensive quantitative proteomic analysis. *Acs Nano* **5**, 7155–7167 (2011).
301. Deng, Z.J., et al. Differential plasma protein binding to metal oxide nanoparticles. *Nanotechnology* **20** (2009).
302. Gessner, A., et al. Influence of surface charge density on protein adsorption on polymeric nanoparticles: Analysis by two-dimensional electrophoresis. *Eur J Pharm Biopharm* **54**, 165–70 (2002).
303. Pustulka, S.M., et al. Protein nanoparticle charge and hydrophobicity govern protein corona and macrophage uptake. *Acs Applied Materials & Interfaces* **12**, 48284–48295 (2020).

304. Oberländer, J., et al. Temperature, concentration, and surface modification influence the cellular uptake and the protein corona of polystyrene nanoparticles. *Acta Biomaterialia* **148**, 271–278 (2022).
305. Wang, W.H., et al. Impact of particle size and pH on protein corona formation of solid lipid nanoparticles: A proof-of-concept study. *Acta Pharmaceutica Sinica B* **11**, 1030–1046 (2021).
306. Zhang, T.X., et al. Protein corona formed in the gastrointestinal tract and its impacts on oral delivery of nanoparticles. *Medicinal Research Reviews* **41**, 1835–1850 (2021).
307. Kumar, A., et al. What are the biological and therapeutic implications of biomolecule corona formation on the surface of inhaled nanomedicines? *Nanomedicine* **10**, 343–345 (2015).
308. Lundqvist, M., et al. The nanoparticle protein corona formed in human blood or human blood fractions. *PLoS One* **12**, e0175871 (2017).
309. Schottler, S., et al. Protein source and choice of anticoagulant decisively affect nanoparticle protein corona and cellular uptake. *Nanoscale* **8**, 5526–36 (2016).
310. Mirshafiee, V., et al. The importance of selecting a proper biological milieu for protein corona analysis in vitro: Human plasma versus human serum. *Int J Biochem Cell Biol* **75**, 188–95 (2016).
311. Colapicchioni, V., et al. Personalized liposome-protein corona in the blood of breast, gastric and pancreatic cancer patients. *Int J Biochem Cell Biol* **75**, 180–7 (2016).
312. Corbo, C., et al. Personalized protein corona on nanoparticles and its clinical implications. *Biomater Sci* **5**, 378–387 (2017).
313. Pattipeiluhu, R., et al. Unbiased identification of the liposome protein corona using photoaffinity-based chemoproteomics. *Acs Central Science* **6**, 535–545 (2020).
314. Crooke, S.T., et al. Phosphorothioate modified oligonucleotide-protein interactions. *Nucleic Acids Research* **48**, 5235–5253 (2020).
315. Koide, H., et al. Particle size-dependent triggering of accelerated blood clearance phenomenon. *International Journal of Pharmaceutics* **362**, 197–200 (2008).
316. Salvati, A., et al. Transferrin-functionalized nanoparticles lose their targeting capabilities when a biomolecule corona adsorbs on the surface. *Nat Nanotechnol* **8**, 137–43 (2013).
317. Francia, V., et al. Interactions at the cell membrane and pathways of internalization of nano-sized materials for nanomedicine. *Beilstein J Nanotechnol* **11**, 338–353 (2020).
318. Su, G.X., et al. Effects of protein corona on active and passive targeting of cyclic rgd peptide-functionalized pegylation nanoparticles. *Molecular Pharmaceutics* **15**, 5019–5030 (2018).
319. Furumoto, K., et al. Effect of coupling of albumin onto surface of peg liposome on its in vivo disposition. *International Journal of Pharmaceutics* **329**, 110–116 (2007).
320. Peng, Q., et al. Preformed albumin corona, a protective coating for nanoparticles based drug delivery system. *Biomaterials* **34**, 8521–8530 (2013).
321. Foote, M. Using nanotechnology to improve the characteristics of antineoplastic drugs: Improved characteristics of *nab*-paclitaxel compared with solvent-based paclitaxel. *Biotechnology Annual Review, Vol 13* **13**, 345–357 (2007).
322. Zhang, J., et al. Polymeric nanoparticles based on chitooligosaccharide as drug carriers for co-delivery of all-trans-retinoic acid and paclitaxel. *Carbohydrate Polymers* **129**, 25–34 (2015).

323. Tonigold, M., et al. Pre-adsorption of antibodies enables targeting of nanocarriers despite a biomolecular corona. *Nature Nanotechnology* **13**, 862–+ (2018).
324. van Asbeck, A.H., et al. Molecular parameters of siRNA-cell-penetrating peptide nanocomplexes for efficient cellular delivery. *ACS Nano* **7**, 3797–807 (2013).
325. Rossi, A., et al. Calcium, mitochondria and cell metabolism: A functional triangle in bioenergetics. *Biochimica Et Biophysica Acta-Molecular Cell Research* **1866**, 1068–1078 (2019).
326. Hepler, P.K. The role of calcium in cell division. *Cell Calcium* **16**, 322–330 (1994).
327. Endo, M. Calcium ion as a second messenger with special reference to excitation-contraction coupling. *Journal of Pharmacological Sciences* **100**, 519–524 (2006).
328. Orrenius, S., et al. Regulation of cell death: The calcium-apoptosis link. *Nature Reviews Molecular Cell Biology* **4**, 552–565 (2003).
329. Bootman, M.D., et al. The regulation of autophagy by calcium signals: Do we have a consensus? *Cell Calcium* **70**, 32–46 (2018).
330. Delos Santos, R.C., et al. Selective regulation of clathrin-mediated epidermal growth factor receptor signaling and endocytosis by phospholipase c and calcium. *Molecular Biology of the Cell* **28**, 2802–2818 (2017).
331. Yao, C.K., et al. A ca2+ channel differentially regulates clathrin-mediated and activity-dependent bulk endocytosis. *Plos Biology* **15** (2017).
332. Lorents, A., et al. Cell-penetrating peptides split into two groups based on modulation of intracellular calcium concentration. *J Biol Chem* **287**, 16880–9 (2012).
333. Melikov, K., et al. Efficient entry of cell-penetrating peptide nona-arginine into adherent cells involves a transient increase in intracellular calcium. *Biochemical Journal* **471**, 221–230 (2015).
334. Hori, S., et al. Ca2+ enrichment in culture medium potentiates effect of oligonucleotides. *Nucleic Acids Research* **43** (2015).
335. Goldshtein, M., et al. Mechanisms of cellular uptake and endosomal escape of calcium-siRNA nanocomplexes. *International Journal of Pharmaceutics* **515**, 46–56 (2016).
336. Baoum, A., et al. "Soft" calcium crosslinks enable highly efficient gene transfection using TAT peptide. *Pharm Res* **26**, 2619–29 (2009).
337. Baoum, A., et al. Calcium condensed cell penetrating peptide complexes offer highly efficient, low toxicity gene silencing. *Int J Pharm* **427**, 134–42 (2012).
338. Baoum, A.A., Berkland, C. Calcium condensation of DNA complexed with cell-penetrating peptides offers efficient, noncytotoxic gene delivery. *J Pharm Sci* **100**, 1637–42 (2011).
339. Thomè, R., et al. Chloroquine: Modes of action of an undervalued drug. *Immunology Letters* **153**, 50–57 (2013).
340. Sperber, K., et al. Inhibition of human-immunodeficiency-virus type-1 replication by hydroxychloroquine in t-cells and monocytes. *Aids Research and Human Retroviruses* **9**, 91–98 (1993).
341. Shibata, M., et al. Mechanism of uncoating of influenza b-virus in mdck cells – action of chloroquine. *Journal of General Virology* **64**, 1149–1156 (1983).
342. Ooi, E.E., et al. In vitro inhibition of human influenza a virus replication by chloroquine. *Virology Journal* **3** (2006).
343. Esdaile, J.M., et al. A randomized trial of hydroxychloroquine in early rheumatoid-arthritis – the hera study. *American Journal of Medicine* **98**, 156–168 (1995).

344. Bezerra, E.L.M., et al. Double-blind, randomized, controlled clinical trial of clofazimine compared with chloroquine in patients with systemic lupus erythematosus. *Arthritis and Rheumatism* **52**, 3073–3078 (2005).
345. Luthman, H., Magnusson, G. High-efficiency polyoma DNA transfection of chloroquine treated-cells. *Nucleic Acids Research* **11**, 1295–1308 (1983).
346. Kneuer, C., et al. A nonviral DNA delivery system based on surface modified silica-nanoparticles can efficiently transfect cells in vitro. *Bioconjugate Chemistry* **11**, 926–932 (2000).
347. Al-Bari, M.A.A. Targeting endosomal acidification by chloroquine analogs as a promising strategy for the treatment of emerging viral diseases. *Pharmacology Research & Perspectives* **5** (2017).
348. Lee, S.H., et al. Activatable cell penetrating peptide-peptide nucleic acid conjugate via reduction of azobenzene peg chains. *J Am Chem Soc* **136**, 12868–71 (2014).
349. El-Sayed, A., et al. Delivery of macromolecules using arginine-rich cell-penetrating peptides: Ways to overcome endosomal entrapment. *AAPS J* **11**, 13–22 (2009).
350. El-Andaloussi, S., et al. A novel cell-penetrating peptide, m918, for efficient delivery of proteins and peptide nucleic acids. *Mol Ther* **15**, 1820–6 (2007).
351. Li, Y.J., et al. Mechanisms of enhanced antiglioma efficacy of polysorbate 80-modified paclitaxel-loaded PLGA nanoparticles by focused ultrasound. *Journal of Cellular and Molecular Medicine* **22**, 4171–4182 (2018).
352. Li, W., et al. Bbb pathophysiology-independent delivery of siRNA in traumatic brain injury. *Sci Adv* **7** (2021).
353. Attia, N., et al. Gene transfer to rat cerebral cortex mediated by polysorbate 80 and poloxamer 188 nonionic surfactant vesicles. *Drug Design Development and Therapy* **12**, 3937–3949 (2018).
354. Zhao, N., et al. Apolipoprotein e, receptors, and modulation of Alzheimer's disease. *Biological Psychiatry* **83**, 347–357 (2018).
355. van de Sluis, B., et al. News on the molecular regulation and function of hepatic low-density lipoprotein receptor and LDLR-related protein 1. *Current Opinion in Lipidology* **28**, 241–247 (2017).
356. Tahara, K., et al. Cellular uptake mechanisms and intracellular distributions of polysorbate 80-modified poly (D,L-lactide-co-glycolide) nanospheres for gene delivery. *European Journal of Pharmaceutics and Biopharmaceutics* **75**, 218–224 (2010).
357. Bost, J.P., et al. Novel endosomolytic compounds enable highly potent delivery of antisense oligonucleotides. *Communications Biology* **5** (2022).
358. Wang, H., et al. Hyperosmotic treatment synergistically boost efficiency of cell-permeable peptides. *Oncotarget* **7**, 74648–74657 (2016).
359. Bell, G.D., et al. MRNA transfection by a xentry-protamine cell-penetrating peptide is enhanced by TLR antagonist e6446. *Plos One* **13** (2018).
360. Guterstam, P., et al. Elucidating cell-penetrating peptide mechanisms of action for membrane interaction, cellular uptake, and translocation utilizing the hydrophobic counter-anion pyrenebutyrate. *Biochimica Et Biophysica Acta-Biomembranes* **1788**, 2509–2517 (2009).
361. Takeuchi, T., et al. Direct and rapid cytosolic delivery using cell-penetrating peptides mediated by pyrenebutyrate. *ACS Chem Biol* **1**, 299–303 (2006).
362. Ma, J.L., et al. Enhanced peptide delivery into cells by using the synergistic effects of a cell-penetrating peptide and a chemical drug to alter cell permeability. *Molecular Pharmaceutics* **12**, 2040–2048 (2015).

363. Rodrigues, B.D., et al. In Vitro and In Vivo Characterization of CPP and Transferrin Modified Liposomes Encapsulating pDNA. *Nanomedicine-Nanotechnology Biology and Medicine* **28** (2020).
364. Kumari, A., et al. Surface-engineered mucus penetrating nucleic acid delivery systems with cell penetrating peptides for the lungs. *Molecular Pharmaceutics* **19**, 1309–1324 (2022).
365. Freimann, K., et al. Formulation of stable and homogeneous cell-penetrating peptide nf55 nanoparticles for efficient gene delivery in vivo. *Mol Ther Nucleic Acids* **10**, 28–35 (2018).
366. HeLa (rrid:Cvcl_0030). Available online: https://www.Cellosaurus.Org/cvcl_0030 (accessed on 15.04.2024).
367. HaCaT (rrid:Cvcl_0038). Available online: https://www.Cellosaurus.Org/cvcl_0038 (accessed on 15.04.2024).
368. Kang, S.H., et al. Up-regulation of luciferase gene expression with antisense oligonucleotides: Implications and applications in functional assay developments. *Biochemistry* **37**, 6235–6239 (1998).
369. HeLa EGFP-654 (rrid:Cvcl_vs42). Available online: www.Cellosaurus.Org/cvcl_vs42 (accessed on 15.04.2024).
370. U-87 MG-Luc2 (rrid:Cvcl_5j15). Available online: https://www.Cellosaurus.Org/cvcl_5j15 (accessed on 15.04.2024).
371. Sazani, P., et al. Nuclear antisense effects of neutral, anionic and cationic oligonucleotide analogs. *Nucleic Acids Res* **29**, 3965–74. (2001).
372. Padari, K., et al. Characterization of peptide-oligonucleotide complexes using electron microscopy, dynamic light scattering, and protease resistance assay. *Methods Mol Biol* **2036**, 127–139 (2019).
373. Wang, L.H., et al. Mis-assembly of clathrin lattices on endosomes reveals a regulatory switch for coated pit formation. *Journal of Cell Biology* **123**, 1107–1117 (1993).
374. Lamaze, C., et al. The actin cytoskeleton is required for receptor-mediated endocytosis in mammalian cells. *Journal of Biological Chemistry* **272**, 20332–20335 (1997).
375. Silva, L., et al. Competitive binding of cholesterol and ergosterol to the polyene antibiotic nystatin. A fluorescence study. *Biophysical Journal* **90**, 3625–3631 (2006).
376. Schnitzer, J.E., et al. Filipin-sensitive caveolae-mediated transport in endothelium – reduced transcytosis, scavenger endocytosis, and capillary-permeability of select macromolecules. *Journal of Cell Biology* **127**, 1217–1232 (1994).
377. Kiss, A.L. Caveolae and the regulation of endocytosis. *Caveolins and Caveolae: Roles in Signaling and Disease Mechanisms* **729**, 14–28 (2012).
378. Nonnenmacher, M., Weber, T. Adeno-associated virus 2 infection requires endocytosis through the clic/geec pathway. *Cell Host & Microbe* **10**, 563–576 (2011).
379. Fretz, M., et al. Effects of na+/h+ exchanger inhibitors on subcellular localisation of endocytic organelles and intracellular dynamics of protein transduction domains HIV-TAT peptide and octaarginine. *J Control Release* **116**, 247–54 (2006).
380. Pearson, A.M., et al. Polynucleotide binding to macrophage scavenger receptors depends on the formation of base-quartet-stabilized 4-stranded helices. *Journal of Biological Chemistry* **268**, 3546–3554 (1993).
381. Terpstra, V., van Berkel, T.J.C. Scavenger receptors on liver Kupffer cells mediate the in vivo uptake of oxidatively damaged red blood cells in mice. *Blood* **95**, 2157–2163 (2000).

382. Kawabata, K., et al. The fate of plasmid DNA after intravenous injection in mice – involvement of scavenger receptors in its hepatic-uptake. *Pharmaceutical Research* **12**, 825–830 (1995).
383. Beppu, M., et al. Recognition of sialosaccharide chains of glycophorin on damaged erythrocytes by macrophage scavenger receptors. *Biochimica Et Biophysica Acta-Molecular Cell Research* **1268**, 9–19 (1995).
384. Brown, M.S., et al. The scavenger cell pathway for lipoprotein degradation – specificity of the binding site that mediates the uptake of negatively-charged LDL by macrophages. *Journal of Supramolecular Structure* **13**, 67–81 (1980).
385. Thelen, T., et al. The class A scavenger receptor, macrophage receptor with collagenous structure, is the major phagocytic receptor for Clostridium sordellii expressed by human decidual macrophages. *Journal of Immunology* **185**, 4328–4335 (2010).
386. Chieosilapatham, P., et al. Keratinocytes: Innate immune cells in atopic dermatitis. *Clinical and Experimental Immunology* **204**, 296–309 (2021).
387. Latreille, P.L., et al. In situ characterization of the protein corona of nanoparticles in vitro and in vivo. *Advanced Materials* **34** (2022).
388. Wang, H.X., et al. Formation of a monolayer protein corona around polystyrene nanoparticles and implications for nanoparticle agglomeration. *Small* **15** (2019).
389. Vitali, M., et al. Simple spectroscopic determination of the hard protein corona composition in aunps: Albumin at 75%. *Nanoscale* **12**, 15832–15844 (2020).
390. Falahati, M., et al. A health concern regarding the protein corona, aggregation and disaggregation. *Biochimica Et Biophysica Acta-General Subjects* **1863**, 971–991 (2019).
391. Sharma, A., et al. Toxicological considerations when creating nanoparticle-based drugs and drug delivery systems. *Expert Opin Drug Metab Toxicol* **8**, 47–69 (2012).
392. Nagayama, S., et al. Fetuin mediates hepatic uptake of negatively charged nanoparticles via scavenger receptor. *Int J Pharm* **329**, 192–8 (2007).
393. Shemesh, C.S., et al. Pharmacokinetic and pharmacodynamic investigations of ion-353382, a model antisense oligonucleotide: Using alpha-2-macroglobulin and murinoglobulin double-knockout mice. *Nucleic Acid Ther* **26**, 223–35 (2016).
394. Vu, V.P., et al. Immunoglobulin deposition on biomolecule corona determines complement opsonization efficiency of preclinical and clinical nanoparticles. *Nat Nanotechnol* **14**, 260–268 (2019).
395. Reddy, S.T., et al. Exploiting lymphatic transport and complement activation in nanoparticle vaccines. *Nat Biotechnol* **25**, 1159–64 (2007).
396. Dunkelberger, J.R., Song, W.C. Complement and its role in innate and adaptive immune responses. *Cell Research* **20**, 34–50 (2010).
397. Lindman, S., et al. Systematic investigation of the thermodynamics of hsa adsorption to n-iso-propylacrylamide/n-tert-butylacrylamide copolymer nanoparticles. Effects of particle size and hydrophobicity. *Nano Lett* **7**, 914–20 (2007).
398. Cruz-León, S., Schwierz, N. Hofmeister series for metal-cation-rna interactions: The interplay of binding affinity and exchange kinetics. *Langmuir* **36**, 5979–5989 (2020).
399. Wang, R.C., et al. Effects of small molecular compounds in soymilk on the protein coagulation process: Ca2+ as coagulant. *Food Research International* **77**, 34–42 (2015).

400. Ju, Z.Y., Kilara, A. Aggregation induced by calcium chloride and subsequent thermal gelation of whey protein isolate. *Journal of Dairy Science* **81**, 925–931 (1998).
401. Isaacs, A.M., et al. Acceleration of amyloid β-peptide aggregation by physiological concentrations of calcium. *Journal of Biological Chemistry* **281**, 27916–27923 (2006).
402. Vaher, H., et al. Mir-10a-5p is increased in atopic dermatitis and has capacity to inhibit keratinocyte proliferation. *Allergy* **74**, 2146–2156 (2019).
403. Bains, S.N., et al. Irritant contact dermatitis. *Clinical Reviews in Allergy & Immunology* **56**, 99–109 (2019).
404. Miliotou, A.N., et al. Development of a novel PTD-mediated ivt-mRNA delivery platform for potential protein replacement therapy of metabolic/genetic disorders. *Molecular Therapy-Nucleic Acids* **26**, 694–710 (2021).
405. Tateshita, N., et al. Development of a lipoplex-type mRNA carrier composed of an ionizable lipid with a vitamin E scaffold and the kala peptide for use as an ex vivo dendritic cell-based cancer vaccine. *Journal of Controlled Release* **310**, 36–46 (2019).
406. Lou, B., et al. MRNA polyplexes with post-conjugated gala peptides efficiently target, transfect, and activate antigen-presenting cells. *Bioconjugate Chemistry* **30**, 461–475 (2019).
407. Kim, Y., et al. The potential of cell-penetrating peptides for mRNA delivery to cancer cells. *Pharmaceutics* **14** (2022).
408. Porosk, L., et al. The development of cell-penetrating peptides for efficient and selective in vivo expression of mRNA in spleen tissue. *Pharmaceutics* **15** (2023).
409. Xie, Z.J., et al. Calcium-induced human keratinocyte differentiation requires src- and fyn-mediated phosphatidylinositol 3-kinase-dependent activation of phospholipase C-gamma1. *Molecular Biology of the Cell* **16**, 3236–3246 (2005).
410. Mahanty, S., et al. Keratinocyte differentiation promotes er stress-dependent lysosome biogenesis (vol 10, 269, 2019). *Cell Death & Disease* **10** (2019).
411. Commisso, C., et al. Macropinocytosis of protein is an amino acid supply route in ras-transformed cells. *Nature* **497**, 633–+ (2013).
412. Chen, Y., et al. Cholesterol sequestration by nystatin enhances the uptake and activity of endostatin in endothelium via regulating distinct endocytic pathways. *Blood* **117**, 6392–6403 (2011).
413. Kumar, G.K., et al. Embelin reduces cutaneous tnf-α level and ameliorates skin edema in acute and chronic model of skin inflammation in mice. *European Journal of Pharmacology* **662**, 63–69 (2011).
414. Nusrat, A., et al. Molecular physiology and pathophysiology of tight junctions iv. Regulation of tight junctions by extracellular stimuli: Nutrients, cytokines, and immune cells. *American Journal of Physiology-Gastrointestinal and Liver Physiology* **279**, G851–G857 (2000).
415. Capaldo, C.T., Nusrat, A. Cytokine regulation of tight junctions. *Biochimica Et Biophysica Acta-Biomembranes* **1788**, 864–871 (2009).

ACKNOWLEDGEMENTS

This work was carried out at the Institute of Technology at the University of Tartu. This work was supported by the Estonian Ministry of Education and Research through grant 0180019s11, the Estonian Research Council through grants PUT1617P, PRG1169, PRG1506, and PRG1259, the Institute of Technology through grant PLTTI20912, and LEO Pharma Research Foundation through grant LF17040.

First, I would like to sincerely thank my supervisor Prof. Margus Pooga for always being supportive and encouraging, appreciating my effort, teaching me to view even negative results positively, and making my PhD years feel like an exciting adventure. I appreciate the help of my co-supervisor Prof. Ana Rebane, whose thorough proofreading and advice have always been highly valuable to me.

I am also thankful to all the current and former colleagues: Kärt Padari, Abhijit Biswas, Kapilraj Periyasamy, Raphael Chimdi, Geeta Arya, İrem Ilgın Gümüşoğlu, Ly Porosk, and Chigozie Chibueze Nkwocha for conducting research together and creating a cooperative and friendly atmosphere within our group.

I am deeply grateful to my family for their support throughout these years, especially to my mother, Alla Piirsoo, for her invaluable help in both everyday and work life.

PUBLICATIONS

CURRICULUM VITAE

Name Maria Maloverjan
Date of birth 14th of September 1996
Citizenship Estonian
E-mail maria.maloverjan@ut.ee

Education and professional employment

2015–2018 University of Tartu, BSc in Biology, *cum laude*
2018–2020 University of Tartu, MSc in Biomedicine, *cum laude*
2020–… University of Tartu, PhD student in Biomedical technology
2022–… University of Tartu, junior research fellow in Technology

Publications

Lorents A†, **Maloverjan M**†, Padari K, Pooga M. Internalisation and Biological Activity of Nucleic Acids Delivering Cell-Penetrating Peptide Nanoparticles Is Controlled by the Biomolecular Corona. Pharmaceuticals. 2021; 14(7):667.

Maloverjan M, Padari K, Abroi A, Rebane A, Pooga M. Divalent Metal Ions Boost Effect of Nucleic Acids Delivered by Cell-Penetrating Peptides. Cells. 2022; 11(4):756.

Biswas A†, **Maloverjan M**†, Padari K, Abroi A, Rätsep M, Wärmländer SKTS, Jarvet J, Gräslund A, Kisand V, Lõhmus R, Pooga M. Choosing an Optimal Solvent Is Crucial for Obtaining Cell-Penetrating Peptide Nanoparticles with Desired Properties and High Activity in Nucleic Acid Delivery. Pharmaceutics. 2023; 15(2):396.

Periyasamy K†, **Maloverjan M**†, Biswas A, Remm A, Pook M, Rebane A, Pooga M. PepFect14 mediates the delivery of mRNA into human primary keratinocytes and in vivo. Front Pharmacol. 2023; 14:1219761.

ELULOOKIRJELDUS

Nimi Maria Maloverjan
Sünniaeg 14. september 1996
Kodakondsus Eesti
E-post maria.maloverjan@ut.ee

Haridus ja töökogemus

2015–2018	Tartu Ülikool, loodusteaduse bakalaureus (BSc) bioloogia erialal, *cum laude*
2018–2020	Tartu Ülikool, loodusteaduse magister (MSc) biomeditsiini erialal, *cum laude*
2020–…	Tartu Ülikool, doktoriõpe biomeditsiini tehnoloogia erialal
2022–...	Tartu Ülikool, tehnoloogia nooremteadur

Publikatsioonid

Lorents A†, **Maloverjan M**†, Padari K, Pooga M. Internalisation and Biological Activity of Nucleic Acids Delivering Cell-Penetrating Peptide Nanoparticles Is Controlled by the Biomolecular Corona. Pharmaceuticals. 2021; 14(7):667.

Maloverjan M, Padari K, Abroi A, Rebane A, Pooga M. Divalent Metal Ions Boost Effect of Nucleic Acids Delivered by Cell-Penetrating Peptides. Cells. 2022; 11(4):756.

Biswas A†, **Maloverjan M**†, Padari K, Abroi A, Rätsep M, Wärmländer SKTS, Jarvet J, Gräslund A, Kisand V, Lõhmus R, Pooga M. Choosing an Optimal Solvent Is Crucial for Obtaining Cell-Penetrating Peptide Nanoparticles with Desired Properties and High Activity in Nucleic Acid Delivery. Pharmaceutics. 2023; 15(2):396.

Periyasamy K†, **Maloverjan M**†, Biswas A, Remm A, Pook M, Rebane A, Pooga M. PepFect14 mediates the delivery of mRNA into human primary keratinocytes and in vivo. Front Pharmacol. 2023; 14:1219761.

DISSERTATIONES TECHNOLOGIAE UNIVERSITATIS TARTUENSIS

1. **Imre Mäger**. Characterization of cell-penetrating peptides: Assessment of cellular internalization kinetics, mechanisms and bioactivity. Tartu 2011, 132 p.
2. **Taavi Lehto**. Delivery of nucleic acids by cell-penetrating peptides: application in modulation of gene expression. Tartu 2011, 155 p.
3. **Hannes Luidalepp**. Studies on the antibiotic susceptibility of *Escherichia coli*. Tartu 2012, 111 p.
4. **Vahur Zadin**. Modelling the 3D-microbattery. Tartu 2012, 149 p.
5. **Janno Torop**. Carbide-derived carbon-based electromechanical actuators. Tartu 2012, 113 p.
6. **Julia Suhorutšenko**. Cell-penetrating peptides: cytotoxicity, immunogenicity and application for tumor targeting. Tartu 2012, 139 p.
7. **Viktoryia Shyp**. G nucleotide regulation of translational GTPases and the stringent response factor RelA. Tartu 2012, 105 p.
8. **Mardo Kõivomägi**. Studies on the substrate specificity and multisite phosphorylation mechanisms of cyclin-dependent kinase Cdk1 in *Saccharomyces cerevisiae*. Tartu, 2013, 157 p.
9. **Liis Karo-Astover**. Studies on the Semliki Forest virus replicase protein nsP1. Tartu, 2013, 113 p.
10. **Piret Arukuusk**. NickFects–novel cell-penetrating peptides. Design and uptake mechanism. Tartu, 2013, 124 p.
11. **Piret Villo**. Synthesis of acetogenin analogues. Asymmetric transfer hydrogenation coupled with dynamic kinetic resolution of α-amido-β-keto esters. Tartu, 2013, 151 p.
12. **Villu Kasari**. Bacterial toxin-antitoxin systems: transcriptional cross-activation and characterization of a novel *mqsRA* system. Tartu, 2013, 108 p.
13. **Margus Varjak**. Functional analysis of viral and host components of alphavirus replicase complexes. Tartu, 2013, 151 p.
14. **Liane Viru**. Development and analysis of novel alphavirus-based multifunctional gene therapy and expression systems. Tartu, 2013, 113 p.
15. **Kent Langel**. Cell-penetrating peptide mechanism studies: from peptides to cargo delivery. Tartu, 2014, 115 p.
16. **Rauno Temmer**. Electrochemistry and novel applications of chemically synthesized conductive polymer electrodes. Tartu, 2014, 206 p.
17. **Indrek Must**. Ionic and capacitive electroactive laminates with carbonaceous electrodes as sensors and energy harvesters. Tartu, 2014, 133 p.
18. **Veiko Voolaid**. Aquatic environment: primary reservoir, link, or sink of antibiotic resistance? Tartu, 2014, 79 p.
19. **Kristiina Laanemets**. The role of SLAC1 anion channel and its upstream regulators in stomatal opening and closure of *Arabidopsis thaliana.* Tartu, 2015, 115 p.

20. **Kalle Pärn**. Studies on inducible alphavirus-based antitumour strategy mediated by site-specific delivery with activatable cell-penetrating peptides. Tartu, 2015, 139 p.
21. **Anastasia Selyutina**. When biologist meets chemist: a search for HIV-1 inhibitors. Tartu, 2015, 172 p.
22. **Sirle Saul**. Towards understanding the neurovirulence of Semliki Forest virus. Tartu, 2015, 136 p.
23. **Marit Orav**. Study of the initial amplification of the human papillomavirus genome. Tartu, 2015, 132 p.
24. **Tormi Reinson**. Studies on the Genome Replication of Human Papillomaviruses. Tartu, 2016, 110 p.
25. **Mart Ustav Jr**. Molecular Studies of HPV-18 Genome Segregation and Stable Replication. Tartu, 2016, 152 p.
26. **Margit Mutso**. Different Approaches to Counteracting Hepatitis C Virus and Chikungunya Virus Infections. Tartu, 2016, 184 p.
27. **Jelizaveta Geimanen**. Study of the Papillomavirus Genome Replication and Segregation. Tartu, 2016, 168 p.
28. **Mart Toots**. Novel Means to Target Human Papillomavirus Infection. Tartu, 2016, 173 p.
29. **Kadi-Liis Veiman**. Development of cell-penetrating peptides for gene delivery: from transfection in cell cultures to induction of gene expression *in vivo*. Tartu, 2016, 136 p.
30. **Ly Pärnaste**. How, why, what and where: Mechanisms behind CPP/cargo nanocomplexes. Tartu, 2016, 147 p.
31. **Age Utt**. Role of alphavirus replicase in viral RNA synthesis, virus-induced cytotoxicity and recognition of viral infections in host cells. Tartu, 2016, 183 p.
32. **Veiko Vunder**. Modeling and characterization of back-relaxation of ionic electroactive polymer actuators. Tartu, 2016, 154 p.
33. **Piia Kivipõld**. Studies on the Role of Papillomavirus E2 Proteins in Virus DNA Replication. Tartu, 2016, 118 p.
34. **Liina Jakobson**. The roles of abscisic acid, CO_2, and the cuticle in the regulation of plant transpiration. Tartu, 2017, 162 p.
35. **Helen Isok-Paas**. Viral-host interactions in the life cycle of human papillomaviruses. Tartu, 2017, 158 p.
36. **Hanna Hõrak**. Identification of key regulators of stomatal CO_2 signalling via O_3-sensitivity. Tartu, 2017, 260 p.
37. **Jekaterina Jevtuševskaja**. Application of isothermal amplification methods for detection of *Chlamydia trachomatis* directly from biological samples. Tartu, 2017, 96 p.
38. **Ülar Allas**. Ribosome-targeting antibiotics and mechanisms of antibiotic resistance. Tartu, 2017, 152 p.
39. **Anton Paier**. Ribosome Degradation in Living Bacteria. Tartu, 2017, 108 p.
40. **Vallo Varik**. Stringent Response in Bacterial Growth and Survival. Tartu, 2017, 101 p.

41. **Pavel Kudrin**. In search for the inhibitors of *Escherichia coli* stringent response factor RelA. Tartu, 2017, 138 p.
42. **Liisi Henno**. Study of the human papillomavirus genome replication and oligomer generation. Tartu, 2017, 144 p.
43. **Katrin Krõlov**. Nucleic acid amplification from crude clinical samples exemplified by *Chlamydia trachomatis* detection in urine. Tartu, 2018, 118 p.
44. **Eve Sankovski**. Studies on papillomavirus transcription and regulatory protein E2. Tartu, 2018, 113 p.
45. **Morteza Daneshmand**. Realistic 3D Virtual Fitting Room. Tartu, 2018, 233 p.
46. **Fatemeh Noroozi**. Multimodal Emotion Recognition Based Human-Robot Interaction Enhancement. Tartu, 2018, 113 p.
47. **Krista Freimann**. Design of peptide-based vector for nucleic acid delivery in vivo. Tartu, 2018, 103 p.
48. **Rainis Venta**. Studies on signal processing by multisite phosphorylation pathways of the *S. cerevisiae* cyclin-dependent kinase inhibitor Sic1. Tartu, 2018, 155 p.
49. **Inga Põldsalu**. Soft actuators with ink-jet printed electrodes. Tartu, 2018, 85 p.
50. **Kadri Künnapuu**. Modification of the cell-penetrating peptide PepFect14 for targeted tumor gene delivery and reduced toxicity. Tartu, 2018, 114 p.
51. **Toomas Mets**. RNA fragmentation by MazF and MqsR toxins of *Escherichia coli.* Tartu, 2019, 119 p.
52. **Kadri Tõldsepp**. The role of mitogen-activated protein kinases MPK4 and MPK12 in CO_2-induced stomatal movements. Tartu, 2019, 259 p.
53. **Pirko Jalakas**. Unravelling signalling pathways contributing to stomatal conductance and responsiveness. Tartu, 2019, 120 p.
54. **S. Sunjai Nakshatharan**. Electromechanical modelling and control of ionic electroactive polymer actuators. Tartu, 2019, 165 p.
55. **Eva-Maria Tombak**. Molecular studies of the initial amplification of the oncogenic human papillomavirus and closely related nonhuman primate papillomavirus genomes. Tartu, 2019, 150 p.
56. **Meeri Visnapuu**. Design and physico-chemical characterization of metal-containing nanoparticles for antimicrobial coatings. Tartu, 2019, 138 p.
57. **Jelena Beljantseva**. Small fine-tuners of the bacterial stringent response – a glimpse into the working principles of Small Alarmone Synthetases. Tartu, 2020, 104 p.
58. **Egon Urgard**. Potential therapeutic approaches for modulation of inflammatory response pathways. Tartu, 2020, 120 p.
59. **Sofia Raquel Alves Oliveira**. HPLC analysis of bacterial alarmone nucleotide (p)ppGpp and its toxic analogue ppApp. Tartu, 2020, 122 p.
60. **Mihkel Örd**. Ordering the phosphorylation of cyclin-dependent kinase Cdk1 substrates in the cell cycle. Tartu, 2021, 228 p.
61. **Fred Elhi**. Biocompatible ionic electromechanically active polymer actuator based on biopolymers and non-toxic ionic liquids. Tartu, 2021, 140 p.

62. **Liisi Talas**. Reconstructing paleo-diversity, dynamics and response of eukaryotes to environmental change over the Late-Glacial and Holocene period in lake Lielais Svētiņu using sedaDNA. Tartu, 2021, 118 p.
63. **Livia Matt**. Novel isosorbide-based polymers. Tartu, 2021, 118 p.
64. **Koit Aasumets**. The dynamics of human mitochondrial nucleoids within the mitochondrial network. Tartu, 2021, 104 p.
65. **Faiza Summer**. Development and optimization of flow electrode capacitor technology. Tartu, 2022, 109 p.
66. **Olavi Reinsalu**. Cancer-testis antigen MAGE-A4 is incorporated into extracellular vesiclesand is exposed to the surface. Tartu, 2022, 130 p.
67. **Tetiana Brodiazhenko**. RelA-SpoT Homolog enzymes as effectors of Toxin-Antitoxin systems. Tartu, 2022, 132 p.
68. **Georg-Marten Lanno**. Development of novel antibacterial drug delivery systems as wound scaffolds using electrospinning technology. Tartu, 2022, 175 p.
69. **Liubov Cherkashchenko**. New insights into alphaviral nsP2 functions. Tartu, 2023, 171 p.
70. **Kristina Kiisholts**. Peptide-based drug carriers and preclinical nanomedicine applications for endometriosis treatment. Tartu, 2023, 138 p.
71. **Kai Rausalu**. Alphaviral nsP2 protease: From requirements for functionality to inhibition. Tartu, 2023, 175 p.
72. **Laura Sandra Lello**. Unraveling the intricate nature of the alphavirus RNA replicase. Tartu, 2023, 219 p.
73. **Houman Masnavi**. Visibility Aware Navigation. Tartu, 2023, 180 p.
74. **Kadir Aktas**. Cosmic Ray Tomography based Object Reconstruction and Recognition. Tartu, 2023, 104 p.
75. **Egils Avots**. Brain abnormality detection using statistical analysis of individual structural connectivity networks and EEG signals. Tartu, 2023, 223 p.
76. **Sainan Wang**. Structure-guided insights into the functions of CHIKV nsP2. Tartu, 2024, 154 p.
77. **Anneli Samel**. Unveiling the characteristics of cancer-testis antigen MAGEA10. Tartu, 2024, 136 p.
78. **Ikechukwu Ofodile**. Fault tolerant attitude control for nanosatellites: ESTCube-2 case. Tartu, 2024, 130 p.
79. **Olena Zamora**. Impacts of plant hormones on controlling stomatal conductance. Tartu, 2024, 166 p.
80. **Mariliis Hinnu**. *In vitro* methods for studying the mechanisms of ribosome-targeting antibiotics. Tartu, 2024, 143 p.
81. **Chung-Yueh Yeh**. Characterization of MPK and HT1 kinases in CO_2-induced stomatal movements. Tartu, 2024, 118 p.
82. **Iman Dadras**. Low power neural network-based control and actuation solutions for insect-scale robots. Tartu, 2024, 149 p.
83. **Fatemeh Rastgar**. Towards reliable real-time trajectory optimization. Tartu, 2024, 158 p.